Optimum Inerter-based Absorbers for Cable Vibration Suppression

Jiannan Luo

Department of Mechanical Engineering

University of Bristol

A dissertation submitted to the University of Bristol in accordance with the requirements of the degree of Ph.D. in the Faculty of Engineering

December 2018

Word count: 37643

Abstract

Cables are widely used in cable-stayed bridges and other civil engineering structures, but they often experience large amplitude vibrations due to their low inherent damping. Compared with conventional viscous dampers, inerter-based vibration absorbers can potentially be more effective to improve damping performance. The inerter is a two-port mechanical element with the property that the applied force is proportional to the relative acceleration between its terminals, with the constant of proportionality termed inertance. This thesis is focused on establishing a systematic methodology for identifying optimum inerter-based cable vibration absorbers. In order to facilitate the investigation of a wide range of candidate absorber layouts, a finite element (FE) taut cable model with a generic vibration absorber represented by its admittance function, is firstly established. Then, three performance measures and an optimisation approach used in this study are introduced.

Based on the established model, the effects of different absorber layouts for cable vibration suppression are investigated. First, potential advantages of all layouts with no more than one inerter, one damper and one spring each, are investigated. Compared with viscous damper only, the three-element inerter-based layouts can provide significant performance improvements with large inertance. However, large inertance leads to difficulties in terms of physical implementation. In order to limit the inertance, while maintaining the performance gain, alternative inerter-based configurations containing more elements are studied. Based on network synthesis theory, a pair of fixed-sized-inerter (FSI) layouts are introduced which cover a set of seven-element network layouts with one inerter and at most six other elements (springs and dampers). The results show that one type of FSI layout can provide much more beneficial results than all those low-complexity layouts (with three elements or fewer), with much smaller inertance. Moreover, a simplification procedure is adopted with which two four-element inerter-based layouts are obtained, with no comprise of the performance for specific ranges of inertance values.

For the identified beneficial layouts, the effects of series compliance at connections are examined, due to the fact that the connections at either end of the absorber are not fully rigid. Results show that without re-optimisation, the series compliance is detrimental, if properly retuned for specific inertance, even better performance can be obtained in some cases. The effects of the installation location of the absorber on damping performance are also investigated for same identified beneficial layouts. Significant influence of location parameter on damping performance has been found.

The study results can be useful for inerter-based absorber for cable vibration problems in engineering application, e.g., in design, tuning and installation of absorbers. Besides, the proposed methodology in this study can be applied to cable vibration problems with other performance criteria, and also other mechanical structures.

For Mom and Dad.

Acknowledgements

Firstly, I would like to thank my supervisor Dr. Jason Zheng Jiang for giving me the opportunity of doing this PhD. I will never forget your support, encouragement and insight throughout the whole study. I would also like to thank my co-supervisor, Dr. John Macdonald, for guiding me to solve the problems nicely and patiently.

Second, I would like to thank all members working in Act Laboratory. An acknowledgement is to Professor David Stoten. Thank you for all the coffee time and the English lessons, which made my work more enjoyable. Thanks are due to my fellow friends, Sara, Yuan and Xiaofu, thank you all for accompanying and understanding, both in the academic study and in the personal life.

Also, I would like to thank my best friend Qingwei Liu, who was my four-year roommate for my undergraduate study in SJTU. By WeChat, we still have a lot of chances to share happiness and sorrow together, though the long distance exists between Shanghai and Bristol.

In the depth of heart, I would like to thank my Mom and Dad, you both are always supportive of all of my endeavours and I would not have the chance to write these words without your countless love, trust, understanding and encouragements.

Finally, I would like to thank Chinese Scholarship Council to offer me this full scholarship for the financial support for my four-year study in UK.

Jiannan Luo

Act Lab, Queen's Building

Bristol

December 2018

Author's Declaration

I declare that the work in this dissertation was carried out in accordance with the regulations of the University of Bristol. The work is original except where indicated by special reference in the text and no part of the dissertation has been submitted for any other degree.

Any views expressed in the dissertation are those of the author and in no way represent those of the University of Bristol.

The dissertation has not been presented to any other University for examination either in the United Kingdom or overseas.

Signed:

Dated:

Publications

As a result of the work conducted in this thesis, the following publications have been produced.

1. Jiannan Luo, Jason Z. Jiang, John H. G. Macdonald, Cable Vibration Suppression with Inerter-based Absorbers. *J. of Engineering Mechanics*. 145(2):04018134, 2019. (DOI: 10.1061/(ASCE)EM.1943-7889.0001554.)
2. Jiannan Luo, John H. G. Macdonald, Jason Z. Jiang, Optimum Absorber Identification Methodology for Cable Vibration Suppression Using Fixed-sized-inerter Layouts. *Mechanism and Machine Theory.* (Submitted)
3. Jiannan Luo, Jason Z. Jiang, John H. G. Macdonald, Damping performance of taut cables with passive absorbers incorporating inerters, *13th Int. Conference on Motion and Vibration Control (MOVIC 2016), July 3-6, 2016, Southampton, UK. J. of Physics: Conference Series.* 2016. 744, EI: 20164502990094.
4. Jiannan Luo, John H. G. Macdonald, Jason Z. Jiang, Use of Inerter-based Vibration Absorbers for Suppressing Multiple Cable Modes, *5th International conference on Structure Dynamics (EURODYN 2017), September 10-13, 2017, Rome, Italy. Procedia Engineering.* 2017. 199:1695-1700*,* EI: 20173904219925.

Contents

List of Figures

List of Tables

List of Symbols and Abbreviations

C	grounded capacitor
DOF	degree of freedom
FE	finite element
FRP	fibre-reinforced plastic
FSI	fixed-sized inerter
I	current
K	coefficient matrix for spring
L	inductor
M	coefficient matrix for mass
R	resister
TID	tuned inerter damper
TMD	tuned mass damper
TMDI	tuned mass damper inerter
V	voltage
VIMD	viscous inerter mass damper
D	cable diameter
F	force
$F(t)$	the force of absorber
L	the total length of cable
M	the total mass of cable
T	the tension along cable
S	sub-layout
U	mean wind speed
$Y(s)$	admittance function
$Z(s)$	impendence function
$a_f{}'$	non-dimensional location parameter of absorber

b	inerter
b'	inertance in non-dimensional form
c	damping coefficient
c'	damping coefficient in non-dimensional form
k	spring stiffness
k'	non-dimensional spring stiffness
k_{sc}'	non-dimensional stiffness of series compliance
m	mass
m_i	unit mass
n	number of degrees of freedom
v	velocity
x_c	distance of viscous damper to one end
x_i	vertical position of unit mass
β	a function of cable orientation and static aerodynamic force coefficients of cross-section
δ_{ij}	Kronecker delta function
ζ	damping ratio
ζ_{ai}	a defined value to prevent galloping
ζ_c	critical damping ratio
$\zeta_{c,\,max}$	maximum optimum critical damping ratio
$\zeta_{c,\,opt}$	optimum critical damping ratio
η_i	minimum product of $\zeta_i\omega_i$
θ_i	rotational angle of unit mass
λ	complex conjugate
ρ	air density
ω	natural frequencies
ω_o	undamped natural frequency
ω'	non-dimensional natural frequency

Chapter 1

Introduction

1.1 Background

Vibration control techniques for mechanical systems have been an attractive research topic for many decades. Various techniques have been proposed to isolate or suppress the unwanted vibrations, which may lead to human discomfort or structure failure and damage. In fact, as a theme in dynamics, vibration control has been used for almost all mechanical engineering applications. Since the unwanted vibrations do exist in most structure systems, these vibrations need to be controlled in most cases, in order to improve comfort and safety performances. Many examples have been successfully applied in different areas, e.g., building structures, civil engineering structures, road and rail vehicles, aircraft systems, etc.

According to whether with the requirement for external energy, the controllers can be classified into active and passive ones. Between them, there is a "hybrid" one which may only need a small external power demand for operation (e.g., a battery) to control electronic control unit or hydraulic valves for instance. This category between active and passive controllers is normally classified as "semi-active" controller. Therefore, in this broad area of vibration control, three categories, i.e., active, semi-active and passive controllers are available for engineering applications.

Although active control can provide the best performance as it can adjust the control force according to feedback in real-time, the required external power resource along with resultant additional cost and weight, and also increased complexity, inevitably limit its practical applications. Besides, active control might result in stability and robustness problems since it can do work on the controlled system itself. In contrast, due to the relatively

simple structure and also low maintenance cost, passive vibration suppression devices have been widely used in practice for a long time.

Stay cables are widely used in cable-stayed bridges and other civil engineering structures to carry static loads, but they are often observed to experience large amplitude vibrations. Cable vibrations are generated depending on different factors and phenomena. Although the exact mechanisms for cables are unclear so far, possible causes include forcing on the cables such as excitations from rain and wind, wake galloping, and excitation from deck or pylon motion, etc. The cable vibrations are coupled with vibration of the bridge deck and pylon towers. It is the vibration occurring on the cables which primarily induces vibration on the other structural members of the bridge. The different wind-induced vibrations are mainly included as aerodynamic galloping, wake galloping, buffeting, vortex shedding and fluttering. Some extreme external disturbances may cause very severe vibrations, which could cause cable or connection failures due to fatigue, as well as damaging the corrosion protection.

To suppress cables from excessive vibrations, various passive, semi-active or even active absorber have been invented, developed and applied. Theoretically, active absorbers can be able to suppress multiple resonances with unknown frequencies. However, due to the system complexity, e.g., external energy demand and additional weight and cost, active control still has been limited to prototype or research domain. In recent decades, some researches have been carried out for semi-active controllers and their prototypes. Recent studies reported that compared with traditional passive absorbers, i.e., viscous dampers, better performance and higher supplemental damping for stay cables can be provided by using semi-active technologies, e.g., by using magnetorheological (MR) fluid dampers. An engineering application example is Shandong Binzhou Yellow River Bridge with forty MR fluid dampers attached to the stay cables to suppress possible vibrations. But compared with passive absorbers, the cost of semi-active dampers can be relatively high, and it is particularly difficult for maintenance.

Currently, passive techniques are still dominant in most application cases. Adding passive absorbers to cables is the most commonly used method for vibration suppression. Among them, viscous dampers have been used in suppressing cable vibrations for many years, e.g. on the Fred Hartman Bridge in Texas, and the Erasmus Bridge in Rotterdam.

Viscous dampers are normally installed normal to the cable with one end fixed to the bridge deck. The optimum achievable damping ratio for a certain mode is larger if the damper is located closer to an anti-node. However, for ease of installation and maintenance, they are usually located close to the deck end of the cable, up to about 5% of the length along the cable.

Tuned mass dampers (TMDs) are another type of passive absorber device that has been used in practice on cables, for example on the Øresund Bridge between Malmo and Copenhagen. Normally, TMDs can be more effective than viscous dampers if they are fixed at the same location along the cable, but they may have to require a relatively large secondary mass in order to be beneficial. An alternative is to use a vibration suppression device incorporating an inerter.

The inerter was proposed as an ideal two-terminal mechanical element with the property that the applied force is proportional to the relative acceleration between its two terminals. The inerter has fundamentally enhanced the absorbers that can be realised mechanically. Furthermore, via gearing, the inertance, which is defined as the constant of proportionality with the unit of mass (i.e., kg), can be much larger than the physical mass of the device itself. Many researches have been carried out to introduce this new device into traditional vibration suppression systems. Performance advantages have been identified for many application areas, e.g., road and railway vehicles, buildings structures, and aircraft landing gear systems, etc. A typical example is the successful application of inerters in Formula one racing car. Significant improvements are provided for ride and handling performances by using inerter-based vibration absorbers (Cambridge, 2008).

For vibration suppression of cables, several theoretical studies have been carried out to investigate the potential benefits of adding a tuned inerter damper (TID) system. For example, a practical tuning methodology for the TID is proposed by Lazar (2016) to minimise the displacement amplitude at the mid-span of the cable for excitation from the motion of both supports. However, cable vibrations caused by forcing on the cables, which is usually considered the key factor, has not been taken into consideration. Furthermore, other passive absorber layouts with different complexity than that specific layout, i.e., the TID, have not been investigated or systematically compared.

As a commonly used technique, network synthesis has been applied in electrical system design for nearly one century. Particularly for electrical circuit design, passive network synthesis has been a sophisticated approach. Many theoretical contributions were made in early time focusing on the realisation of positive-real transfer functions with electrical elements. Due to the introduction of inerter, the network synthesis theory has extended its application from electrical systems to mechanical systems.

The general Bott-Duffin procedure always results in large numbers of elements required, though something that was not a significant issue in electrical circuit design. But when applying network synthesis to mechanical device design, minimising network complexity is particularly important due to some practical constraints, e.g., space, weight and cost. Unlike electrical circuits or other complicated electrical systems, it is more difficult for high-complexity mechanical structure systems to be implemented in practice in most cases. For example, it is not practical for high-complexity configurations of inerter-based vibration absorbers to be physically implemented and applied in the case of long bridge cables for vibration suppression, with difficulty for maintenance as well.

In order to obtain mechanical network realisations that are as simple as possible, some significant contributions have been made over recent decades. Due to the space and cost constraints in a mechanical implementation, it is necessary to find an efficient and systematic identification methodology for optimum configuration, in order to obtain optimum damping performance for multiple modes meanwhile with less number of elements, and also with practical small inertance values for mechanical implementation in engineering applications.

The difficulty for the identification of these inerter-based absorber configurations lies in the fact that the number of possible absorber layouts goes up exponentially with the increase of element number. In addition, it is understood that larger inertance implies more difficulties in terms of physical implementation. These difficulties include space and weight constraints in mechanical structure realisation, as well as extra wear and parasitic damping that large inertance may cause. Due to the difficulties both in identifying optimum absorber configurations among increased number of possible candidates and also in identifying the optimum values of increased the number of structure elements, network synthesis can be an efficient approach for optimum inerter-based absorber layouts in a systematic way.

To limit the number of elements, and also size and weight, fixed-sized-inerter (FSI) layouts are introduced by Zhang et al. (2017) which can be realised by a seven-element network comprising four dampers, two springs and one inerter. In addition, FSI layouts also have the benefit that the inertance value of the inerter-based absorber can be controlled within a realistic range. Thus, for an inerter-based absorber with limited size and weight, its maximum inertance provided need to be constrained by gearing ratio and rotating weight, depending on the type of inerter for example, fly-wheel, external helical tube or fluid inerters, etc.

In order to systematically identify beneficial layouts with both relatively high-performance gain and also relatively realistic structure for practical applications, among many candidate layouts, fixed-sized inerter layouts can be adopted. However, the identified beneficial FSI absorber layouts with seven elements still are complicated considering practical structure implementation. Therefore, simplification approaches are in need which attempting to reduce absorber structure elements as possible, and meanwhile maintaining their original optimum performance as possible. In addition, a general representation for absorber configuration in modelling has to be considered, e.g., by using a general admittance function, which can represent an arbitrary absorber configuration. Meanwhile, a good balance between calculation efficiency and accuracy is also important for the comprehensive investigation.

Obviously, it is crucially important to propose optimisation criterion reasonably for any optimisation problem. In previous research literature on cable vibrations, damping ratio is the most commonly used measure for assessing the vibration suppression effect. Although the lowest frequency mode, i.e., the first mode, is most susceptible to the cable vibration, higher modes (including the first six modes) may also need to be considered for some severe cases. The current guidelines on cable stay specify the requirements of damping systems also in terms of the damping ratio. Therefore, for comparing and evaluating the effectiveness of the different absorber layouts for cable vibration suppression, damping ratio can be considered as the key parameter for optimisation in this study. However, considering different forcing conditions (e.g., different aerodynamics cases) and also for different cable cases (e.g., different length), optimisation measures should be proposed properly. As the

optimisation measures are essential in assessing and quantifying the effectiveness, for identifying optimum layouts and all interested modes, they should be considered sufficiently.

For general purpose and making comparisons efficient for different layouts or various absorber configurations with different structure parameter values, all structure parameters of the absorber may need to be non-dimensionally scaled in the modelling. Besides, other parameters for the system of absorber and cable, e.g., circular natural frequencies of the damped system and the location of the absorber, are also need to be represented in non-dimensional forms. The purpose is to make comparisons of different layouts or various absorber configurations with different structure parameter values more efficiently and also to interpret the obtained results more clearly.

Hence, for the purpose of identifying and investigating the beneficial layouts systematically, a generic mathematical model of a cable combined with an arbitrary linear passive absorber needs to be built, along with all system parameters non-dimensionalised. In addition, for more efficient calculations, some considerations, e.g., adequate modelling approach, selections for degrees of freedoms and calculation tools in used software, also need to be justified and properly selected.

An efficient and systematic optimum configuration identification methodology is presented. The methodology is used to comprehensively investigate the damping performance of different absorber layouts in a systematic way. The purpose is to identify beneficial inerter-based configurations which can obtain optimum damping performance for multiple modes meanwhile with practical small inertance values and with less number of elements. First, all low-complexity layouts with no more than one inerter, one damper and one spring, are to be examined for their damping ratio enhancement considering multiple modes.

However, layouts with more elements are likely to provide greater improvements with smaller inertance. Since the number of possible layouts increases exponentially with the number of elements grows, thus, a systematic optimum configuration identification methodology needs to be adopted. For inerter-based vibration absorber layouts with more elements, network synthesis theory, which originated in the electrical domain, provides a promising way for systematic investigation. It is understood that larger inertance implies more difficulties in terms of physical implementation. Fixed-sized-inerter (FSI) layouts can

be adopted in the study due to their advantages for limiting weight and size. By making use of two types of fixed-sized-inerter (FSI) layouts, an efficient and systematic optimum configuration identification methodology can be proposed for identifying more beneficial absorber layouts than those low-complexity layouts, being classified as the all possible layouts with three or fewer elements in this study. A simplification procedure also can be adapted to reduce the number of elements to the minimum while not compromising the performance gains.

For the identified beneficial layouts, based on the proposed mathematical approach for the study, some other effects, e.g., series compliance at connection and location of absorber also can be investigated for the potential application of the identified configurations.

Due to the fact that the connections at either end of the absorber (with the support and with the cable) practically are not fully rigid in most cases, the effects of series compliance should be considered for more realistic situations. Since the effects of absorber structure parameters along with series compliance are normally coupled with each other, many computations may need for re-tuning each parameter in performance optimisation. Hence, for the identified inerter-based absorber configurations, the effects of series compliance and the coupling effect of the series compliance and structure parameters on optimisation performance need to be investigated.

In practical applications, absorbers are usually installed near the cable support on the deck, which may reduce their vibration suppression effectiveness to some extent. Due to the physical restriction, inerter-based absorbers also need to be installed near the cable support on the deck, for their vibration mitigation effectiveness. The problem of the optimal damping constant of a viscous damper located close to one end of a taut cable, studied previously, e.g., Pacheco et al. (1993) suggested that the maximum "normalised damping ratio" that could be obtained by a concentrated viscous damper, which would be about half the relative distance of the damper from the support for a viscous damper within a realistic range. Meanwhile, when the damper is close to a support, an approximate value of the optimal external damping constant for the lower modes of vibration is also found. However, no literature has been found for investigating location effect of inerter-based absorber installed on cables. So, it is worth examining the location of inerter-based absorber relative to the total length of the cable, and its effect for cable vibration suppression.

Therefore, based on an established generic model with all non-dimensionalised parameters, other effects, e.g., series compliance at connection and location of absorber, need to be investigated for the identified beneficial layouts. The investigation results for the identified beneficial layouts may be useful in practice for suppressing cable vibrations.

1.2 Research objectives

The aim of this work is to study and to propose an optimum absorber configuration identification approach for suppressing cable vibration in a systematic way. For limiting vibration of cables, and also to efficiently compare the effectiveness of identified inerter-based absorber configurations with others in previous studies, damping ratio is taken as key parameter in optimisations, and all concerned modes are considered.

To be specific, the main objectives of the thesis respectively are,

- to propose an efficient modelling and optimisation approach used in the present study, i.e., by using finite element method to establish a cable model combined with an arbitrary linear passive absorber, and to propose optimisation measures which considering all modes concerned with the cable-absorber system dynamics, for comprehensively investigating and identifying inerter-based absorber layouts in a systematic way;
- based on the established model and proposed a mathematical approach to investigate the low-complexity inerter-based absorber layouts with three elements or fewer firstly, for identifying beneficial layouts among all these low-complexity absorber layouts systematically;
- making use of two types of fixed-sized-inerter (FSI) layouts which are realised by a seven-element network, including a new FSI layout which is firstly introduced in this study, to investigating all possible layouts covered by the two FSI layouts, i.e., a set of layouts with one inerter and at most six other damper and spring elements, and to identify beneficial FSI layouts for suppressing cable vibration;
- to propose a simplification procedure for the identified beneficial FSI layout in order to further reduce the number of elements to the minimum while not compromising the performance gains, and then to identify overall beneficial configurations

simplified from the identified beneficial FSI layout, i.e., with similar optimum performance and with fewer elements compared with the original FSI layout, meanwhile with relatively small inertance values considering its physical implementation in practice;

- for identified beneficial layouts, to investigate the effects of the series compliance at connections and also the location of the absorber, which can be useful for potential applications in practice.

1.3 Thesis outline

The thesis focuses on the study of the optimum inerter-based absorber for cable vibration suppression. Throughout the whole thesis, a layout is defined as a network representing the topological connections of spring, damper and inerter elements, and a configuration refers to a layout with element values specified. Based on the research objectives of the present study introduced in Section 1.2, the structure of the thesis is organised as below.

In Chapter 2, a literature review is carried out, introducing stay cable modelling, vibration control techniques and inerter-based absorbers. First, the literature on mathematical modelling methods for investigating stay-cable dynamics is reviewed. Two commonly used methods for cable-absorber system dynamics, i.e., finite element method and Galerkin's method, are introduced in detail. Their advantages and disadvantages for the present cable vibration suppression problem are analysed. Relevant researches and applications are comprehensively reviewed. Then, an analysis of the advantages and disadvantages of active, semi-active and passive vibration control approaches are provided. Finally, the researches on network synthesis in mechanical systems are reviewed. Previous studies on passive absorbers incorporating an inerter used for cable vibration suppression is particularly reviewed. Considering increased attention and research focuses on inerter-based absorbers for other mechanical systems, the existing research works to this study are also briefly reviewed.

In Chapter 3, the modelling methodology and optimisation approach used in the present study is introduced, an integrated cable model with admittance function representing absorber is firstly established. By using finite element (FE) method, and also neglecting the

cable inclination, sag, out-of-plane motion and elasticity of the cable, a lumped mass FE model with an arbitrary linear passive absorber is used for comprehensively identifying optimum absorbers. Considering damping performance of the cable for the first mode and higher modes concerned with the present study, three optimisation measures are respectively proposed and described. In order for this study to be more representative for general cable vibration suppression problems, all parameters for the whole absorber-cable system are scaled in non-dimensional forms. Also, based on computational accuracy and efficiency considerations, i.e., selection of degrees of freedoms and MATLAB (MathWorks, 2010) tools used for performance calculations, are made and justified.

Chapter 4 focuses on identifying optimum absorber layouts with at most one spring, one damper and one inerter. First, all candidate inerter-based absorber layouts with two and three elements are presented. Based on the proposed mathematical approach, i.e., the established finite element cable model with a generic representation for different absorber layouts along with all non-dimensionalised parameters, by using two performance measures, i.e., Measures one and two depending on whether higher mode constraints are taken into consideration, the damping performance of all absorber layouts with two and three elements are comprehensively investigated. According to the analysis of optimisation results, the beneficial inerter-based absorber configurations for cable vibration suppression are identified, along with their corresponding parameter values presented.

Chapter 5 focuses on a systematic beneficial layout identification using fixed-sized-inerter (FSI) layouts. Based on the proposed mathematical approach, by using Measures two and three, a systematic investigation is carried out for all possible layouts covered by a pair of FSI layouts, i.e., a set of layouts with one inerter and at most six other elements including dampers and springs. First, two different FSI absorber layouts synthesized by seven-element networks are introduced, including a new one introduced in this study. Their respective corresponding admittance functions are also derived. Then, the damping performance of the FSI layouts along with the parameter values of their elements are systematically investigated to quantify the damping performance for multiple modes. Based on the results, a simplification procedure is adopted. Still by using the two performance measures criteria, simplified four-element optimum configurations are examined and identified along with their parameters presented. Finally, an overall beneficial, simplified configuration, with

similar optimal damping performance and with fewer elements compared with the original, beneficial FSI layout is identified, along with its element parameter values presented.

In Chapter 6, for the identified beneficial layouts, some other effects on the performance are investigated. First, due to the fact that the connections at either end of the absorber are not fully rigid, the effects of series compliance at connections are investigated. The effects of series compliance are examined for both cases, i.e., before and after re-tuning cases. Then, the effects of the installation location of the absorber on damping performance are also investigated for identified beneficial layouts.

Chapter 7 provides a summary of the main contributions of the thesis, along with remarks and outlook for future work.

Chapter 2

Literature review

This chapter presents a comprehensive literature review for the present study which focuses on a systematic identification of absorber layouts for suppressing cables vibration, typically for long cables applied in cable-stayed bridges.

First, cable-stayed bridges and their vibrations are introduced, the vibration mechanisms and different excitation sources are preliminarily analysed. Then, control techniques for suppressing stay-cables vibration, e.g., by using passive, active and semi-active controllers, are introduced respectively. Relevant researches and applications based on these techniques for stay cables vibration suppression are mainly reviewed. For passive control, the literature on the researches of inerter-based absorber and its engineering applications are reviewed. Considering the potential applications of inerter-based absorbers in increased number of areas, the literature on the structural characteristics and recent developments of inerter-based absorbers prototypes are also reviewed.

Finally, this chapter reviews the researches on network synthesis techniques in mechanical systems. Particularly, the Fixed-sized inerters and their advantages are introduced and reviewed.

2.1 Introduction for stay cables vibration

In this section, the structure of stay-cable for bridges is introduced. Then, their vibration mechanisms are discussed. Relevant theoretical researches, experimental works and practical applications are reviewed for cable vibration suppression as below.

Cable-stayed bridges are competitive for spans in the range 200 meters to 1100 meters, (and beyond) thus covering approximately 90% of the present span range (Krenk, 2000). The cables usually weight 100kg per meter (Caetano, 2007), thus a typical long cable of 200 meters could weight about 20 tons. The structural system of cable supported bridges consists of four main components: the stiffening girder (or truss) with the bridge deck, the cable system supporting the stiffening girder, the towers (or pylons) supporting the cable system, and the anchor blocks (or piers) support the cable system vertically and horizontally or only vertically at the extreme ends (Caetano, 2007).

Many applications of stay-cable for bridges can be found in the world. Two examples introduced previously are presented here. The Øresund Bridge, presented in Figure (2.1a), is nearly sixteen kilometres long, between Sweden and Denmark (Peeters et al., 2009). This famous stay-cable bridge also can be an application example to use tuned mass dampers for vibration suppressions. Another example of using semi-active dampers is Shandong Binzhou Yellow River Bridge in China, which was put into use in 1974 and rebuilt in 1984 with forty magnetorheological fluid dampers to suppress possible vibration shown in Figure (2.1b).

(a)

(b)

Figure 2.1: Examples of cable-stayed bridges. (a) The Øresund Bridge (Peeters et al., 2009), and (b) Shandong Binzhou Yellow River Bridge (Ou, 2003).

Stay cables are important in securing the safety of the entire structure (Main and Jones, 2002). However, the resonance of cables will cause large-amplitude vibrations due to their low inherent damping, typically 0.1% of the critical damping structure (Main and Jones, 2002). So, unless suppressed, external disturbances and dynamic loads on cables either from

wind, rain etc., or minor motion on the supporting ends on deck and towers due to the vehicle or even severe earthquake, etc., will lead to large-amplitude vibrations. Excessive vibration may cause fatigue and decrease durability, which reduces the overall safety of bridges.

Researchers and engineers have tried various methods to improve the cable dynamic properties, and many methods are proved to be effective to some extent. Typically, the most commonly used methods include, e.g., to treat the cable surface with different techniques in order to improve the aerodynamic properties (Flamand, 1995); to use bind several cables together (Langsoe and Larsen, 1987); or to provide mechanical vibration absorbers(Gimsing and Georgakis, 2011). However, each method has its own advantages and limitations.

Experiment in a wind tunnel has proved that cable surface treatment method has some advantages, e.g., effective over a wide range of wind speeds and performs even better at high wind speeds; generally cost-effective and demands little maintenance effort; easily implemented in the field and thus can be designed to be aesthetically pleasing; and also active in the sense that it reduces the energy input from the moving air (Sarkar, 1999). But, this method is not able to deal with vibration caused by minor motion on the supporting ends. Besides, a direct relationship has not been found between the surface treatment and the improved cable aerodynamics performance yet. Therefore, these uncertainties make it extremely difficult to design a suitable or optimum treatment.

Using crossing-ties to bind several cables together, can enhance the cable reducing the effective length by adding constraints on each cable and thereby avoid resonance (Caetano, 2007). They also somewhat increase cable damping (Lankin et al., 2000). The drawbacks include that crossing-ties are too obvious that may conflict with original aesthetics of the bridge (Pacheco et al., 1993). Hence, they could easily fatigue and wear out comparing with other methods.

The vibration of stay cable due to moderate wind, sometimes in conjunction with light rain, has been observed with increasing frequency in recent years. This problem is not new and has been studied extensively over a period of several decades. However, gaps still remain in our understanding of the problem. With a growing inventory of cable-stayed bridges and development of new application techniques, there is a significant increase for reporting large amplitude cable vibrations. Some structures have been retrofitted to mitigate these vibrations.

Cable-stayed bridges under design and construction are currently incorporating dampers, cross-ties, and/or aerodynamic surface treatments into the cable system.

The cables of a cable-stayed bridge are made by winding together strands or wires of materials like steel or Fibre-Reinforced Plastic (FRP) (Tang and Yan, 2018; Hanselka and Hoffmann, 1999). Some materials, e.g., FRP are popularly used for cables because of their lightness, flexibility and also low damping characteristics. However, they are excited easily and can oscillate severely when subjected wind. Cable vibrations are generated depending on different factors and phenomena. The cable vibrations are coupled with the vibration of the bridge deck and pylon towers. So, it is the vibration occurring on the cables which primarily induces vibration on the other structural members of the bridge. The different wind-induced vibrations are included as follows.

Aerodynamic galloping is a type of galloping due to wind effect, referring to the wave-like motion of elongated bodies, which are not aerodynamic in shape (bluff bodies). In the case of a cable-stayed bridge, the bluff body is usually the bridge deck. So aerodynamic galloping is the oscillation of bridge deck when acted upon by wind. It is a low-frequency situation and therefore does not create an adverse effect usually.

Wake galloping is the vibration of the bridge deck induced due to the wake effect formed between cables. When the wind is acted on two cables, which are spaced close to each other, a force or wake effect is developed between the cables. Under the action of this force, the cables tend to rotate in opposite directions which induces torsional oscillations. This vibration is transmitted to the bridge deck, which in turn causes galloping effect on the deck.

Buffeting is the sudden instability occurred due to shock wave oscillations or air flow separation created when two objects strike each other. The sudden impact of a seismic load or dynamic load leads cables to strike one another. This sudden shock induces vibration on the whole structure. Buffeting is a high-frequency phenomenon.

Vortex shedding occurs when air flows past a slender and tall body at certain velocities, an oscillation is experienced. This oscillating force is called vortex shedding. In the case of a cable-stayed bridge, pylons are prone to experience this effect. When wind flows past the pylon, low-pressure vortices are formed on the downstream side of it. This vortex force will be likely to move the pylon from side to side. If the vortex shedding frequency becomes

equal to the resonance frequency of the structure, the whole structure will vibrate with harmonic oscillations. Vortex shedding is a higher frequency phenomenon and it depends mainly on the size and shape of the pylon.

Fluttering is an unstable vibratory motion of the structure due to the coupling between elastic deformation of the structure and the aerodynamic force acted on it. Fluttering occurs due to the combined effect of bending and torsion. Long span bridges like suspension bridge and cable-stayed bridges are more prone to fluttering because of their high ratio value, i.e., the depth of structure parallel with the wind to the least lateral dimension.

Resonant buffeting occurs in bridges with parallel planes of cables. This phenomenon happens mainly due to the wake effect formation between the cables. Wind striking the upwind and downwind portions of the cable with a time delay induces the whole cables to move laterally.

Many researches have been carried out for investigating stay cable vibration induced with different winds and external disturbances. Although the exact excitation mechanisms are rather complex, but possible causes include aerodynamic forcing on the cables such as galloping (Den Hartog, 1933; Macdonald and Larose, 2006), wake galloping (Tokoro et al., 2000), rain–wind excitation (Hikami and Shiraishi, 1988; Matsumoto et al., 1990) and excitation from deck or pylon motion (Lilien and Pinto, 1994; Macdonald, 2016). It has been commonly accepted that large cable vibrations are more often caused by aerodynamic forcing which introduces aeroelastic instabilities. Several studies carried out to understand this dynamic behaviour, are typically reviewed as below.

Furthermore, the largest problematic cable vibrations are rain-wind induced vibrations and inclined cable galloping (Zuo & Jones, 2010). These mechanisms can be characterised by negative aerodynamic damping. Hence to mitigate them, sufficient positive structural damping is required. If the total damping is negative the vibrations grow exponentially from very small initial vibrations, whereas if the total damping is positive any vibrations decay exponentially. Hence, it is not a matter of the amplitude of the vibrations but the total damping, which governs the dynamic stability. Therefore, providing sufficient structural damping is important for preventing these types of vibrations. This is also in agreement with existing guidelines which specify the minimum damping level required.

The current guidelines on stayed cable specify the requirements of damping systems in terms of the damping ratio (or logarithmic decrement or Scruton Number, which are proportional to damping ratio) (SETRA, 2002; Caetano, 2007; Post-Tensioning Institute, 2012). Also damping ratio affects both the amplitude of vibrations due to buffeting or vortex shedding and the critical wind speed for the onset of aeroelastic galloping and rain-wind-induced vibrations (Post-Tensioning Institute, 2012), as well as the critical amplitude of deck vibrations to cause parametric excitation (Lilien and Pinto, 1994; Macdonald, 2016). Moreover, Zuo and Jones (2010) observed large amplitude vibrations of various cables due to rain-wind excitation and similar vibrations in dry conditions up to the sixth mode, whereas Acampora et al. (2014) identified significant vibrations in the first five modes.

For cable dynamics modelling, linear two-dimensional motion models are used in most cases, by neglecting the effect of inclination and sag of the cable. There are a few methods in building the cable model together with the absorber. Galerkin's methods are a class of methods which can simplify a continuous operator problem, for example converting a partial differential equation to a set of discrete problem. This method is introduced (Pacheco et al., 1993) to simplify the partial differential equation of stay cable into a series of ordinary differential equations. However, a very large member of DOFs is required to reach a relatively accurate result, since this method can reach the exact solution only with infinity DOFs, theoretically.

Krenk and Nielsen's modelling method (Krenk and Nielsen, 2002) provides the full solution for the lower modes which is then evaluated numerically. An explicit approximate solution for both taut cables and shallowed cables are provided, giving the modal damping as well as the optimal tuning of the damper. Although rather accurate analytical approximation can be obtained, generalising recent results for a taut cable, this method has a disadvantage that it cannot reach the exact solution for different configurations since it is only suitable for viscous damper only.

Being independent of the damper coefficient, Main and Jones (2002) provided a method using expression for the eigenvalues which is derived giving the range of attainable damping ratios and corresponding oscillation frequencies in every mode for a given damper location. This formulation reveals the importance of damper-induced frequency shifts in characterising the response of the system. It has benefits in reaching the accurate results

without approximation. But, it requires solving partial differential equation, and the boundary conditions varies for different absorber locations and structures.

However, considering the more realistic situation that cables in cable-stayed bridges are under three-dimensional parametric excitation, nonlinear inclined cables with small sags under such situation were also studied with a Finite Element model (Xu and Yu, 1998; Ouni et al., 2012).

2.2 Vibration control and applications

Vibration control techniques have been an attractive research topic for many decades. Various techniques have been proposed to isolate or suppress unwanted vibrations, which may lead to human discomfort or structure damage. In this section, vibration control techniques, applications and researches, particularly for stay cables, are reviewed in the categories of passive, active and semi-active control respectively.

2.2.1 Active and semi-active control

In order to suppress cables from excessive vibrations, various passive, semi-active, or even active absorber have been invented.

Theoretically, by using external power sources, active vibration absorbers are able to more effectively suppress multiple resonance with unknow frequencies (Ou, 2003). Some experimental studies have also shown that active (Tseng and Hrovat, 2015) and semi-active (Karnopp et al., 1974; Hrovat, 1983; Christenson et al., 2001; Jalili, 2002) control techniques usually provide better performance than traditional passive absorbers.

The active control system requires a large power source for actuators to generate a force to resist the unwanted motion. As active controllers are able to provide the real-time optimal control force according to the sensed feedback information for obtaining the best overall performance, they have attracted attention from both researchers and engineers for some civil engineering applications.

It has been theoretically proved that active vibration absorbers are more capable to suppress multiple resonances. The simulation study showed that active dampers are more capable to suppress multiple resonances with unknown frequencies because a superimposed

negative stiffness force can shape damping force (Wang et al., 2014). Also, feasibility studies of active control of cable-stayed bridges were carried out (Yang and Giannapolous, 1979; Ni et al., 2001). Simulation results showed that seismic response can be significantly reduced by the implementation of active mass drivers using only a few dominant modes in the control design. However, active control systems are normally expensive, not reliable enough and cost-effective, because they require an external power source, which is difficult to be supplied and maintained especially in extreme conditions such as power failure. Therefore, the development of active control is still at its early stage for cable vibration control.

A semi-active control system can be defined as a system which typically requires a small external power source for operation (e.g., a battery) and utilises the motion of the structure to develop the control forces, the magnitude of which can be adjusted by the external power source. Unlike active control, semi-active systems do not need energy input and hence is unconditionally stable but with performance worse than active control systems. Experimental study verified that semi-active vibration absorbers are also able to provide much higher supplemental damping of stay-cables than passive damper (Christenson et. al., 2001).

Although significant benefits of active and semi-active controllers have been proved by both theoretical and experimental studies, for the application of stay-cable vibration suppression, passive absorber is more widely used due to their reliable and simple structures, and also easy maintenance. So far, passive absorbers still are more cost-effective compared with active or semi-active absorbers in practical applications for suppressing stay-cable vibrations.

2.2.2 Passive control

Although active control provides the best performance as it can adjust the control force in real time, it typically requires large energy and maintenance cost. While, due to the relatively simple structure and low cost in terms of size, weight and maintenance, passive techniques are still dominant in most application cases currently.

In most studies, passive dampers, including viscous damper, tuned inerter damper, etc., are installed with one end on the deck and the other end connected to the cable at a distance

of approximately 2 ~ 4% of the total cable span length starts from the support on the deck (Gimsing and Georgakis, 2011). While hanged dampers with a secondary mass, such as tuned mass dampers (TMDs), can be located at any position on the cable. Previous studies showed that (Koo et al., 2004; Fisco and Adeli, 2011; Pinkaew and Fujino, 2001) passive absorbers are not as effective as active or semi-active dampers. However, with the invention of inerter and usage of force-current analogy (Smith, 2002), mechanical circuits can be translated to classical electrical circuits in a completely analogous way. Meanwhile, inerter can provide large inertance with only small amount of mass. So the invention of inerter may allow engineers and researchers to develop more beneficial inerter-based passive absorbers compared with conventional viscous dampers.

It was showed (Pacheco et al., 1993) that an optimal damper size exists and a "universal" design curve was developed to facilitate the design of passive dampers for stay cables. Transverse passive viscous dampers have been applied to the cables on many cable-stayed bridges. However, the damper location is typically restricted to be close to the bridge deck for aesthetic and practical reasons. For longer bridge cables, passive dampers cannot provide enough supplemental damping to eliminate vibration effects without significant changes of the structure.

The problem of the optimal damping constant of a viscous damper located close to one end of a taut cable was studied by some researchers, e.g., by Pacheco et al. (1993), Cardenas et al. (2008), Xu and Yu (1998), etc. The results (Pacheco et al., 1993) showed that the maximum normalised damping ratio that could be obtained by a concentrated viscous damper, which would be about half the relative distance of the damper from the support. Due to the constraints, e.g., space, if the distance of damper from the end support is reduced to half, optimal damping for Mode 1 will be obtained by doubling the damper size. Meanwhile, when the damper is close to a support, an approximate value of the optimal external damping constant for the lower modes of vibration is also found.

Due to their stability, reliability, robustness and easy maintenance, passive absorbers are more preferred for civil engineering applications to suppress vibrations. Two types of passive control are reviewed more concisely, i.e., viscous damper and tuned mass damper (TMD). Some vibration suppression devices incorporating inerter are also discussed and reviewed here, considering their potentials for applications.

2.2.2.1 Viscous dampers

Viscous damper is one of the suitable structures which are thoroughly studied to suppress cable vibrations. Several researchers have proposed passive control of cables using viscous dampers attached transverse to the cables. Viscous damper is considered ideal as a linear damping device, in which its force is exactly proportional to the relative velocity between its two ends. Many application examples of cable with viscous damper used in cable-stayed bridges, showing fluid viscous damper is an efficient way to suppress cable vibration (Pacheco et al., 1993; Duflot and Taylor, 2008). Normally, the viscous damper is installed with one end on the deck and the other end connected to the cable at a distance of approximately 2~ 4% of the total cable span length starts from the support on the deck A typical structure of these viscous dampers is presented for practical application, illustrated in Figure (2.2a). Totally 160 dampers are installed on Waldo Hancock Bridge, shown in Figure (2.2b) (TERATEC Inc., 2018).

(a) (b)

Figure 2.2: Viscous damper and its installation. (a) Structure of absorber (TERATEC Inc., 2018) and (b) cable dampers installed on Waldo Hancock Bridge (TERATEC Inc., 2018).

Many studies have been carried out for investigating viscous dampers applied in cable vibration suppression, here, several of them are typically reviewed as below.

Carne (1981) was one of the first to study the vibrations of a taut cable with an attached damper. He developed an approximate, analytical solution by obtaining a transcendental

equation for the complex eigenvalues and an approximation for the damping ratio for the first mode as a function of the damper coefficient and location. The study showed that to suppress vibration of a particular mode, the viscous damper is most effective if it is located at the anti-node of that mode.

Pacheco et al. (1993) formulated a free-vibration problem using Galerkin's method with sinusoidal functions of an undamped cable as mode shapes, and several hundred terms were required for an adequate convergence of the solution. This work also introduced non-dimensional parameters to develop a "universal curve"(shown below as Figure 2.3) where a "normalised damping ratio" is adopted as $\zeta_i / (x_c/L)$. The universal curve is useful and applicable in many practical design situations. Moreover, a basic study of the influence of cable sag is also included.

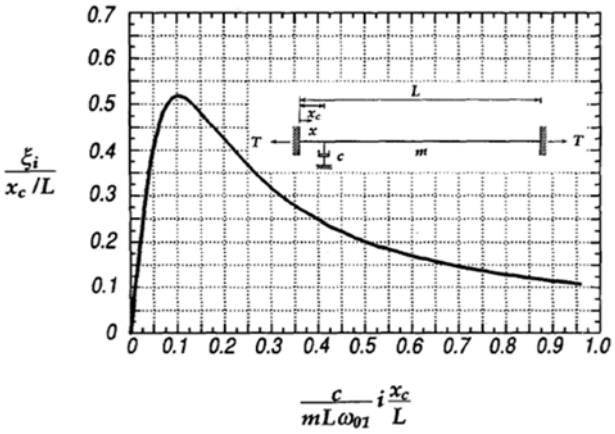

Figure 2.3: Universal curve from Pacheco et al. (1993) rating modal damping ratio ζ_i with damping coefficient c, location x_c, mode number i, and cable mass per unit length m, cable length L and the first mode circular natural frequency of ω_{01}.

Krenk (2000) and later Krenk and Nielsen (2002) developed an exact analytical solution of a free-vibration problem for a taut cable, and by using an iterative method, obtained an asymptotic approximation for the damping ratios for all modes for damper locations near the end of the cable.

Main and Jones (2002) similarly discussed a horizontal cable with a linear viscous damper theoretically, using analytical formulations of a complex eigenvalue problem. They discussed the theoretical solutions and the physical situations that those solutions represent.

In addition, they pointed out the importance of damper-induced frequency shifts in characterising the response of the cable-damper system.

Based on the previous researches, the dynamics of the cable with viscous damper have been well investigated. According to the "universal estimation curve", the viscous damper cannot provide enough damping ratio for all six modes if the damper is too close to one end. But if the absorber device is too far away from one end, it will not only influence aesthetics, but also make the installation and maintenance more difficult.

2.2.2.2 Tuned Mass Dampers

The concept of the tuned mass damper (TMD) dates back to the 1920s. TMDs can provide frequency-dependent properties (by tuning its parameter values). It consists of a secondary mass with properly tuned spring and damping elements. Compared with those conventional mechanical dampers, tuned mass dampers are relatively new countermeasures for stay cable vibrations.

Some studies were carried out for investigation on TMD, including its location and scale, etc., both theoretically and experimentally. For example, Tabatabai and Mehrabi (1999) reported an experimental investigation on TMD performance.

Andersson et al. (2013) made a comparison showing that a TMD located at 40% distance from the support is more efficient than a viscous damper located very close to the support. The tuned mass dampers have been recommended for full-scale implementations for two major reasons. First, the TMD is observed to be more efficient than other countermeasures in damping out the free vibration. Second, the TMD can be physically installed at any location along the cables (but the efficiency is different at each location).

The other types of mechanical dampers are usually limited to the cable ends, and their effectiveness cannot be fully realised. The limitation of tuned mass damper is difficult to install as they locate far away from one end. Besides, performance of TMD is limited by the amount of mass that can be added to the cable, usually, mass ratio between the secondary mass and cable might not be large enough. Besides, a so-called "hybrid damper system", which combines a viscous damper and a TMD, can overcome the shortcoming of single damping system and mitigate undesired cable vibration (Cu and Han, 2015).

2.2.2.3 Vibration suppression device incorporating inerters

It has been reviewed that adding passive viscous absorbers to cables is the most commonly used method for vibration suppression. Tuned mass dampers (TMDs) are another type which can be more effective than viscous dampers if they are fixed at the same location along the cable, but they may have to require a relatively large secondary mass in order to be beneficial. An alternative is to use a vibration suppression device incorporating an inerter.

By introducing the concept of the inerter, the theory of network synthesis can be extended in its application from electrical systems to mechanical systems (Smith, 2002). Mechanical network synthesis provides a methodology for investigating highly-complex mechanical systems (Papageorgiou and Smith, 2005; Wang et al., 2009a, b). The inerter was proposed as an ideal two terminal mechanical element (Smith, 2002), with the property that the applied force is proportional to the relative acceleration between its two terminals. The inerter has fundamentally enlarged the range of absorbers that can be realized mechanically. Furthermore, via gearing, the inertance (i.e., the constant of proportionality between the relative acceleration and force, with dimensions of mass) can be much larger than the physical mass of the device.

Performance advantages of the vibration suppression device incorporating an inerter have been identified for road vehicles (Smith and Wang, 2004; Jiang et al., 2015a), railway vehicles (Wang et al., 2009a, b, 2012; Jiang et al., 2015b), aircraft landing gear systems (Liu et al., 2015; Li et al., 2017a,b), and civil engineering structures (Ikago et al., 2012; Lazar et al., 2014; Makris and Kampas, 2016; Yang, 2016; Zhang et al., 2017; Bakis et al., 2017).

For experimental and innovative use of inerters, following current trends of performance-based design, an optimum tuned mass damper inerter (TMDI) design framework with uncertain structure properties and seismic excitation is built with the help of analytical and simulation-based tools (Giaralis and Taflanidis, 2018). Inerters are also used as vibration absorber in robots. A biped robot with inerters, springs and dampers at its ankle shows a more excellent walking when compared with traditional ones without such optimisation (Hanazawa et al., 2011).

The potential benefits of adding a Tuned Inerter Damper (TID) system has been analysed by Lazar et al. (2016) for suppressing cable vibration. A practical tuning

methodology for the TID was proposed to minimise the displacement amplitude at the mid-span of the cable for excitation from motion of both supports. Furthermore, Lu et al. (2017) examined the damping enhancement potential of a viscous inerter mass damper (VIMD) system. Significant improvement of the achievable damping ratio over that of a conventional viscous damper was found. Both of these previous investigations on this topic were focused on specific network layouts (i.e. topological connections of spring, damper and inerter elements), although many alternative layouts exist. Further study was carried out on three-element damping layouts with optimisation results considering a constraint regarding the performance in higher modes, showing that the identified beneficial inerter-based vibration absorbers can enhance damping performance over multiple cable modes significantly (Luo et al., 2017).

2.3 Inerter and network synthesis in mechanical systems

Network synthesis is a general technique that can be used for passive, semi-active and active control. In this section, the theoretical research work on network synthesis is reviewed firstly. A complete summary for analogy between the electrical and mechanical systems is presented. From engineering viewpoint, recent research interests on the realisation of biquadratic transfer functions with minimum elements haven been also reviewed. Particularly, Fixed-sized inerters, which to limit size and weight for constraints in terms of more realistic physical implementation, are reviewed and introduced.

2.3.1 Analogy between electrical and mechanical systems

To apply the electrical network analysis to the mechanical structure, an analogy between the electrical and mechanical domains has been investigated by some researchers. The first was the force-voltage analogy in 1907 (Poincare, 1907). An alternative force-current analogy was then proposed by Firestone (Firestone, 1933), this analogy preserves the topology of the elements in the network. As shown in Figure 2.4, for a one-port electrical network, the force-current analogy can be set up by the following correspondences, i.e.,

Electrical ↔ Mechanical

current (I) ↔ force (F)

voltage (V) ↔ velocity (v)

electrical ground ↔ mechanical ground

electrical energy ↔ kinetic energy

magnetic energy ↔ potential energy

inductor (L) ↔ spring (k)

resistor (R) ↔ damper (c)

grounded capacitor (C) ↔ mass (m)

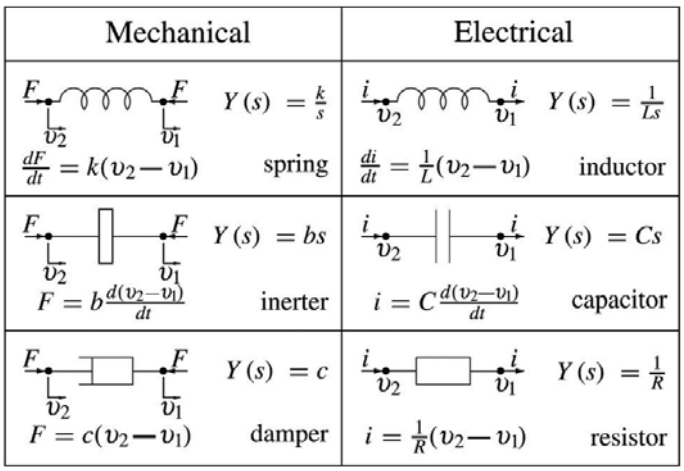

Figure 2.4: Electrical and mechanical symbols and correspondences (Smith 2002).

It should be noticed that one terminal of the mass is always grounded, implying that the electrical analogy to a mass is a grounded capacitor. In order to establish the analogy between electrical and mechanical systems, Smith introduced a new mechanical device, i.e., inerter (Smith, 2002).

The inerter is a mechanical two-terminal device with the property that the exerted force is proportional to the relative acceleration between its two terminals. This force F can be represented by $F = b(\dot{v}_2 - \dot{v}_1)$, where b is the inertance with unit of kg, and v_1, v_2 are the velocity of the corresponding terminals. The introduction of the inerter completes the force-current mechanical-electrical analogy with springs, inerters and dampers corresponding to

inductors, capacitors and resistors, respectively, as shown in Figure 2.4. This makes that all the positive-real mechanical transfer functions can be realised by the passive mechanical networks consisting of springs, inerters and dampers by using the network synthesis procedure.

Although transfer function is most commonly-used in control theory, however, sometimes it is also convenient to use other terms to refer to a complex number which may be either the impedance (e.g., ratio of voltage to current in electrical circuits), or the admittance (e.g., ratio of current to voltage) of a system. Throughout this thesis, these terms are often used in the introduction and literature review of the first two chapters, while admittance function are most frequently used in the present study.

2.3.2 Structure and characteristics of inerter prototypes

Three prototypes of inerter have been proposed, i.e., rack-pinion inerter (Smith, 2002), ball-screw inerter (Chen et al., 2009) and fluid inerter (Swift et al., 2013), which are shown in Figure (2.5a), (2.5b) and (2.5c) respectively. However, an important feature of all these designs for the different inerter prototypes is that they can provide much larger inertance than their real mass because of the gearing generated by the mechanism.

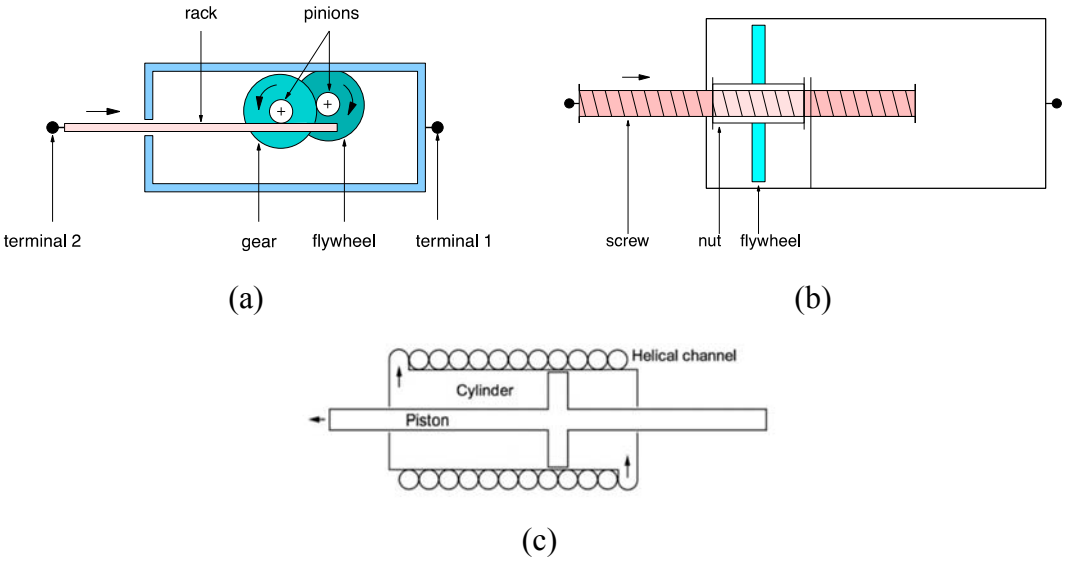

Figure 2.5: Different inerters. (a) Rack-pinion inerter, (b) Ball-screw inerter, and (c) Fluid inerter (Swift et al., 2013).

As shown in Figure (2.5a), rack-pinion inerter consists of rack, gear, pinions and flywheel, which drives the flywheel by the plunger sliding. It has been employed in Formula one racing cars in 2005 under the name of J-damper (Cambridge University, 2008).

Ball-screw inerter can be formulated using the mechanism shown in Figure (2.5b), which transforms the translational motion to the rotational one. A ball-screw inerter has been made in the University of Bristol with the real mass of 2.5kg and the inertance of 70kg, almost 30 times of the mass itself. However, such inerter prototypes may suffer low durability due to the gearing, especially under large periodic forcing. The fluid inerter was introduced in (Swift et al., 2013), which may have the ability to counter this problem.

Fluid inerters were experimentally studied by some researchers, e.g., by Swift et al. (2013). From its mechanism shown in Figure (2.5c), it can be seen that when an external force applied to the inerter, the inner piston moves, pushing the encased liquid in the external thin helical channel, from one side of the cylinder to the other. The inertial force is generated by the mass flow of liquid through this channel. Gearing is provided through the choice of channel diameter and length. The inerter considered to generate a purely inertial force may be referred to as an ideal inerter. However, in practice, some nonlinear effects affect the device behaviour. So, several modelling studies considering these effects have been proposed and experimentally tested, with the aim of capturing the nonlinear nature of the inerters, respectively reviewed as below.

The nonlinear effects, e.g., friction, backlash and elastic effect, etc. were experimentally studied (Wang and Su, 2008; Gonzalez-Buelga et al., 2016; Li et al., 2012). To investigate the nonlinear effects on the inerter-based vibration suppression device, the performance of the TID device using an off-the-shelf inerter has been experimentally tested, showing that with appropriate retuning of the components in the TID device, the TID incorporating the real inerter device is close to the ideal inerter device (Gonzalez-Buelga et al., 2016).

With the introduction of the inerter, various types of vibration suppression devices are expanded and the possibility to obtain the controller providing the superior performance can be enlarged. By selecting the fixed-structure inerter-based networks as candidate layouts, performance improvement of various mechanical systems have been identified, such as automotive (Smith and Wang, 2004), railway vehicles (Jiang et al., 2011, 2015b; Wang and

Liao, 2010a) and buildings (Lazar et al., 2014; Ikago et al., 2012; Marian and Giaralis, 2014; Wang et al., 2010b; Krenk and Høgsberg, 2016).

With the electrical mechanical analogy introduced in Section 2.3.1, new possibilities for mechanical device design are available and have been applied to a wide range of systems (Wang et al., 2009a, 2009b; Zhang et al., 2017). Apart from pure mechanical absorbers, mechatronic designs, which enables the controller's immittance to be realised through a combination of mechanical and electrical networks, have also been proposed and proved to be beneficial (Wang and Chan, 2011b; Pires et al., 2013; Gonzalez-Buelga et al., 2015).

2.3.3 Network synthesis

As a commonly used technique, network synthesis has been successfully applied in electrical system design for nearly one century. Due to the introduction of inerter, the network synthesis theory has extended its application from electrical systems to mechanical systems. Many theoretical contributions were made in early time focusing on the realisation of positive-real transfer functions with electrical elements, e.g., from Forster (Foster, 1924) in 1924 to Bott-Duffin (Bott and Duffin, 1949) in 1949, focusing on the realisation of positive-real transfer functions with electrical elements. For a given impedance *Z(s)* which exists and is real-rational meanwhile, all these approaches were investigated for a two-terminal network, i.e., current i and voltage v, shown in Figure 2.3 (Smith, 2002).

The synthesizing networks approach from a given transfer function was firstly proposed by Foster, indicating that a transfer function with a certain property can be realised with an electric network built by using two of the three elements, i.e., resistors, inductors and capacitors. The realizability of such a function as the driving-point immittance of electrical networks consisting of inductors and capacitors only was established in Fosters Reactance Theorem (Foster, 1924).

Afterwards, Brune carried out the study for the networks consisting of all types of three elements, i.e., resistors, inductors and capacitors, (Brune, 1931) and concluded that the network is passive if and only if its impedance function *Z(s)* is positive-real. The necessary and sufficient conditions for an immittance function to be positive-real was also provided in (Brune, 1931). Many similar investigations were carried out for deriving the equivalent

condition for positive-realness and well summarised in (Chen and Smith, 2009), also showing that any positive-real function can be realised with a two-terminal network comprising resistors, capacitors, inductors and transformers. The network realisations were used to be represented as the Brune cycle.

Two decades later after Brune's synthesis approach, the further relevant studies showed that transformers are unnecessary in the synthesis of positive-real functions (Bott and Duffin, 1949), meaning that any positive-real functions can be realised only with capacitors, inductors and resistors. While transformers can be eliminated from Brune cycle, e.g., by using of Richards's transformation (Richards, 1947).

Same as the Brune's synthesis, Bott-Duffin procedure also begin with Foster Preamble (Van Valkenburg, 1962; Storer, 1957), i.e., extracting poles and zeros on the imaginary axis or at infinity, along with a constant less than or equal to the minimum value of the real part of the positive-real function, in order to obtain a "minimum function" (Seshu, 1959). Many studies have been carried out for realisation of biquadratic impedances, with minimum set of elements, e.g., to derive the necessary and sufficient realisability condition (Wang et al., 2012). Comparatively, for a given positive-real function, the realisation by using the Bott-Duffin procedure may need more synthesis steps than Brune's approach. This may result in a much larger number of elements required.

Some studies showed that, it is more difficult for high-complexity mechanical structure systems to be implemented in practice in most cases. Hence, minimising network complexity is important for practical applications. Studies showed that high-complexity configurations of inerter-based vibration absorbers are more difficult to be physically implemented and applied in the case of long-stay cables of bridge for vibration suppression, with difficulty for maintenance for example. Recent experimental studies showed that for inerter prototypes that larger inertance implies more difficulties in terms of physical implementation. These difficulties include space and weight constraints in mechanical structures, as well as extra wear and parasitic damping that large inertance may cause.

Since the number of possible layouts goes up exponentially corresponding to the increase of each number of structure elements, and due to the increased difficulty for choosing optimum absorber configurations, network synthesis can be an efficient approach for the present study, i.e., identifying optimum layouts in a systematic way.

The difficulty for the identification of these configurations lies in the fact that, according to graph theory, the number of possible absorber layouts goes up exponentially with the increase of element number (Riordan and Shannon, 1942). In addition, researches showed that larger inertance implies more difficulties in terms of physical implementation because physical realisations of inerter is either via mechanical gearing (Smith, 2002; Papageorgiou and Smith, 2005; Lazarek et al., 2018) or hydraulic gearing (Wang et al., 2011a; Swift et al., 2013; Liu et al., 2018), and both methods can only achieve a limited range of inertance to mass ratios. Some significant works have been carried out to reduce the element number required, and most of them focused on the realisation of biquadratic transfer functions due to the fact that most engineering mechanical problem can be represented by a biquadratic function effectively. Typically, a biquadratic transfer function is expressed as,

$$Z(s) = \frac{As^2 + Bs + C}{Ds^2 + Es + F}. \tag{2.1}$$

For the realisation of "biquadratic minimum functions", i.e., a biquadratic function that is minimum, it was proved in (Seshu, 1959) both that at least two resistors are required without the use of transformers and that seven elements are generally required, except for specific cases where a five-element bridge network is needed. According to (Pantell, 1954), the seven-element realisations were identified to be the modified structure of the Bott-Duffin realisation. Hence, it was concluded that for any given positive-real biquadratic function, eight elements are required for the realisation, i.e., with one resistor to reduce a positive-real function to a minimum function. However, Wang et al. (2012) had attempted to derive the necessary and sufficient realisability condition for realising biquadratic impedances with at most four elements.

It should be mentioned that Ladenheim firstly classified the simple RLC networks with up to two "reactive" (i.e. inductors and capacitors) and three "resistive" elements (Ladenheim, 1948), over one hundred networks were obtained by an enumeration method and various transformations. For each network, the realisability conditions were derived and expressed with the parameters *A, B, ..., F* in Equation (2.1). Although the study work is quite comprehensive but no complete summary of the results were presented, so it is still not clear

how many networks are required to cover the whole set of biquadratic realisable by the five-element two-reactive networks considered.

Later, a network containing one inductor, one capacitor and three resistors in the form of an unbalanced bridge with one of the reactive elements being in the cross arm of the bridge was investigated by Foster and Ladenheim (1964), the realisability conditions for the biquadratic were derived and it was shown that under certain conditions, the network can realise some functions that cannot be realised by the other five-element two-reactive networks. Besides, the realisation of the biquadratic with all the three-reactive five-element networks was studied (Ladenheim, 1964), where the realisability conditions and the corresponding element values were also provided. The investigation to realise the biquadratic by using all these series-parallel six-element networks with three reactive and four reactive elements also appeared in (Ladenheim, 1948; Foster and Ladenheim, 1963).

Basic frequency-response functions and their corresponding causal time-response functions of elementary inertia-elastic and inertia-viscous models are systematically summarised recently by Makris (2017) in which different layouts incorporating the inerter were presented and the relevant admittance functions were defined.

To be specific, for an inerter of limited size and weight, the maximum inertance provided is constrained by gearing ratio and the rotating weight (design of fly-wheel or external helical tube and liquid) depending on the type of inerter (Papageorgiou and Smith, 2005; Liu et al., 2018).

In order to limit the number of elements, and also size and weight, Fixed-sized inerter (FSI) layouts are introduced by Zhang et al. (2017) which can be realised by a seven-element network comprising four dampers, two springs and one inerter. It should be mentioned that FSI layouts also have the benefit that the inertance value of inerter can be controlled in a realistic range. The motivation for proposed FSI layouts is to investigate more different candidate configurations in a systematic way so as to facilitate the identification of beneficial absorbers with practical inertance values.

2.4 Summary

Based on over one hundred and fifty literature, including 149 published papers, 3 patents and also a few resources from the internet, this chapter reviews the literature relevant to the present study on the methodology and identification approach of inerter-based absorbers for cables vibration suppression, typically for long cables applied in cable-stayed bridges.

First, the structure of cable-stayed bridges and their cables are briefly reviewed and introduced. Also, the cable vibration mechanisms and different excitation sources are preliminarily analysed. Considering the potential applications of inerter-based absorbers in increased number of areas, the literatures on the structures and recent developments of inerter-based absorbers prototypes are also reviewed.

Focusing on the researches and applications for stay cables vibrations are mainly reviewed. To be specific, vibration control techniques for suppressing stay-cable vibration, including passive, active and semi-active control techniques, are reviewed respectively. For passive control, the researches and engineering applications of viscous damper, tuned mass damper and inerter-based absorber are mainly reviewed.

The literature review shows that passive absorbers are more preferred for civil engineering applications due to their stability, reliability and easy maintenance. On cable vibrations, damping ratio is still the most commonly used measure in previous research papers. Also, the first six modes should be considered for longer cables or cable in extreme forcing conditions.

Finally, the researches on network synthesis in mechanical systems are reviewed. For relatively complex inerter-based absorber layouts with more elements, network synthesis can be an efficient approach for identifying beneficial layouts in a systematic way. Besides, Fixed-sized inerter (FSI), along with its benefits to limit the weight and size of absorber devices for relatively practical, physical implementation, are reviewed and introduced. Since the number of possible layouts goes up exponentially corresponding to the increase of each number of structure elements, the difficulty for identifying optimum absorber layouts may increases. Therefore, FSI layouts can be adopted in the present study, to limit the number of elements, and to control the inertance in a realistic range meanwhile.

Chapter 3

Modelling and mathematical approach

The mathematical modelling and optimisation in the present study are for a comprehensive identification of optimum absorbers for suppressing cable vibration.

First, a few methods in building the cable model together with the absorber are introduced. Due to the advantages of finite element (FE) methods for investigating absorber-cable systems dynamics, both in terms of computational efficiency and accuracy, a lumped mass FE model of cable, with a generic vibration absorber represented by its admittance function, is established for the present study. In the modelling, all parameters for the absorber-cable system are non-dimensionalised. Three optimisation performance criteria are proposed to assess and qualify the effects of candidate absorber layouts. Some considerations in computation, e.g., properly selection of degrees of freedom and used computational tools in MATLAB software environment, are also described.

In this chapter, the mathematical approach for modelling and optimisation procedure used in the present study is presented and described in detail as below.

3.1 Introduction

In this section, two methods basically used in previous literatures for an absorber on a taut cable are mainly introduced. Firstly, the procedure of using Galerkin's method is reviewed. Then two different type of finite element methods are introduced. The effects

of lumped mass FE model and consistency mass FE models, are also justified for the present study.

There are a few methods in building the cable model together with the absorber. As the most commonly used numerical method for structural analysis, the Finite Element (FE) method can be used for investigating cable vibration. By using the idea of FE method, taut cable can be considered as a system consisting *n* unit masses, in which *n* tends to be infinity, on a massless cable under tension force. In general, both types of FE method are more accurate than Galerkin's method for limited degrees of freedom. One of the most important reasons is that the two FE methods can represent the discrete change in gradient of the cable (i.e. the kink), which is caused by the absorber force. Galerkin's methods are a class of methods which can simplify a continuous operator problem, for example converting a partial differential equation to a set of discrete problem. This method is introduced (Pacheco et al., 1993) to simplify the partial differential equation of stay cable into a series of ordinary differential equations. However, a very large member of DOFs is required to reach a relative accurate result, since this method can reach the exact solution only with infinity DOFs, theoretically. The method used refers to a class of weighted residuals, which is a class of approaches to simplify a continuous operator problem for solving differential equations, for example converting a partial differential equation to a set of discrete problems. However, Galerkin's method presents a set of sinusoid curves, which needs much more modes to present the kink. This could result in Galerkin's method less accurate than finite element method in the present study. Other methods intorduced by Krenk (2000) and Main and Jones (2002) requires nonlinear equations which is more difficult to solve and to incorporate the absorber. Moreover, the form of the equation is different for each different absorber layout so there is not a general analytical solution. While, the proposed finite difference form, with the absorber represented by a generic admittance function, has the benefits of the form of the matrix equation being the same for any absorber layout and a simple, consistent method can be used for its solution for the eigenvalues. By discretising the cable into a sufficiently large number of lumped masses, this formulation converges on the exact solution.

In principle, the number of DOFs n should be as great as manageable in order to minimise the error due to approximation. However, considering computational efficiency, suitable DOFs should be selected, so n has to be limited properly for the present study. Based on the comparison of results respectively using FE and Galerkin's methods, FE method is more suitable for present study, either in term of computation accuracy and efficiency, or more capable to exhibit the kink in the cable mode shape caused by the damper. Therefore, in this study, a FE model is used with properly selected degrees of freedom (DOFs), which will be discussed in Sub-section 3.4.2.

For modelling of cable and absorber, Krenk and Nielsen (2002) provided the full solution for the lower modes. An explicit approximate solution for both taut cables and shallow cables are provided, giving the modal damping as well as the optimal tuning of the damper. Although by using Krenk and Nielsen's modelling method, rather accurate analytical approximation can be obtained, this method has a disadvantage that it cannot reach the exact solution for different configurations since it is only suitable for viscous damper only.

Besides, Main and Jones (2002) provided a method using expression for the eigenvalues which is derived giving the range of attainable damping ratios and corresponding oscillation frequencies in every mode for a given damper location. This formulation reveals the importance of damper-induced frequency shifts in characterising the response of the system. It has benefits in reaching the accurate results without approximation. But, it requires solving partial differential equation, and the boundary conditions varies for different absorber location and structures.

Normally, large vibration of bridge cables are observed in the first few modes in practice. So, it should be sufficient to consider the first six modes here. Also, different cases are considered, including long cable or severe forcing conditions, e.g., for preventing the negative damping resulted from high-speed wind. Considering damping performance of the cable for the first mode and higher modes concerned, three optimisation measures for assessing and quantifying the effectiveness of absorber layouts are respectively proposed for the optimisation and identification in the study.

In this study, a new method is introduced for simplicity in calculation and versatility for different absorber layouts. An integrated cable model with admittance functions

representing absorbers is established, along with three optimisation measures to assess and quantify the effectiveness, for identifying optimum layouts. For balancing computation accuracy and efficiency, the lumped mass model rather than a consistent mass model is used here, with a properly selected degrees of freedom, introduced as below.

3.2 Cable model with an admittance function representing absorbers

In the present study, by using finite element method, an integrated cable model with admittance function representing absorber is built. The mathematical approach for modelling is described as below. Since the equilibrium condition is used for the present dynamic modelling and analysis, the tension force of cable resulted from the static load of the cable is not considered in the present study.

With an arbitrary linear passive absorber represented by an admittance function *Y(s),* and also neglecting the cable inclination, sag, out-of-plane motion and elasticity of the cable, a lumped FE model with n DOFs is built, as shown in Figure 3.1. The tension along the cable is denoted T, the total mass of the cable is M, and the total length of the cable is L. There are n masses, each of mass m spread along the cable and two masses of mass $m/2$ connected directly to the supports. Hence, $m = M/(n+1)$. These masses divide the cable into $n+1$ elements, each of length l equal to $L/(n+1)$. The a^{th} mass has an associated vertical position $x_a(t)$, which equals zero at equilibrium. The absorber is connected to mass a_f. Since the masses at the end-points are connected directly to the supports, x_0 and x_{n+1} always equal zero.

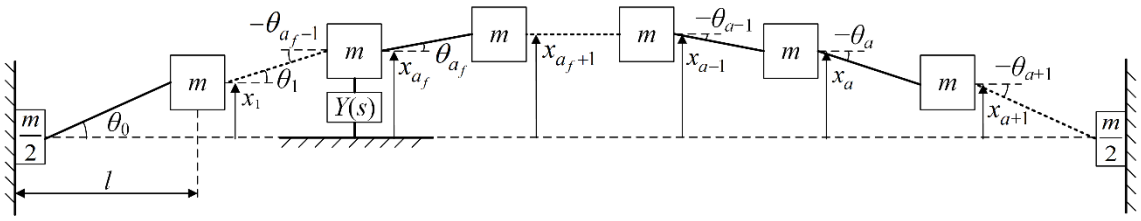

Figure 3.1: Finite element model of a taut cable with an admittance function of arbitrary absorber.

The displacement of the masses from their equilibrium positions leads to an angle θ_a between mass a and mass a+1. As the vertical displacements of each mass element $x_{a+1} - x_a$ are small compared to the element length $L/(n+1)$, so $\arctan\{(x_{a+1} - x_a)/[L/(n+1)]\}$ can be approximated using $\arcsin\{(x_{a+1} - x_a)/[L/(n+1)]\}$. Thus the angle θ_a can be presented as,

$$\theta_a = \arcsin\left(\frac{x_{a+1} - x_a}{L/(n+1)}\right) \tag{3.1}$$

The circular natural frequency of the first mode of the undamped cable can be expressed as (SETRA, 2002; Caetano, 2007),

$$\omega_0 = \pi\left(\frac{T}{ML}\right)^{0.5} \tag{3.2}$$

The equation of motion for mass a, without any external force, can be expressed as,

$$m\ddot{x}_{a_f} = T\sin\theta_{a_f} - T\sin\theta_{a_f-1}. \tag{3.3}$$

Similarly, the equation of motion for mass a_f, where the absorber is located, can be expressed as,

$$m\ddot{x}_{a_f} = T\sin\theta_{a_f} - T\sin\theta_{a_f-1} + F(t), \tag{3.4}$$

where $F(t)$ is the force provided by the absorber. By substituting Equations (3.1) and (3.2) into Equations (3.3) and (3.4), Equations (3.5) and (3.6) can be obtained as below,

$$\frac{1}{n+1}\ddot{x}_a = (n+1)\left(\frac{\omega_0}{\pi}\right)^2 (x_{a+1} - 2x_a + x_{a-1}), \tag{3.5}$$

$$\frac{1}{n+1}\ddot{x}_{a_f} = (n+1)\left(\frac{\omega_0}{\pi}\right)^2 (x_{a_f-1} - 2x_{a_f} + x_{a_f+1}) + \frac{F(t)}{M}. \tag{3.6}$$

Taking Laplace transforms on both sides of Equations (3.5) and (3.6), and assuming zero initial conditions, the following equation for each mass is obtained as,

$$\frac{1}{n+1}s^2\tilde{x}_a = (n+1)\cdot\left(\frac{\omega_o}{\pi}\right)^2 \cdot (\tilde{x}_{a-1} - 2\tilde{x}_a + \tilde{x}_{a+1}), \tag{3.7}$$

$$\frac{1}{n+1}s^2\tilde{x}_{a_f} = (n+1)\cdot\left(\frac{\omega_0}{\pi}\right)^2\cdot\left(\tilde{x}_{a_f-1} - 2\tilde{x}_{a_f} + \tilde{x}_{a_f+1}\right) + \frac{Y(s)}{M}\cdot s\cdot\tilde{x}_{a_f}(s), \qquad (3.8)$$

where tildes indicate Laplace transforms and $Y(s) = \tilde{F}(s)/\left[s\cdot\tilde{x}_{a_f}(s)\right]$ represents the admittance function of the absorber, which is defined as the ratio of force to velocity.

It has been shown that all admittance functions representing linear, passive absorbers are positive-real functions (Brune, 1931). By arranging the displacement of each mass in the vector $\boldsymbol{x}=[x_1, x_2, x_3, \ldots, x_n]^T$, Equations (3.7) and (3.8) can be rewritten in matrix form as,

$$\mathbf{M}s^2\tilde{\boldsymbol{x}} + \mathbf{C}s\tilde{\boldsymbol{x}} + \mathbf{K}\tilde{\boldsymbol{x}} = \mathbf{0}. \qquad (3.9)$$

In Equation (3.9), the elements of matrices **M**, **C** and **K** are respectively described in Equations (3.10) ~ (3.12), in which δ_{ij} is the Kronecker delta function.

$$m_{ij} = \frac{\delta_{ij}}{n+1}, \qquad (3.10)$$

$$c_{ij} = 0 \ \ except \ \ c_{a_f a_f} = -Y(s)/M\ , \qquad (3.11)$$

$$k_{ij} = (n+1)\cdot\left(\frac{\omega_o}{\pi}\right)^2\cdot\left(2\delta_{ij} - \delta_{i(j+1)} - \delta_{i(j-1)}\right). \qquad (3.12)$$

Complex eigenvalues of the system, represented by $[\lambda\ \ \lambda^{*T}]^T$ (the superscript * refers to the complex conjugate), are calculated as roots of Equation (3.13), where $\boldsymbol{\lambda} = [\lambda_1\ \lambda_2\ \lambda_{3....}\ \ldots]$, **0** is the square null matrix of size n and **I** is the identity matrix of size n.

$$\det\left(\begin{bmatrix}\mathbf{0} & \mathbf{I}\\ -\mathbf{M}^{-1}\mathbf{K} & -\mathbf{M}^{-1}\mathbf{C}\end{bmatrix} - \begin{bmatrix}s\mathbf{I} & \mathbf{0}\\ \mathbf{0} & s\mathbf{I}\end{bmatrix}\right) = 0\ . \qquad (3.13)$$

It should be noted that **C** is a function of s, so the eigenvalues of the system cannot be found by conventional numerical methods. However, Equation (3.13) is still fundamentally valid, giving a polynomial in s, the roots of which are the eigenvalues. By using a similar FE model of a cable with a TID (Lazar et al., 2016), in which the internal DOF of the TID was explicitly represented in the matrix equation of motion, making the vector $\boldsymbol{x}(n+1)$ element long and the matrices **M**, **C** and **K** $(n+1)\times(n+1)$. Using that method,

the matrices need to be reformulated for each alternative absorber layout. The advantage of the current method is that a system with any passive linear absorber can be represented by equation of the same form as Equations (3.9) along with Equations (3.10) ~ (3.12), with **x** always being (is) n elements long and the size of matrices **M**, **C** and **K** are always $n \times n$. The only difference is the admittance function $Y(s)$ representing the absorber.

The roots of Equation (3.13), i.e., $[\lambda \quad \lambda^{*\mathrm{T}}]^{\mathrm{T}}$, are in complex conjugate pairs. The number of pairs is given by n plus the number of internal DOFs of the absorber. However, normally only a few pairs, representing low-frequency modes, are of interest. Either eigenvalue λ_e (with positive imaginary part, e = 1, 2, 3…) or its complex conjugate eigenvalue λ_e^* can be used to calculate damping ratio ζ_e and circular natural frequency ω_e of mode e of the damped cable, which respectively are (Thomson and Dahleh, 1997),

$$\zeta_e = -\mathrm{Re}(\lambda_e) / \sqrt{\mathrm{Re}(\lambda_e)^2 + \mathrm{Im}(\lambda_e)^2}, \tag{3.14}$$

$$\omega_e = \sqrt{\mathrm{Re}(\lambda_e)^2 + \mathrm{Im}(\lambda_e)^2}. \tag{3.15}$$

These exact expressions for the damping ratio and circular natural frequency are used here, rather than the common approximations $\zeta_e \approx -\mathrm{Re}(\lambda_e)/-\mathrm{Im}(\lambda_e)$ and $\omega_e \approx \mathrm{Im}(\lambda_e)$, since with the absorber the damping ratios can become relatively high so the approximations become inaccurate.

For observing mode shape of a cable with a viscous damper, a set of samples is examined. Obviously, for a cable of free vibration, i.e., with non-dimensional *c'* as zero, the real part shows a half sinusoidal curve, with imaginary part equals to zero. The mode shape in two other representative cases are shown in Figure 3.2, with the damper at 5% of the total length of cable. It can be seen that the real and imaginary parts of the mode shape at the location of the damper are of similar magnitude, but for damping coefficients far from the optimum the imaginary parts of the mode shape are small.

For cable with the damper which provides optimum damping ratio, the real part and imaginary part versus non-dimensionalised position along the cable, i.e., *x/L*, are shown in Figure (3.2a), here *x* is the distance along the cable. The obtained results presented in Figure (3.2a) fit with the previous results provided by Pacheco et al. (1993). While for

the case of cable with extreme large damper (here taking the non-dimensional *c'* as 1000), shown in Figure (3.2b), it can be seen from the real part that the damper can be considered as a fixed node at the cable, and the rest of the cable vibrates freely. The imaginary part shows a similar trend as Figure (3.2a), but with much smaller scale due to the large damper. Note that the example shows the first mode in each case. The half sine mode shape for the undamped cable is of course the first mode. There are of course many other modes, with integer numbers of half sines.

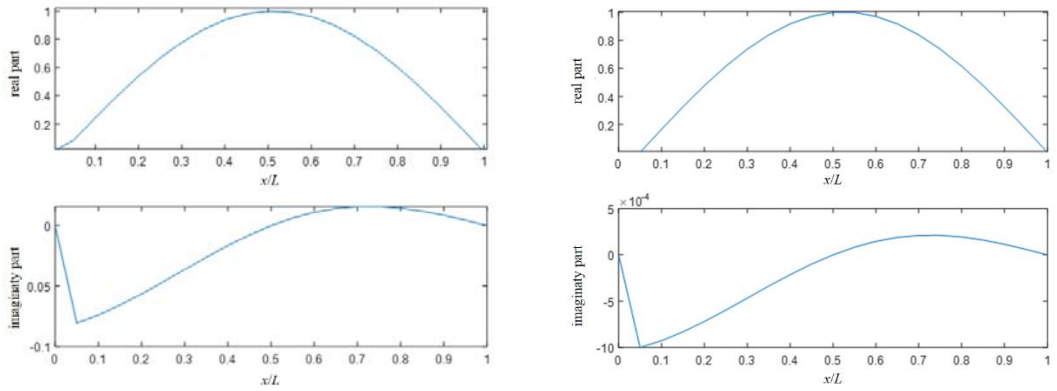

(a) (b)

Figure 3.2: Samples of mode shape of cable with viscous damper. (a) Optimised damper and (b) extreme large damper (*c'*=1000) versus non-dimensionalised position along the cable.

3.3 Performance measures

Three performance measures are introduced as examples in the present study to assess the damping performance of the absorbers for different cases, though some other performance measures can also be adopted with the methodology presented in this thesis. A potential cost function is the internal cable loads. However, as stated in Section 2.1, for the most problematic cable excitation mechanisms, they are governed by the total damping, so the key to preventing them is to provide enough structural damping. If the total damping is positive, the vibrations do not grow, so the amplitude, and hence the internal loads, never become significant. As the lowest frequency mode is often most

susceptible to vibrations (Gimsing and Georgakis, 2011), the first performance measure considers only the modes with natural frequencies close to the first mode of the undamped cable, without considering higher frequency modes. However, long cables or cables in extreme conditions may be susceptible to vibrations in multiple modes, other measures are also needed to be proposed to take higher modes into consideration, by proposed Measures two or three, introduced as below.

3.3.1 Measure one

For shorter cables, the lowest frequency mode (i.e., the first mode) is often susceptible to vibrations, while vibrations of other modes can be neglected (Pacheco, 1993). However, when an absorber involves both an inerter and a spring, it can have an internal resonance which can interact with a cable mode in a similar way to a tuned mass damper. Hence, the one mode of the cable only can be split into two close modes of the cable-absorber system. Dynamic instabilities such as galloping, rain-wind induced vibrations or parametric excitation could occur in either mode, hence it is the lower damping ratio of the two modes that is important. In order to capture both potential modes with natural frequencies close to that of the first mode of the undamped cable, a natural frequency range of $0 \sim 1.5\omega_0$ is chosen, i.e., covering all modes up to halfway between the first and second natural frequencies of the undamped cable. Hence, the critical damping ratio ζ_c which is defined as the lowest damping ratio of all modes in the frequency range from 0 to $1.5\omega_0$, is introduced as the key parameter to identify the effectiveness of the absorber layouts.

Therefore, in the present study, the first performance measure is proposed, i.e., to maximise the damping ratio of any modes with natural frequencies around that of the first undamped mode of the cable, but without considering a constrain for higher mode consideration. To be specific, Measure one is to maximise the minimum damping ratio of all modes with frequencies in the range $\omega_e \in (0,\ 1.5\omega_0)$ without considering higher-frequency modes.

The performance criterion of Measure one is to optimize the critical damping ratio, denoted as $\zeta_{c,opt}$, without considering higher-frequency modes.

3.3.2 Measure two

Because longer cables or cables in extreme conditions may suffer from vibrations in multiple modes, in some cases, more low-frequency modes should be considered. The frequency range of $1.5\omega_0 \sim 6.5\omega_0$ covers the natural frequencies of the next five modes of the undamped cable and, again, allows for changes in the natural frequencies due to the absorber. The reason for this choice is that the first six modes of cables have typically been observed to be excited in the field. For example, Caetano (2007) suggested considering natural frequencies up to approximately 3 Hz, which typically corresponds to the first six modes for cables approximately 250 meters long, or fewer modes for shorter cables.

Hence, the second measure is $\zeta_{c,opt}$ with an extra constraint to ensure that the damping ratios of modes with natural frequencies in the range $[1.5\omega_0, 6.5\ \omega_0]$ are no less than those for a cable with a viscous damper optimised for the first mode. In the optimisation process, the damping ratio of each mode in the frequency range $[1.5\omega_0, 6.5\ \omega_0]$ is compared with the damping ratio of the corresponding mode of a cable with an attached viscous damper, optimised for the first mode, calculated via the universal curve (Pacheco et al., 1993). If the damping ratio of any of the higher modes of the cable-absorber system is less than for the corresponding mode for the viscous damper, a penalty is added to the objective function to realise the constraint.

Therefore, in this study, Measure two is to maximise the minimum damping ratio $\zeta_{c,opt}$ of all modes with frequencies in the range $\omega_e \in (0,\ 1.5\omega_0)$, meanwhile with the constraint that modes with natural frequencies in the range $\omega_e \in [1.5\omega_0,\ 6.5\omega_0)$ have no less damping than those for a cable with a viscous damper optimised for Mode 1.

It should be noted that this solution is the same performance measure as previously used for considering multiple modes (Luo et al., 2017). The reference damping ratios for the cable with a viscous damper are taken from the universal curve (Pacheco et al., 1993). Then, all modes in the frequency range $\omega_e \in [1.5\omega_0,\ 6.5\omega_0)$ are included to ensure that the first six modes of the undamped cable are covered, i.e., by using Measure one with this constraint included.

3.3.3 Measure three

Still considering some extreme conditions, e.g., long cable vibrations in multiple modes, a third performance measure is proposed for this study. It is well known that the motion of the cable in the wind causes changes in the aerodynamic forces which based on quasi-steady theory can be considered as equivalent to $\zeta_{ai} = [\rho DUL/(4M\omega_i)]\beta$, where ρ is the density of air, D is the cable diameter, U is the mean wind speed, M is the cable mass per unit length and β is a function of the cable orientation and the static aerodynamic force coefficients of the cross-section. If β is negative, structural damping of at least $(-\zeta_{ai})$ is required to prevent galloping, i.e. dynamic instability of the cable (Macdonald and Larose 2006).

Since ρ, D, U, L, M and β are all independent of the mode number, galloping of mode i occurs if the product $\eta_i = \zeta_i \cdot \omega_i$ is less than a certain value. Hence the minimum value of η_i for all modes of interest determines the threshold at which galloping would occur. Since lower modes are more concerned in general, without less of generality, all modes in the frequency range $\omega_e \in (0, 6.5\omega_0)$ are included to ensure that the first six modes of the undamped cable are covered for this measure.

Hence, the third performance measure is proposed for suppressing cable vibration, i.e., avoiding galloping to occur is the optimised (minimum) value of $\zeta_i \cdot \omega_i$ (defined as η_i). That is, Measure three is to maximise the minimum η_i over all modes of interest.

3.4 Optimisation approach

A lumped mass FE model of a taut cable combined with an arbitrary linear passive absorber layout is built. Based on proposed three performance measures, by using the corresponding optimisation criteria, the effectiveness of different absorbers in terms of their damping performance can be assessed and quantified in the present study.

For the purpose of comprehensively investigating different absorber layouts and also making comparison fair, a generalised modelling work is necessary, all parameters of absorber elements and also for absorber-cable system need to be non-dimensionalised for a general purpose in comparisons.

3.4.1 The non-dimensionalised parameters

Since the established FE cable model with admittance function which can represent different absorbers, it will provide a general approach to the comprehensive investigation of different absorber configurations. For generality, the parameters of the absorber layouts need to be expressed in non-dimensional form. Thus, in the present study, the inertance is considered in non-dimensional scaled compared with the total weight of the cable by letting $b'=b/M$. Similarly, the circular natural frequencies of the damped system and the location of the damper relative to the total cable length are also presented in non-dimensional forms as $\omega'= \omega_e/\omega_0$ and $a_f' =a_f/(n+1)$ respectively. Since the location of all candidate absorbers has been set to be at 5% length of the whole cable, thus $a'_f = 0.05$.

For generality, all parameters of the absorber layouts are presented in non-dimensional form. Here, for all structural elements of absorbers, the values of the elements are all scaled in the non-dimensional forms. The other parameters, i.e., damping coefficient and stiffness of the absorber elements are defined as $c' = (c/M)/(\omega_0/\pi)$ and $k' = (k/M)/(\omega_0/\pi)^2$ respectively. The non-dimensional expressions will be used throughout this thesis unless being pointed out particularly.

Besides, for focusing on a systematic approach to identify beneficial absorber layouts, and also for a fair comparison, the location of all candidate absorbers in this study are set to be at 5% length of the whole cable.

3.4.2 Optimisation process and computational concerns

Some computational considerations are presented in this section. First, the suitable number n of DOFs for optimisation computation is explained. The results respectively with different DOFs are compared and analysed. Then, computational tools used in MATLAB software environment for this study are also introduced.

In principle, the number of DOFs of the cable n should be large enough to increase accuracy as possible for the FE analysis approximation. In order to balance accuracy and computational time, a lumped mass model rather than consistent mass model is used and

a suitable number of DOFs are selected. From preliminary analysis for a number of absorber layouts, it was typically found that a lumped mass model with 99 DOFs provides similar accuracy to a consistent mass model with 60 DOFs, but the consistent mass model took nearly twice the computational time. This is because the mass matrix for the consistent mass model is non-diagonal, which leads to a non-trivial inverse in Equation (3.13). Hence for similar accuracy, the lumped mass model is more computationally efficient. The maximum relative difference in the damping ratio ζ_e between lumped mass models with 99 and 999 DOFs was found to be typically less than 0.1%, considering only low-frequency modes with natural frequencies below 6.5 ω_0. Therefore, a 99-DOFs lumped mass FE model is used in the present study.

The computations throughout the thesis are performed in the software environment of MATLAB. By determine the matrix shown by equation 3.13, a high order polynomial can be found. Then the roots of the high order polynomial can be considered as the eigenvalues, which is calculated via solve function. The eigenvalues are then shown in complex conjugate pairs. After sorted their imaginal parts in ascending order, the results with satisfy the measures are analysed and optimized. A sample code for calculation of a simple loop is shown in the appendix.

For each performance measure, for a given non-dimensional inertance, the optimum critical damping ratio ζ_e is found by using the MATLAB optimisation command “patternsearch” followed by “fminsearch”. This “patternsearch” uses genetic algorithms and is capable to get out of local minimums. The “fminsearch” is gradient-based, and has been found to be suitable for accurate identification of the minimum within a convex parameter space. Depending on the number of variables that need to be optimised and the complexity of the constraints, multiple initial conditions are often needed for both optimisations.

Both "patternsearch" and "fminsearch" in MATLAB require a starting point for the minimum/maximum search. Both functions could be sensitive to starting point selection, especially for the three-element layouts. It should be mentioned that multiple initial conditions are often needed for both optimisations, depending on the number of variables that need to be optimised and the complexity of the constraints. MATLAB is used for the optimisation, the results can be found by using MATLAB genetic optimisation command

"patternsearch" to obtain a rough solution, which is then used as initial condition for a gradient-based MATLAB function "fminsearch" for fine-tuning. Typically, a set of 16 starting points evenly distributed for each non-dimensional variable c' and k' (if it exists) as the starting points for "patternsearch". The solution identified by "patternsearch" is then used as the starting point for "fminsearch". Note that for the solutions obtained by "fminsearch", if the value of a parameter is larger than 1×10^6, then it is considered as "infinity".

3.5 Summary

Aiming to propose an adequate mathematical model with reasonable optimisation criteria for comprehensively identifying beneficial absorber configurations, a mathematical modelling and optimisation approach is studied and introduced in this chapter.

An integrated finite element of cable model with admittance functions representing absorbers is first established. Using this method, the matrices need not to be reformulated for each alternative absorber layout. The advantage of the current method is that a system with any passive linear absorber can be represented by equation of the same form as Equations (3.9) along with Equations (3.10) ~ (3.12), with **x** always being (is) n elements long and the size of matrices **M**, **C** and **K** are always $n \times n$. The only difference is the admittance function $Y(s)$ which representing the absorber.

Then, in order to assess and qualify the performance of suppressing cable vibrations for all modes concerned, three measures are proposed in this study. Measure one is to maximise the minimum damping ratio ζ_c of all modes with frequencies in the range of (0, $1.5\omega_0$). If with the constraint that modes with natural frequencies in the range of ($1.5\omega_0$, $6.5\omega_0$) have no less damping than those for a cable with a viscous damper optimized for Mode 1, the second performance measure is proposed. Measure two to maximise the minimum damping ratio $\zeta_{c,opt}$ of all modes with frequencies in the range $\omega_e \in (0, 1.5\omega_0)$, meanwhile with the constraint that modes with natural frequencies in the range $\omega_e \in [1.5\omega_0$, $6.5\omega_0$) have no less damping than those for a cable with a viscous damper optimised for Mode 1. This the same performance measure as previously used for multiple modes (Luo et al. 2017).

For extreme cases, Measure three used here is to maximize the minimum η_i , defined as the product of $\zeta_i \cdot \omega_i$, focusing on that the motion of the cable in the wind causes the changes in the aerodynamic forces equivalent to negative damping effect. This measure is motivated and justified in Sub-section 3.3.3 previously, which is applicable to galloping-type aerodynamic instabilities.

In the present study, all parameters of the cable-absorber system are non-dimensionalised for generality and easy comparisons. For the structure parameters of inerter-based absorber, the inertance is also non-dimensionalised compared with the total

weight of the cable by letting $b'=b/M$. Similarly, the non-dimensional damping coefficient and stiffness are defined as $c'=(c/M)/(\omega_0/\pi)$ and $k'=(k/M)/(\omega_0/\pi)^2$ respectively. The circular natural frequencies ω_e of the damped system and the location of the damper relative to the total length of the cable a_f are also presented in non-dimensional forms as $\omega'=\omega_e/\ \omega_0$ and $a'_f=a_f/(n+1)$, respectively.

Some computational considerations are analysed, e.g., the selection of the degrees of freedoms. The maximum relative difference in the damping ratio ζ_e between lumped mass models with 99 and 999 DOFs was found to be typically less than 0.1%, considering only low-frequency modes with natural frequencies below $6.5\omega_0$. Based on a number of results compared with different DOFs by using lumped mass FE model which showed as relative efficient in computation, a 99-DOFs lumped mass model is used for the analysis in the present study.

For each performance measure, MATLAB optimisation command "patternsearch" followed by "fminsearch" are used to search the optimum critical damping ratio. However, multiple initial conditions are often needed for both optimisations, depending on the number of variables that need to be optimised and the complexity of the constraints.

The numerically-obtained performance analysis results can be verified by applying the Real-Time Dynamic Substructure technique to physical inerter-based damping devices. Alternatively, as the analysis is presented in the non-dimensional form, it may be useful for scaled and physical model testing. Also, a few suggestions are made which could be useful for future work, the detailed outlook will be presented in Section 7.2.

Chapter 4

Identification of low-complexity inerter-based absorber layouts

4.1 Introduction

In this chapter, using the proposed mathematical approach introduced in Chapter 3, potential advantages of low-complexity inerter-based absorber layouts are systematically investigated. These low-complexity passive vibration absorber layouts include all possible absorber layouts with no more than one damper, one inerter and one spring each, i.e., all layouts with three elements or fewer.

To be specific, based on established integrated FE cable model with a generic vibration absorber represented by its admittance function, introduced in Section 3.2, and by using the proposed performance measures, i.e., Measures one and two respectively introduced in Sub-sections 3.3.1 and 3.3.2, all these low-complexity absorber layouts are investigated, including the layout with a viscous damper only which is taken as standard for comparison throughout the whole thesis. Then the most beneficial low-complexity inerter-based absorber configurations are identified along with their corresponding element values presented.

4.2 Candidate layouts with two and three elements

In the previous study by Lazar et al (2016), only one configuration, i.e., a specific layout, namely a Tuned Inerter Damper (TID) structure is considered. Since less complicated

layouts are more preferred due to space and weight limits in mechanical structures, all low-complexity absorber layouts with no more than one damper, inerter and spring each are considered as candidate layouts for the investigation in this chapter.

Because neither an inerter nor a spring can dissipate energy, a damper must be present in each candidate layout. The single-element layout with a viscous damper only is taken as standard for comparison, denoted as Layout I in the thesis. Apart from Layout I, there are in total four two-element absorber layouts that contain one damper, which are illustrated by Figure 4.1 as below.

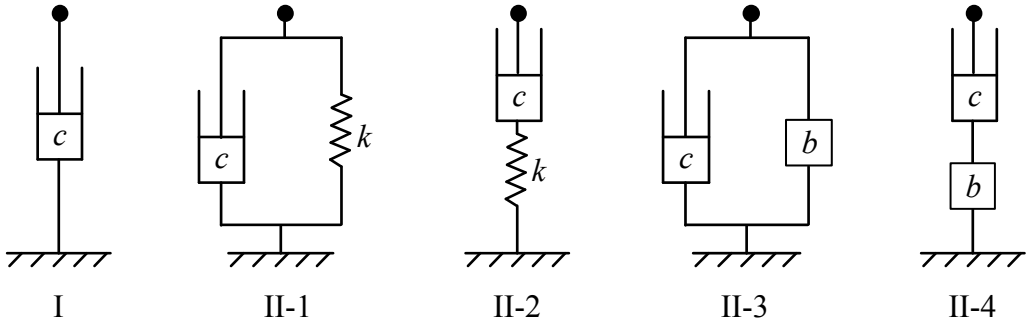

Figure 4.1: Candidate absorber layouts with one or two elements.

Since the inerter is an energy-storage element, the inertance identified in the beneficial layouts will always be in combination with damping (and stiffness) factors. This means the inertance needs to be combined with a traditional damper, so the integrated device can be installed on cable systems in the same way as viscous dampers. There are totally eight possible three-element absorber layouts that contain one damper, one inerter and one spring each. All these candidate absorbers with three elements presented in Figure 4.2.

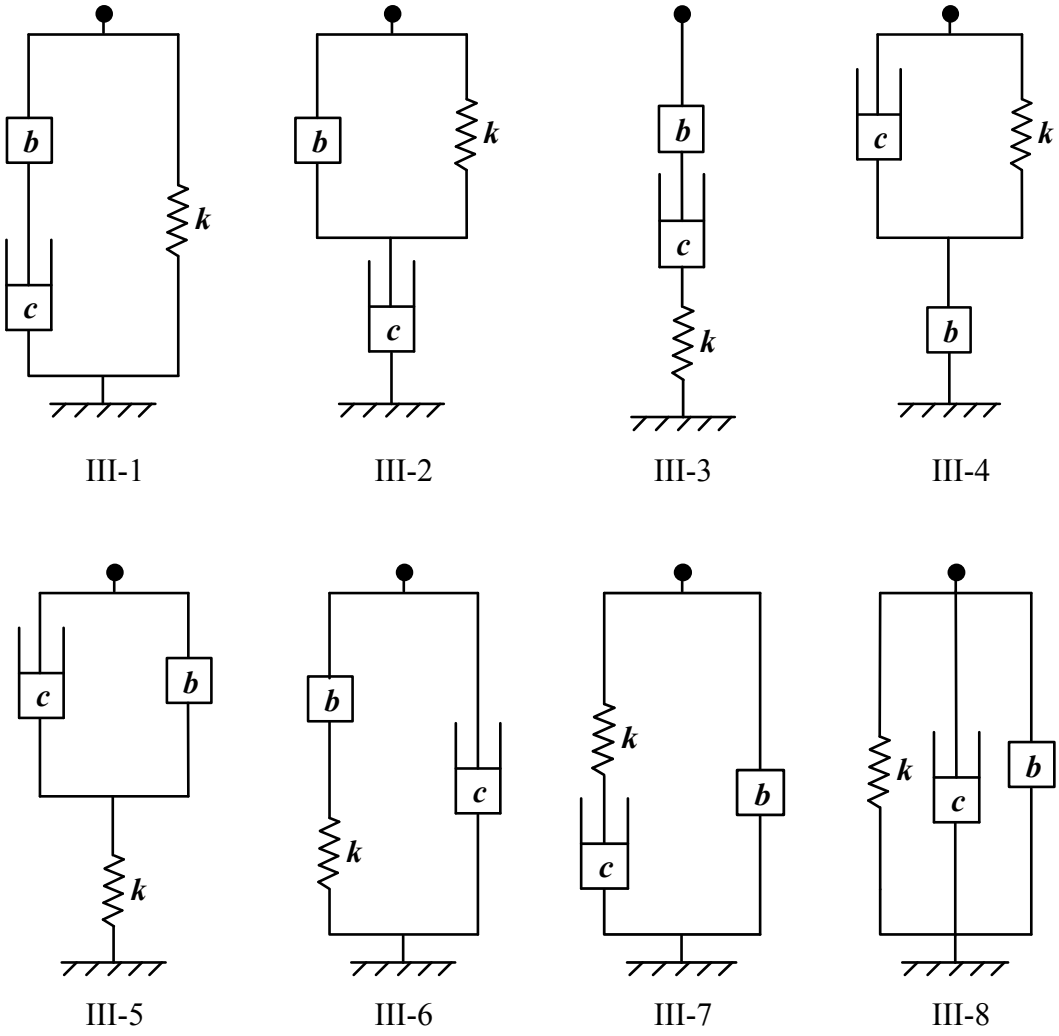

Figure 4.2: Candidate absorber layouts with three elements.

Therefore, all low-complexity absorber layouts that need to be considered are covered by Figures 4.1 and 4.2, totally thirteen including Layout I, i.e., a viscous damper only, with properly selected damping coefficient for comparison as a standard.

For each layout, one terminal is connected to the cable at mass a_f and the other is attached to a fixed support. The admittance functions of all low-complexity candidate absorber layouts are derived and summarized in TABLE 4.1. It should be mentioned that similar work has been done and some simple layouts have also been presented with corresponding admittance functions very recently (Makris, 2017).

TABLE 4.1: Admittance function $Y(s)$ for all low-complexity candidate absorbers.

Layout	Admittance function
I	c
II-1	$c+ks$
II-2	$1/[(1+c)+(s/k)]$
II-3	$bs+c$
II-4	$1/[(1+c)+(1/bs)]$
III-1	$1/[(1+c)+(1/bs)]+(k/s)$
III-2	$1/[(1+c)+(1/bs)+c]$
III-3	$1/[(1+c)+(1/bs)]+(s/k)$
III-4	$1/[(1+c)+(1/bs)+c]$
III-5	$1/[1/(c+bs)+(s/k)]$
III-6	$1/[(1/bs)+(s/k)]+c$
III-7	$1/[(s/k)+(1/c)]+c$
III-8	$bs+c+k/s$

Before the systematic identification for these low-complexity absorber layouts, a preliminary analysis is carried out to examine the optimum critical damping ratios $\zeta_{c,opt}$ for all candidate layouts. Initially, a very large range of non-dimensional inertance values, b', e.g., from 0 to 10^6, are considered. The results for all candidate absorbers show that the maximum optimum critical damping ratio always occurred for b' less than 2.5, with larger inertance decreasing the performance of the absorbers. Therefore, only b' ranging from 0 to 2.5 is considered, with the optimisation results presented in Section 4.2 and 4.3 correspondingly. However, since lower inertance is more realistic and typically less expensive to realise, more detailed discussions focus on a relatively realistic range, e.g., with b' from 0 to 0.5, as presented in Section 4.5 afterwards.

For generality, all parameters of the absorber layouts have been non-dimensionally scaled, as introduced in Section 3.4.1. The new added circular natural frequencies ω_e of the damped system are presented in non-dimensional forms as $\omega' = \omega_e / \omega_0$.

4.3 Optimisation results using Measure one

For all considered low-complexity absorber layouts illustrated in Figures 4.1 and 4.2, by using Measure one described in Sub-section 3.3.1, this section aims to find the largest critical damping ratio ζ_c for the first mode or around, i.e., in the range $\omega_e \in (0, 1.5\omega_0)$, without considering the effect on higher modes.

In this section, all low-complexity layouts, with three elements or fewer, are examined. Their optimisation results are presented in the order of complexity from low to high, i.e., Layouts respectively with a damper only, two and three elements, in sequence, as below.

4.3.1 Layout with a viscous damper only

Based on the lumped-mass FE model with 99 DOFs, the results of the eigenvalue analysis for Layout I, i.e., a viscous damper only, are presented in Figure 4.3 for a range of non-dimensional damping coefficients c' of 0 ~ 20. The resulted relationship between critical damping ratio ζ_c and non-dimensional damping coefficient c' is shown in Figure (4.3a) which follows the universal curve (Pacheco et al., 1993), and also similar with the results from other literatures. The corresponding non-dimensional natural frequency ω' is shown in Figure (4.3b).

It can be seen from Figure (4.3a) that for Layout I, i.e., a viscous damper, its optimum critical damping ratio $\zeta_{c,opt}$ is 0.0264, which matches with the maximum value on the universal curve, showing the validity of the proposed optimisation approach. While Figure (4.3b) shows the corresponding non-dimensional natural frequency ω', which indicates that the viscous damper has a marginal influence on the frequency of the first mode. The results for the viscous damper can be taken as a standard in comparison for inerter-based beneficial layout identification afterwards.

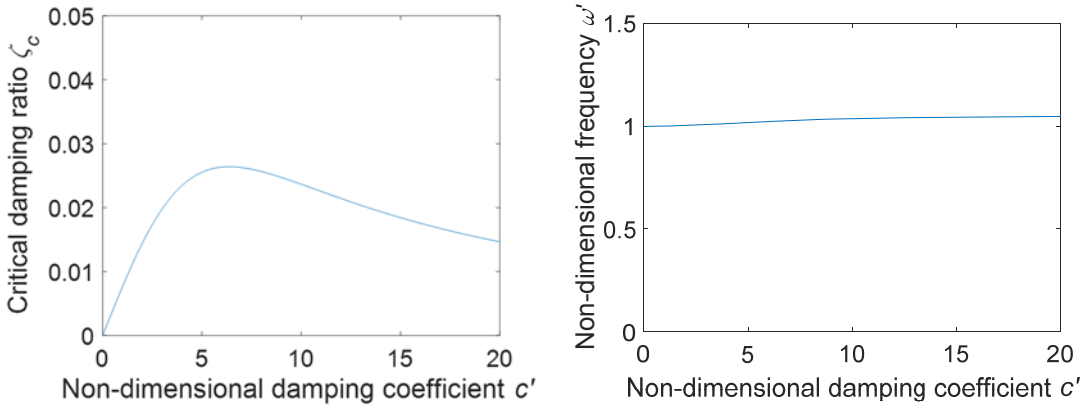

(a) (b)

Figure 4.3: Results for Layout I (viscous damper only). (a) Critical damping ratio, and (b) corresponding non-dimensional natural frequency, versus non-dimensional damping coefficient.

4.3.2 Layouts with two elements

Then, for low-complexity absorber layouts with two elements, i.e., the four candidate absorber layouts shown in Figures 4.1, by using Measure one, optimisations are carried out and beneficial layouts are identified. Here, for absorber layouts with two elements, layouts that can provide a larger maximum optimum critical damping ratio than a damper only are considered beneficial.

The optimum critical damping ratios $\zeta_{c,opt}$ of both Layouts II-1 and II-2 (one damper in parallel or series with one spring), are found to be $\zeta_{c,opt} = 0.026$, which is the same as that for the viscous damper only. The corresponding non-dimensional damping coefficient and stiffness are respectively $c' = 6.430$, $k' = 0$ for Layout II-1 and $c' = 6.430$, $k' = \infty$ for Layout II-2 (i.e. both without the spring). In fact, for any tested c' in the range of 0 to 30, adding a spring always decreases the damping ratio for these two layouts. Therefore, these two layouts are not beneficial. Hence, only Layouts II-3 and II-4 (one damper in parallel or series with one inerter) are discussed below, together with the damper only (i.e., Layout I).

Figure 4.4 presents a three-dimensional shaded surface plot of the critical damping ratio ζ_c for Layout II-3 with $0 \leq c' \leq 20$ and with $0 \leq b' \leq 2.5$. The bold solid curve indicates the optimum critical damping ratio for a given non-dimensional inertance.

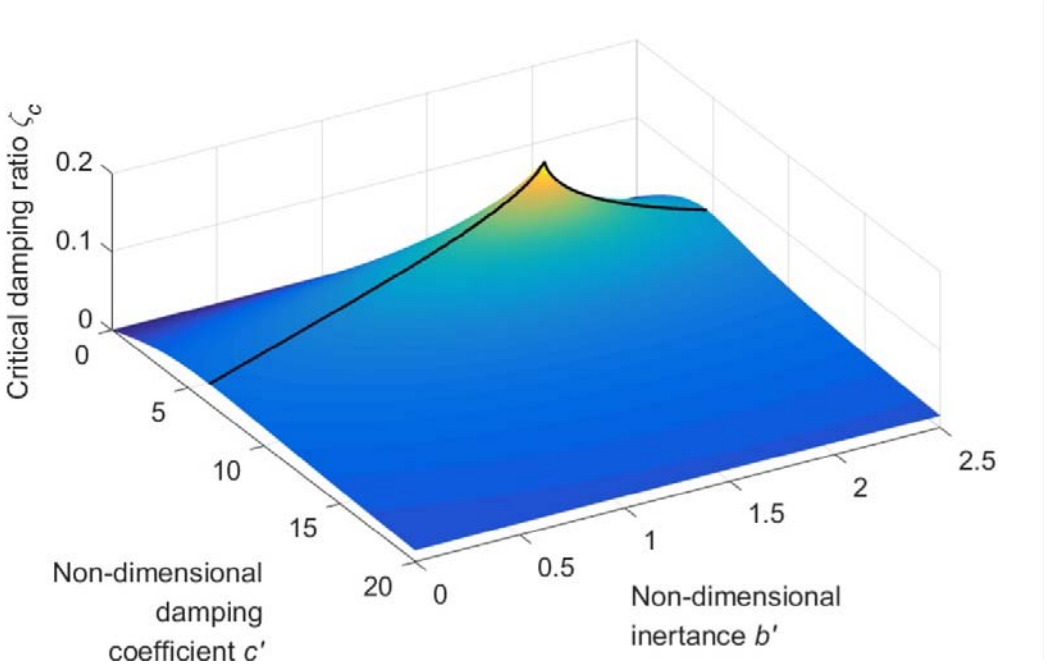

Figure 4.4: Three-dimensional plot of damping ratio versus non-dimensional inertance and damping coefficient for Layout II-3.

Optimisation results for Layout II-3 are presented in Figure 4.5. In Figure (4.5a), the solid curve presents the optimum critical damping ratio as a function of the non-dimensional inertance, which corresponds to the bold solid curve in Figure 4.4, while, the dashed curve shows the damping ratio for a simultaneously occurring non-critical mode also in non-dimensional frequency range $0 \leq \omega' \leq 1.5$. As there are more than one modes in the frequency range considered, the one with provides the lowest damping ratio is considered critical and the others are considered as non-critical modes. The corresponding non-dimensional natural frequencies of both modes are shown in Figure (4.5b). The representation of lines for other layouts in Figures 4.6~4.9 are consistent in style with those presented in Figure 4.5.

As shown in Figure (4.5a), with $b' = 0$, as expected, the optimised critical damping ratio is the same as that for a viscous damper only. For $b' > 0$, Layout II-3 provides a

greater optimum critical damping ratio than that for a viscous damper only for any inertance b' investigated. It can be seen from the solid curve that among all the optimised results with varying b', the maximum optimum critical damping ratio $\zeta_{c,max}$ which is defined as the maximum $\zeta_{c,opt}$, that can be achieved for any inertance, is 0.155 for $b' = 1.760$, i.e. 5.9 times that for a viscous damper only. As b' increases from zero, the damping ratio of the original first mode (the mode with the lowest natural frequency, which is the initially the critical one) increases, but that of the original second mode decreases. At $b' = 1.760$, the damping ratios of the two modes are equal and above that value, the damping ratio of the second mode is lower than that of the first mode, so the second mode becomes the critical one.

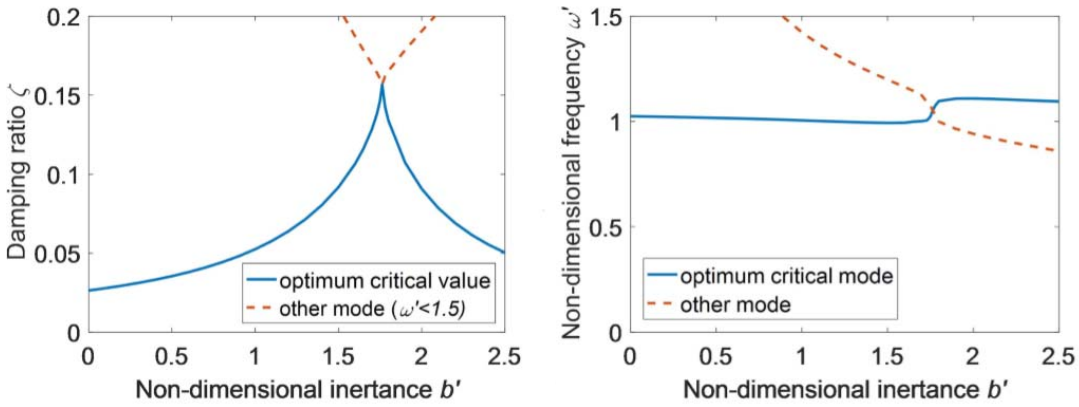

(a) (b)

Figure 4.5: Optimisation results for Layout II-3. (a) Damping ratio, and (b) corresponding non-dimensional frequency, versus non-dimensional inertance.

It can be seen from Figure (4.5b) that the natural frequency of the second mode decreases as b' increases and at $b' = 1.760$ there is a switch of which mode is the critical one. It is notable that in all cases the natural frequency of the critical mode is similar to that of the original undamped first mode, showing that the frequency is not greatly influenced by the absorber. At $b' = 1.760$, the solutions for the critical and the non-critical

modes cross over each other, which lead to the breakpoint seen in Figure 4.4 and Figure (4.5a).

Figure 4.6 presents the optimisation results for Layout II-4. The results are of a similar form to those for Layout II-3. Layout II-4 is hence another beneficial layout compared with a viscous damper only if the non-dimensional inertance is sufficiently large. It can be seen from Figure (4.6a) that among all the optimised results with varying b', Layout II-4 can provide $\zeta_{c,max} = 0.159$ for $b' = 2.250$, which is marginally better than the maximum for Layout II-3. However, Layout II-4 has the drawback that large optimum critical damping ratio $\zeta_{c,opt}$ cannot be achieved with relatively small b'. The optimum critical damping ratio $\zeta_{c,opt}$ for Layout II-4 is larger than that of a viscous damper if $b' > 1.15$. Similar to the case for Layout II-3, the breakpoint at $b' = 2.250$ in Figure (4.6a) is due to a switch of which mode is the critical one and it can be seen in Figure (4.6b) that the natural frequency of the critical mode is always close to that of the original undamped first mode.

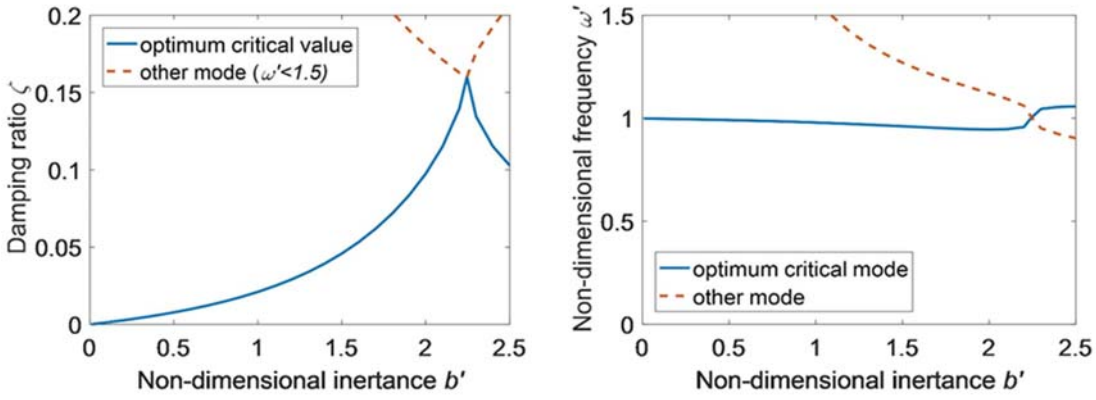

(a) (b)

Figure 4.6: Optimisation results for Layout II-4. (a) Damping ratio, and (b) corresponding non-dimensional frequency, versus non-dimensional inertance.

Therefore, based on the comparisons of optimisation results, by using Measure one, Layouts II-3 and II-4 are considered as beneficial two-element layouts.

4.3.3 Layouts with three elements

Still by using Measure one, this sub-section is to investigate all eight possible three-element absorber layouts shown in Figure 4.2. Based on the optimisation results, only Layouts III-3, III-4, III-5 and III-6 can provide greater optimum critical damping ratio $\zeta_{c,opt}$ than the discussed layouts with fewer elements, i.e., Layouts I, II-3 and II-4, with relatively small non-dimensional inertance b'. However, the other four can only provide same damping ratio as ether II-3 or II-4 in the selected frequency range. Among these four three-element layouts, Layout III-6 is less preferable than the other three due to $\zeta_{c,opt}$ being lower for a wide range of b'. Therefore, optimisation results for only Layouts III-3, III-4 and III-5 are discussed and compared in this sub-section.

Optimisation results for Layout III-3 are presented in Figure 4.7, showing damping ratio and corresponding non-dimensional frequency versus non-dimensional inertance b' in the range of 0 ~ 2.5. It can be seen from Figure (4.7a) that among all the optimum results with varying b', Layout III-3 can provide a maximum optimum critical damping ratio of $\zeta_{c,max} = 0.159$, for $b' = 2.250$, which is the same as Layout II-4, but Layout III-3 is more effective than Layout II-4 when $b' < 2.250$.

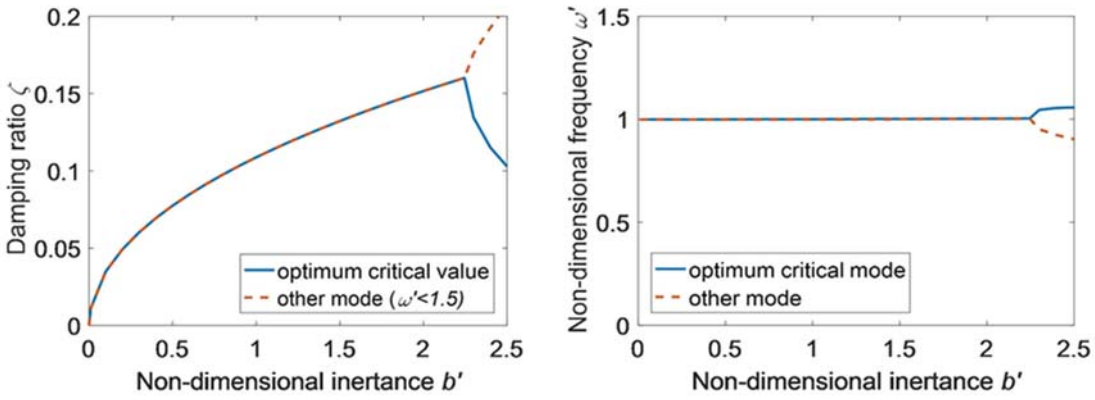

(a) (b)

Figure 4.7: Optimisation results for Layout III-3. (a) Damping ratio, and (b) corresponding non-dimensional frequency, versus non-dimensional inertance.

Also, it can be found from Figure (4.7a) that, for any optimum critical damping ratio with a given $b' \leq 2.250$, the two modes of the system with non-dimensional frequency ω'<1.5 provide the same damping ratio and very similar natural frequencies. This indicates that the inerter and the spring provide a resonance to target the first mode. When $b' = 2.250$, the two modes bifurcate, since the corresponding non-dimensional stiffness reaches infinity. For $b' \geq 2.250$ the optimum results are the same as for Layout II-4, i.e. the spring in Layout III-3 has become a rigid connection.

Optimisation results of Layout III-4 are presented in Figure 4.8, by using Measure one. In fact, the Layout III-4 is equivalent to a TMD when one terminal is grounded (Lazar et al., 2016). The results show that among all the optimum results with varying b', Layout III-4 can provide a maximum optimum critical damping ratio $\zeta_{c,max} = 0.159$, for non-dimensional inertance of $b' = 2.250$ as shown in Figure (4.8a), which is the same as for Layout II-4 as seen in Figure (4.6a). It should be noted that this is in line with the finding in Lazar et al. (2016), which qualitatively stated that the modal damping limitation of a viscous damper can be overcome through the use of a TID.

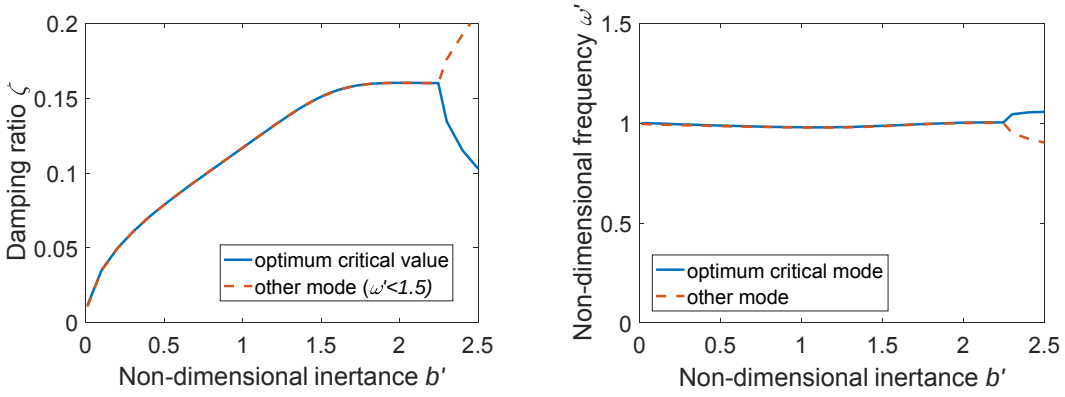

(a) (b)

Figure 4.8: Optimisation results for Layout III-4. (a) Damping ratio, and (b) corresponding non-dimensional frequency, versus non-dimensional inertance.

Compared with Layout II-4, Layout III-4 is more effective when b' is smaller. Similar to the results of Layout III-3, Layout III-4 also has the property that for any $\zeta_{c,opt}$ for (with a) given $b' \leq 2.250$, the two modes of the system with $\omega' < 1.5$ provide the same damping ratio and very similar natural frequencies. When $b' = 2.250$ the two modes bifurcate since the non-dimensional stiffness k' for the optimum result reduces to zero. Since k' cannot physically be negative, for $b' > 2.250$, $\zeta_{c,opt}$ is the same as for Layout II-4.

Optimisation results of Layout III-5 are presented in Figure 4.9, showing the damping ratio and corresponding non-dimensional frequency versus non-dimensional inertance respectively. It can be seen in Figure (4.9a) that among all the optimum results with varying non-dimensional inertance b', Layout III-5 can provide $\zeta_{c,max} = 0.155$, for $b' = 1.760$, which is the same as for Layout II-3. Due to resonance provided by the inerter and spring, for $0.065 \leq b' \leq 1.760$, optimised results for Layout III-5 are better than those for Layout II-3. Figure (4.9b) shows that the two modes of the system with $\omega' < 1.5$ provide the same damping ratio and very similar frequencies. When $1.760 < b'$ or $b' < 0.065$, the optimised results of Layout III-5 are the same as those of Layout II-3, which lead to kinks in Figure (4.9a). The optimum value of k' is then infinity, so the spring acts as a rigid link.

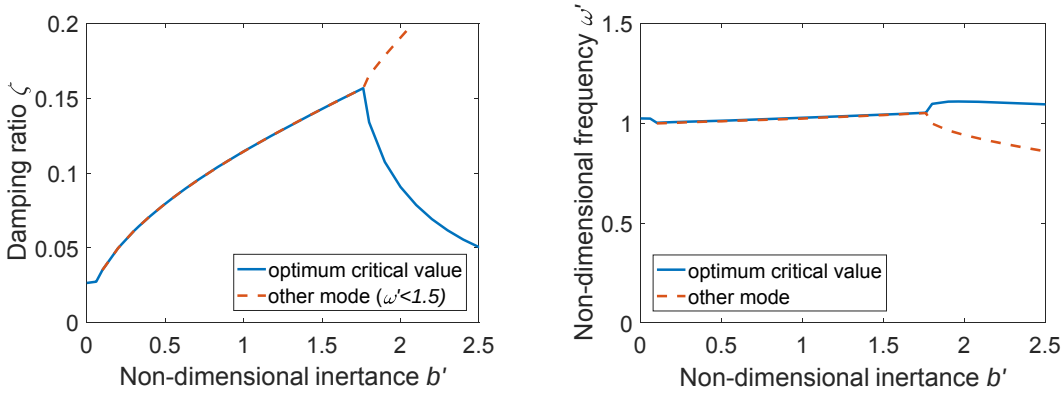

(a) (b)

Figure 4.9: Optimisation results for Layout III-5. (a) Damping ratio, and (b) corresponding non-dimensional frequency, versus non-dimensional inertance.

4.4 Optimisation results using Measure two

By using Measure two described in Section 3.3.2, optimisation results for all low-complexity absorber layouts with three elements or fewer, presented in Figures 4.1 and 4.2, are computed and analysed in this section.

Measure two is to maximise $\zeta_{c,opt}$ of all modes with frequencies in the range $\omega_e \in (0, 1.5\omega_0)$, with the constraint that modes with natural frequencies in the range $\omega_e \in [1.5\omega_0, 6.5\omega_0)$ have no less damping than those for a cable with a damper optimised for Mode 1. So, this optimisation measure considering six modes is similar to the Measure one, except that the additional constraint is implemented to consider the performance of higher modes. Hence, in this section, all optimisation results, by using Measure one or two, are presented in form of without or with the higher mode constrain correspondingly, for observing the influence of the constraint more clearly via the comparison.

The results in Section 4.3. show that, for all absorber layouts for Measure one, i.e., without the higher modes constraint, Layouts II-3, II-4, III-3, III-4 and III-5 are considered beneficial. In this section for Measure two, i.e., with the constraint, optimization results show that for two-element layouts, Layouts II-3 and II-4 can provide better results than a viscous damper only. While for three-element layouts, Layouts III-4 and III-6 perform better than the other three-element layouts. Hence, the optimisation results for beneficial two-element layouts, i.e., Layouts II-3, II-4, and three-element layouts III-4 and III-6, are respectively presented as below.

4.4.1 Beneficial layouts with two elements

First, two two-element layouts, i.e., Layouts II-3, II-4, are examined by using Measure two. Figure 4.10 presents the optimisation results of beneficial Layouts II-3 respectively with and without the higher mode constraint, showing damping ratio versus non-dimensional inertance in Figure (4.10a) and damping ratios for higher modes optimised with b' as 0.195 versus non-dimensional frequency in Figure (4.10b) respectively.

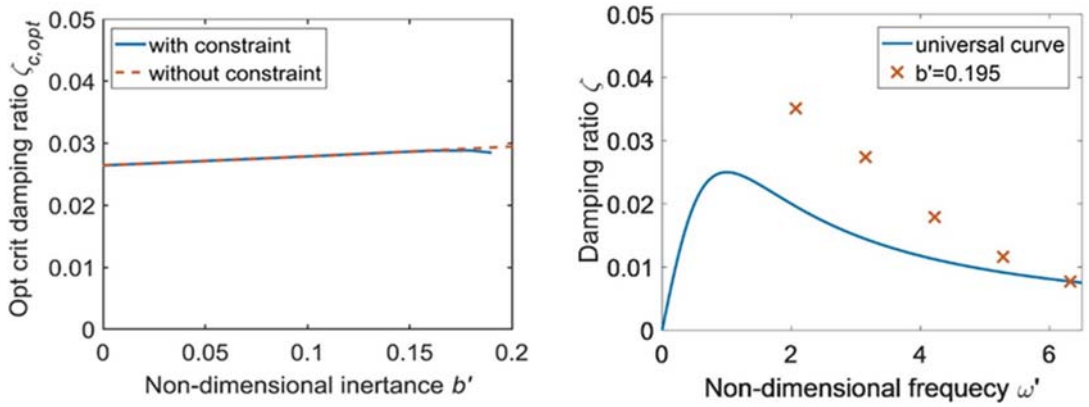

(a) (b)

Figure 4.10: Optimisation results of Layout II-3 with and without the constraint. (a) Damping ratio versus non-dimensional inertance, and (b) damping ratios for higher modes optimised with b' as 0.195 versus non-dimensional frequency.

As shown in Figure (4.10a), for Layout II-3 with non-dimensional inertance $b' = 0$, as expected, the optimised critical damping ratio is the same as that for a viscous damper only, i.e. $\zeta_{c,opt} = 0.026$. For $b' > 0.170$ the constraint affects the results, so $\zeta_{c,opt}$ is lower with the constraint than without it. For $b' > 0$, Layout II-3 provides a slightly greater optimum critical damping ratio than a damper only. It can be seen from the solid curve that among all the optimised results with varying b', $\zeta_{c,max}$ is 0.028 for $b' = 0.160$. When optimised with $b' < 0.170$ without the constraint, the damping ratio of the higher modes are all above the constraint. Therefore, results both with and without the constraint are the same.

In Figure (4.10b), the crosses show the damping ratio for the higher modes for the optimised system with b' as 0.195. The optimum critical damping ratio $\zeta_{c,opt}$ is restricted by the damping ratio of the sixth mode, which is on the boundary provided by the solution of the viscous damper. However, for $b' > 0.195$, the sixth mode cannot meet the boundary condition that no worse than that for a viscous damper optimised for the first mode. Therefore, the solid curve in Figure (4.10a) terminates. Similar situations can occur for the other layouts.

The optimisation results of Layout II-4 with and without the constraint is shown in Figure 4.11. The maximum optimum critical damping ratio $\zeta_{c,max}$ with the higher mode constraint is 0.062 for $b' = 2.172$, which is much greater than for a damper only, but large inertance is required. The solid curve starts at $b' = 0.160$ since for small b' the damping ratio of the second mode cannot satisfy the constraint. For $b' > 1.50$, the optimum solution is limited by the sixth mode, giving reduced result compared with the case without the constraint.

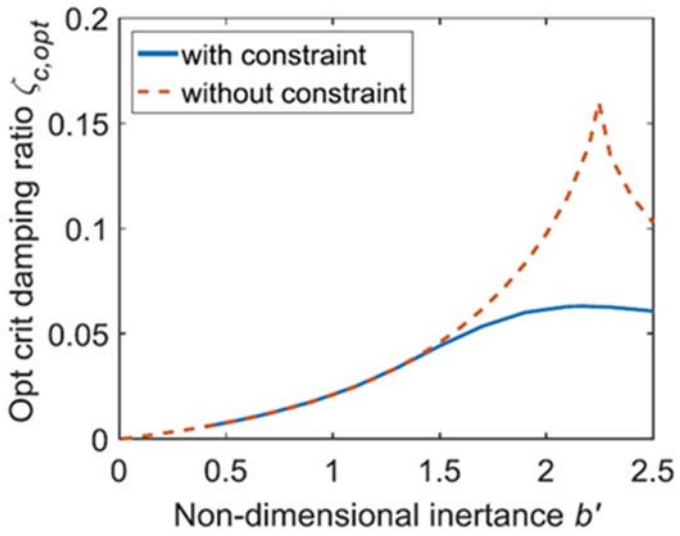

Figure 4.11: Optimisation results of Layout II-4 with and without the constraint.

4.4.2 Beneficial layouts with three elements

In this subsection, the performance of three-element layouts using Measure two is presented. Based on the optimisation results, it is found that with suitable amount of inertance, all candidate layouts with three elements can provide greater $\zeta_{c,opt}$ than layouts with fewer elements, i.e., Layouts I, II-3 and II-4. Since Layouts III-4 and III-6 are the most beneficial ones, therefore, their results are presented as below.

Figure 4.12 shows the optimisation results for Layout III-4. The maximum optimum critical damping ratio $\zeta_{c,max}$ is 0.141 for $b' = 1.40$, which provides 451% more damping ratio than a viscous damper only. The solid curve allowing the additional constraint starts at $b' = 0.390$ since below that the damping ratio of the second mode cannot satisfy the

constraint. For $b' < 0.90$, the optimum solution is limited by the second mode, and for $b' > 1.40$ it is limited by the sixth mode. For $0.90 < b' < 1.40$, the results are not limited by the additional constraint, so the optimum solution is the same as when only considering the critical damping ratio.

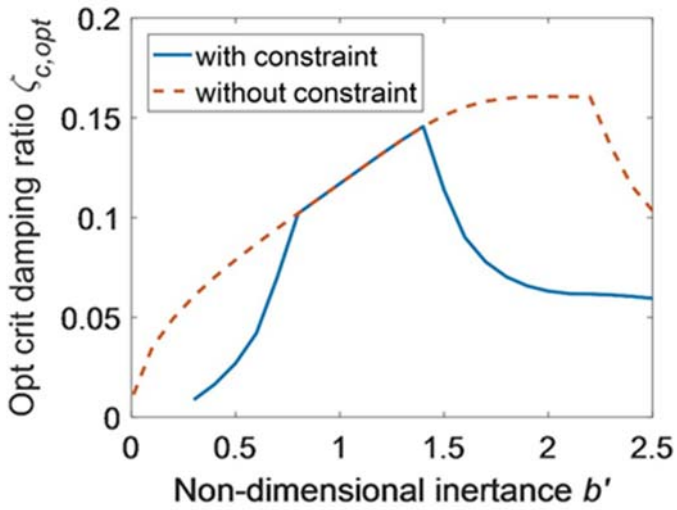

Figure 4.12: Optimised damping ratio versus non-dimensional inertance with and without the constraint for Layout III-4.

Figure 4.13 shows the optimisation results for Layout III-6. The maximum optimum critical damping ratio $\zeta_{c,max}$ is 0.033 for $b' = 0.215$. When $b' < 0.070$, the corresponding k' becomes a rigid connection, and it can be simplified to Layout II-3. For $b' > 0.340$, since the corresponding stiffness $k' = 0$, Layout III-6 reduces to a damper only, so there is no further change in $\zeta_{c,opt}$. Hence, Layout III-6 is considered not as effective as Layout III-4.

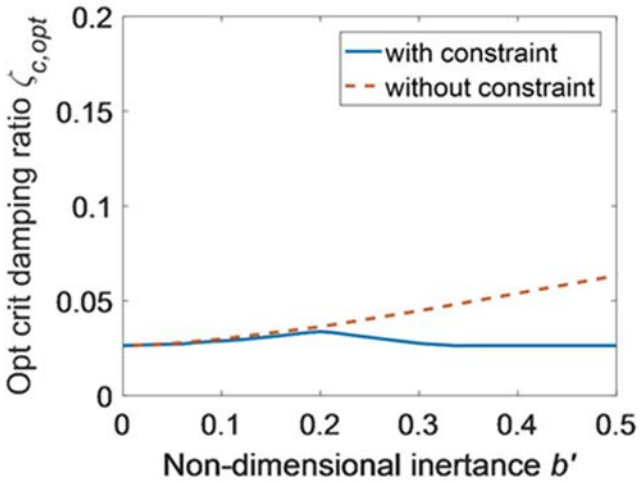

Figure 4.13: Optimised damping ratio versus non-dimensional inertance with and without the constraint for Layout III-6.

4.5 Identified beneficial layouts

Although inerters can realise large inertance by using gearing, with relatively small actual mass, it has been understood that it is difficult and currently uneconomical to realise an inerter with extremely large inertance. Therefore, based on the optimisation results presented in Sections 4.3 and 4.4 respectively without and with the higher mode constraint i.e., for Measures one and two, the identified low-complexity beneficial absorber layouts are summarised, further with a more realistic, small range of non-dimensional inertance $0 < b' < 0.5$ in this section.

By using Measure one, optimisation results show that Layouts II-3, II-4, III-3, III-4 III-5, are more beneficial among all low-complexity absorber layouts, i.e., layouts with three elements or fewer. The performance improvements for these five low-complexity layouts using Measure one, including their beneficial inertance region, maximum improvement (in percentage terms) compared with a damper only and benefit ranges for non-dimensional inertance, respectively within $0 \le b' \le 2.5$ and $0 \le b' \le 0.5$, are summarized in Table 4.2.

TABLE 4.2: Relative improvement of beneficial low-complexity layouts for Measure one.

		$b' \in (0, 2.5]$		$b' \in (0, 0.5]$	
Beneficial layout	Range of Beneficial b'	Maximum Improvement	Corresponding b'	Maximum Improvement	Correspnding b'
II-3	(0, 2.5]	487%	1.760	34%	0.5
II-4	(1.150, 2.5]	502%	2.250	N/A	N/A
III-3	(0.080, 2.5]	502%	2.250	196%	0.5
III-4	(0.2, 2.5]	502%	2.250	203%	0.5
III-5	(0, 2.5]	487%	1.760	202%	0.5

First, for relatively small non-dimensional inertance range, two-element beneficial layouts are examined by using Measure one. Without considering the constraint for higher modes, for $b' \leq 0.5$ the optimum critical damping ratios $\zeta_{c,opt}$ of Layouts II-3 and II-4, and their corresponding non-dimensional damping coefficients c' are compared in Figure 4.14, along with the results for a damper only. Layout II-3 provides higher $\zeta_{c,opt}$ than Layout II-4 and Layout I (a damper only) in this range. Also, a lower damping coefficient is required than that of Layout I. Layout II-4 is only more beneficial than Layout II-3 for $b' > 1.950$ and it can provide a slightly better maximum optimum critical damping ratio $\zeta_{c,max} = 0.159$ compared with $\zeta_{c,max} = 0.155$ for Layout II-3. However, for $0 \leq b' \leq 0.5$, only Layout II-3 is beneficial. Up to 34% increase in the critical damping ratio can be realised compared with a viscous damper only by Layout II-3, as shown in Table 4.2.

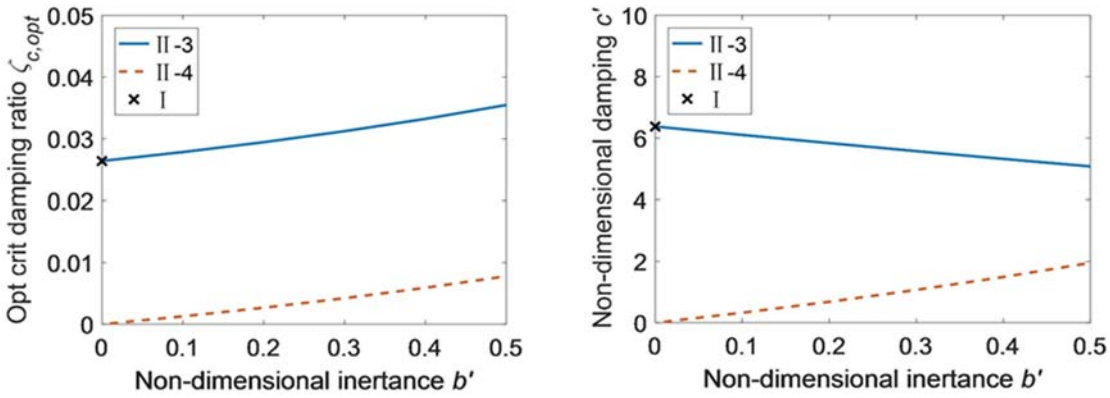

(a) (b)

Figure 4.14: Optimisation results of beneficial layouts with two elements for Measure one. (a) Damping ratio, and (b) corresponding non-dimensional damping coefficient, versus non-dimensional inertance.

Then, still for relatively small non-dimensional inertance in range of $0 \leq b' \leq 0.5$, the identified three beneficial layouts with three elements are investigated by using Measure one. Without the higher mode constraint, for $b' < 0.5$, the optimisation results of the identified beneficial layouts, i.e. Layouts III-3, III-4 and III-5, are presented in Figure 4.15. Note that the gaps between zero and the start point of the curve, and the dotted curve shown in Figure (4.15b) is due to the density chosen in b'.

It can be seen from Figure (4.15a) that, Layout III-4 provides the largest optimum damping ratio $\zeta_{c,opt}$ over a wide range of non-dimensional inertance values b', though the difference with the other two layouts are often small. For $b' \leq 0.065$, Layout III-5 is the most beneficial where it reduces to Layout II-3. For $b' > 0.065$, Layout III-5 provides different solutions with greater $\zeta_{c,opt}$, which lead to the jump in c' as shown in Figure (4.15b). For $0.065 \leq b' \leq 0.5$, there is little difference in performance between the three-element layouts, while much lower non-dimensional damping coefficients c' are required for Layouts III-4 and III-5 compared with Layout III-3.

Figure (4.15c) shows that the corresponding non-dimensional stiffness k' are about π^2 times b' for all three layouts, indicating that the inerter and spring provide resonance to target the first mode.

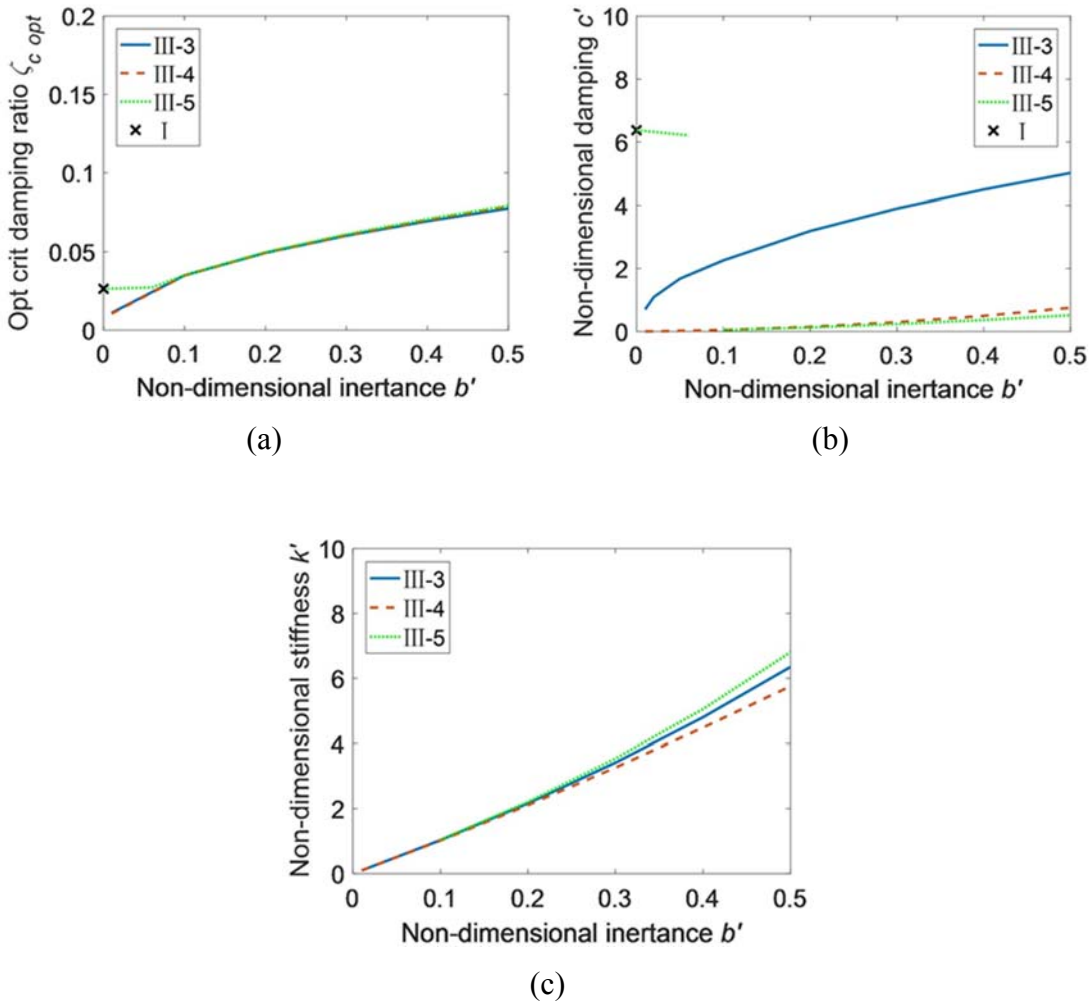

Figure 4.15: Optimisation results for beneficial layouts with three elements for Measure one. (a) Damping ratio, (b) corresponding non-dimensional damping coefficient, and (c) corresponding non-dimensional stiffness, versus non-dimensional inertance.

Therefore, by using Measure two, i.e., with the higher mode constraint, only Layouts II-3, II-4, III-4 and III-6 are considered beneficial. The performance improvements of these four low-complexity layouts using Measure two, including their beneficial inertance region, maximum improvement (in percentage terms) compared with a damper only and benefit ranges for non-dimensional inertance, respectively within $0 \leq b' \leq 2.5$ and $0 \leq b' \leq 0.5$, are summarized in Table 4.3.

TABLE 4.3: Relative improvement of beneficial low-complexity layouts for Measure two.

		$b' \in (0, 2.5]$		$b' \in (0, 0.5]$	
Beneficial layout	Range of Beneficial b'	Maximum improvement	Corresponding b'	Maximum Improvement	Correspondin g b'
II-3	(0, 2.5]	8.96%	0.160	8.96%	0.160
II-4	(1.150, 2.5]	150%	2.250	N/A	N/A
III-4	(0.080, 2.5]	451%	1.400	N/A	N/A
III-6	(0, 2.5]	27.6%	0.215	27.6%	0.215

For relatively small non-dimensional inertance in range of $0 \leq b' \leq 0.5$, the identified beneficial layouts with three elements or fewer are investigated by using Measure two. The optimisation results show that Layout III-6 in the range $0 \leq b' \leq 0.510$ and Layout III-4 in the range $0.510 \leq b' \leq 2.5$ provide more beneficial optimised critical damping ratios than the other layouts.

With the higher mode constraint, for $b' < 0.5$, the optimisation results of Layouts II-4 and III-6 are presented in Figure 4.16, along with the element values presented. As shown in Figure (4.16a), only Layouts II-3 and III-6 can provide results better than a viscous damper for $b' \leq 0.5$. It can be found from Figures (4.16b) and (4.16c) that. Note that, for $b' < 0.08$, k' can be considered infinity, thus the layout III-6 can be simplified in the layout II-3, and for $b' > 0.36$, $k' = 0$, thus layout III-6 can considered as a damper only. Compared with the results without the constraint, resulted non-dimensional damping coefficient c' and spring coefficient k' are of the same order of magnitude, but the higher mode constraint has greatly reduced $\zeta_{c,opt}$ for all the beneficial absorber layouts.

Optimisation results show that by using Measures one and two, Layout III-4 provides the overall optimum critical damping ratio compared with other low-complexity layouts. Whereas Layout III-6 is still worth considering in practice, since it provides reasonable benefits with relatively small inertance.

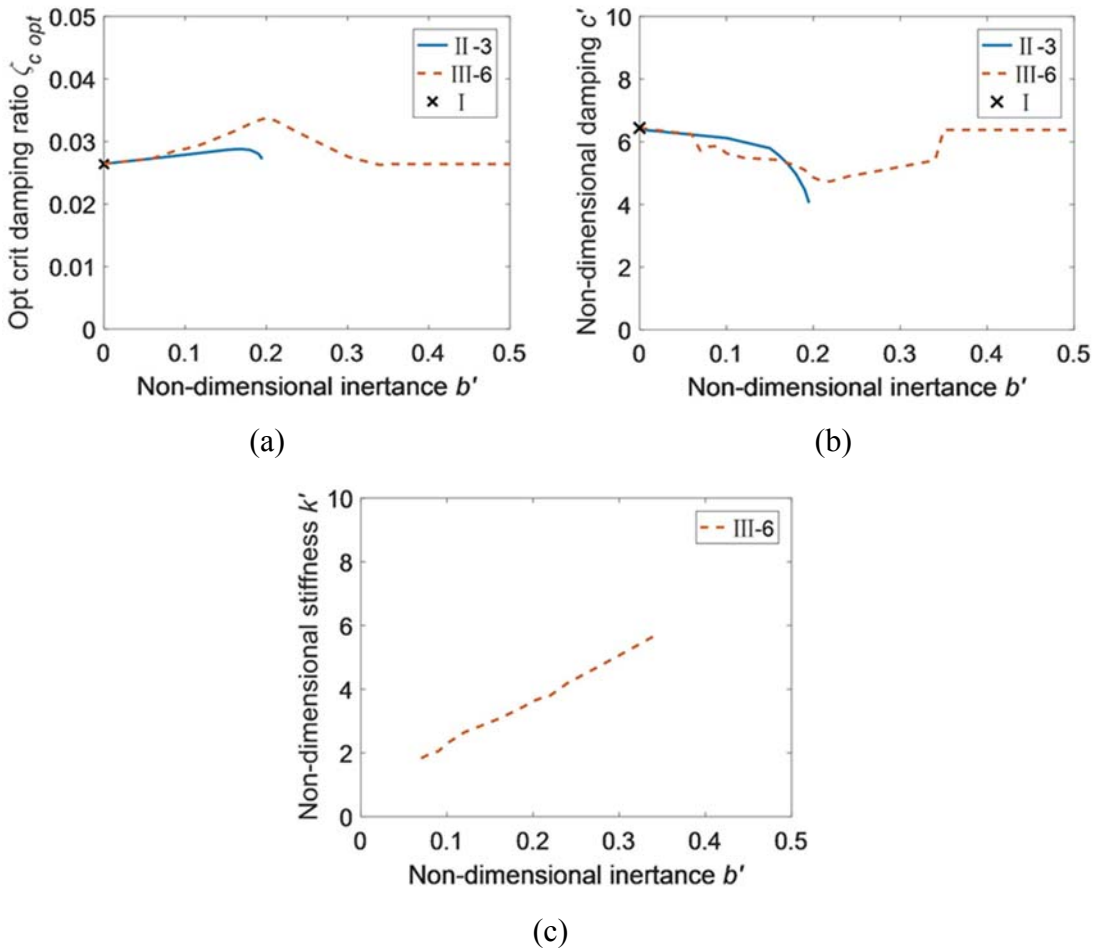

Figure 4.16: Optimisation results for beneficial layouts for Measure two. (a) Damping ratio, (b) corresponding non-dimensional damping coefficient, and (c) corresponding non-dimensional stiffness, versus non-dimensional inertance.

4.6 Summary

Based on the established integrated cable model with an arbitrary absorber layout represented by admittance function, the damping performance of all possible low-complexity absorber layouts, i.e., with three elements or fewer along with a viscous damper only, taken as a standard layout, are investigated. By using proposed performance measures, optimisation results are presented and analysed to identify beneficial low-complexity inerter-based absorber layouts for cable vibration suppression, with non-

dimensional inertance b' within the range of 0 to 2.5, with further focus on the more practical range of 0 to 0.5.

The results show that all layouts incorporating inerters can provide more beneficial optimum critical damping ratios than for a viscous damper only. Compared with two-element layouts for small inertance, three-element layouts can provide greater damping performance.

By using Measure one, i.e., to maximise the minimum damping ratio of all modes with frequencies in the range $\omega_e \in (0, 1.5\omega_0)$, without the higher mode constraint, three beneficial absorber layouts with three elements, i.e. Layouts III-3, III-4 and III-5, are found to be most beneficial, offering much greater damping ratios than other layouts when the inertance is small.

While for considering the performance of higher modes, by using Measure two, i.e., with the constraint that modes with natural frequencies in the range $\omega_e \in [1.5\omega_0, 6.5\omega_0)$ have no less damping than those for a cable with a damper optimised for Mode 1, two low-complexity layouts, i.e., Layouts III-4 and III-6, are found to be beneficial, even though their performance is restricted by the constraint.

Based on optimisation result comparisons for all low-complexity inerter-based absorber layouts, the most beneficial layout is identified as Layout III-4, i.e., the layout with overall beneficial damping performance within relatively large range of non-dimensional inertance. Compared with a viscous damper only, Layouts III-4 can provide significant performance improvement, up to 502% for Measure one and 451% for Measure two respectively.

Chapter 5

Identification of optimum cable vibration absorbers using fixed-sized-inerter layouts

5.1 Introduction

In Chapter 4, all layouts with no more than one inerter, one damper and one spring, and identified beneficial configurations for damping ratio enhancement considering multiple modes, have been analysed. The results showed that inerter-based vibration absorber layouts with two or three elements can provide significant performance improvements compared with a viscous damper when the inertance in these absorbers is sufficiently large. However, in practice, large inertance implies more difficulties in terms of physical implementation. Meanwhile, there are many alternative inerter-based configurations containing more elements, which could potentially provide better performance with significantly smaller inertance. Although the layouts with more elements are likely to provide greater improvements with smaller inertance meanwhile, nevertheless, with the number of elements grows, the number of possible layouts increases exponentially, according to graph theory (Riordan and Shannon, 1942). Thus, a systematic optimum configuration identification and simplification methodology needs to be adopted for the layouts with more elements compared with those low-complexity layouts discussed in Chapter 4.

For inerter-based vibration absorber layouts with more elements, network synthesis theory, which originated in the electrical domain, provides a promising way forward for systematic investigation. A Fixed-sized-inerter layout was introduced by Zhang et al. (2017) which covers a set of seven-element network layouts with one inerter and at most six damper and spring elements. However, this study on Fixed-sized-inerter is for building vibration suppression, it may not so effective for cable vibration suppression with performance improvements obtained with this FSI. Therefore, to further expand the range of network layouts covered, another FSI layout can be introduced which covering a different set of networks. With these two FSI layouts, a wider range of candidate layouts can be covered for investigation and also fully control their inertance meanwhile.

In this chapter, another FSI layout is introduced to further expand the range of network layouts covered. The newly introduced FSI layout may significantly enhance the performance with small inertance values. However, for realistic and useful considerations in terms of practical implementations, a simplification procedure is needed and then adopted to reduce the identified FSI layout from seven to less elements as possible.

Therefore, for inerter-based vibration absorber layouts with more elements, using two types of fixed-sized-inerter (FSI) layouts, optimum inerter-based absorbers for cable vibration suppression is investigated. A simplification procedure is also adopted to reduce the number of elements to the minimum while not compromising the performance gains. So, in Chapter 5, with these two FSI layouts, an approach for the identification of optimum cable vibration absorber configurations is introduced. An efficient and systematic optimum configuration identification methodology is studied and presented.

It worth to point out that in this chapter, in order to be consistent with the second paper in publication list of the thesis, non-dimensional damping coefficients and spring stiffinesses are defined as $c' = (c/M)/\omega_0$ and $k' = (k/M)/{\omega_0}^2$, instead of $c' = (c/M)/(\omega_0/\pi)$ and $k' = (k/M)/(\omega_0/\pi)^2$ (as introduced in Sub-section 3.4.1).

5.2 Network synthesis and Fixed-sized-inerter layouts

It has been shown in the previous study (Luo et al., 2019) that, with small inertance, only limited performance advantages compared with a viscous damper can be achieved

from the three-element absorber configurations which consisting of at most one spring, one damper and one inerter. However, for inerter-based vibration absorber layouts with more elements, network synthesis theory, which originated in the electrical domain, provides a promising way forward for systematic investigation. A Fixed-sized-inerter layout was introduced by Zhang et al. (2017) which covers a set of seven-element network layouts with one inerter and at most six damper and spring elements, for building vibration suppression However, it may not effective for cable vibration suppression with performance improvements obtained with this FSI. Therefore, to further expand the range of network layouts covered, another FSI layout is introduced which covering a different set of networks. With these two FSI layouts, a wider range of candidate layouts can be covered for investigation and also fully control their inertance.

The motivation for proposed FSI layouts is to investigate more different candidate configurations in a systematic way so as to facilitate the identification of beneficial absorbers with practical inertance values.

In this section, two Fixed-sized-inerter (FSI) layouts are introduced which include one inerter and two sub-networks with admittance functions S_1 and S_2 respectively. The FSI-I, shown in Figure (5.1a) was defined by Zhang et al. (2017), demonstrating the benefits of vibration suppression for multi-story buildings. A new FSI layout, i.e., FSI-II shown in Figure (5.2b) which covering a different set of networks, is introduced in this study.

Figure 5.1: The two possible FSI layouts. (a) FSI-I, and (b) FSI-II.

The admittance functions of FSI-I and FSI-II can be derived as $Y_1(s)$ and $Y_2(s)$ respectively, as below,

$$Y_1(s) = \frac{S_2(s)[bs + S_1(s)]}{bs + S_1(s) + S_2(s)}, \tag{5.1}$$

$$Y_2(s) = \frac{bs \cdot S_1(s)}{bs + S_1(s)} + S_2(s). \tag{5.2}$$

In these two functions, S_1 and S_2 are restricted to be first-order admittance functions, respectively expressed as,

$$S_1(s) = \frac{\alpha_1 s + \beta_1}{\gamma_1 s + \delta_1}, \tag{5.3}$$

$$S_2(s) = \frac{\alpha_2 s + \beta_2}{\gamma_2 s + \delta_2}. \tag{5.4}$$

To guarantee that S_1 and S_2 can be realised with damper(s) and spring(s) only, following two conditions need to be satisfied according to relevant network synthesis theory (Storer, 1957),

$$\alpha_1\gamma_1 - \beta_1 \leq 0, \tag{5.5}$$

$$\alpha_2\gamma_2 - \beta_2 \leq 0. \tag{5.6}$$

These two FSI layouts cover a wide range of candidate network layouts for investigation and also fully control the inertance b, so as to facilitate the identification of beneficial absorber configurations with practical inertance values.

5.3 Optimum performance of FSI layouts

For the two FSI layouts synthesised by seven-element networks, the two proposed optimisation measures, i.e., Measures two and three, introduced in Sub-sections 3.3.2 and 3.3.3 respectively, are used here to quantify the effectiveness of suppressing cable vibrations. Measure two is to maximise the minimum damping ratio $\zeta_{c,opt}$ of all modes with frequencies in the range $\omega_e \in (0, 1.5\omega_0)$, meanwhile with the constraint that modes with natural frequencies in the range $\omega_e \in [1.5\omega_0, 6.5\omega_0)$ have no less damping than those for a cable with a viscous damper optimised for Mode 1. While Measure three is to

maximise the minimum product $\zeta_i \cdot \omega_i$, defined as η_i. The damping performance of FSI layouts along with their parameter values of elements are then systematically investigated.

By using Measure two, all modes in the frequency range $\omega_e \in [1.5\omega_0, 6.5\omega_0)$ are included to ensure that the first six modes of the undamped cable are covered by considering the high-mode constraint. For extreme cases, Measure three used here is to maximize the minimum $\eta_i = \zeta_i \cdot \omega_i'$, mainly focusing on that the motion of the cable in the wind causes the changes in the aerodynamic forces equivalent to negative damping effect. Note that ω_i' is the value after non-dimensionalisation introduced in Section 3.4.1. This measure is motivated and justified in Sub-section 3.3.3 previously, which is applicable to galloping-type aerodynamic instabilities. Here, non-dimensional damping coefficients and spring stiffinesses are defined as $c' = (c/M)/\omega_0$ and $k' = (k/M)/{\omega_0}^2$ respectively.

Based on the introduced matFor a given non-dimensional inertance, all the other parameter values in S_1 and S_2 inertance b', ranging from 0 to 1, all the other parameter values in S_1 and S_2 are optimised according to each measures used here. The optimisation results of the two FSI layouts are obtained and analysed, respectively for Measures two and three as below.

5.3.1 Optimum results for Measure two

Firstly, for Measure two, the optimum critical damping ratio, denoted as $\zeta_{c,opt}$, are obtained, and presented in Figure 5.2, in which the dash-curve represents the optimum results for FSI-I, solid-curve for FSI-II, along with two layouts with fewer elements for comparison. The dotted-curve is for the most beneficial low-complexity layout, i.e., Layout III-4 identified in Chapter 4, which representing optimum performance that can be achieved by all low-complexity configurations. And the "cross" represents the optimised damping ratio of Mode 1 for a viscous damper only, i.e., Layout I, with a value of 0.026.

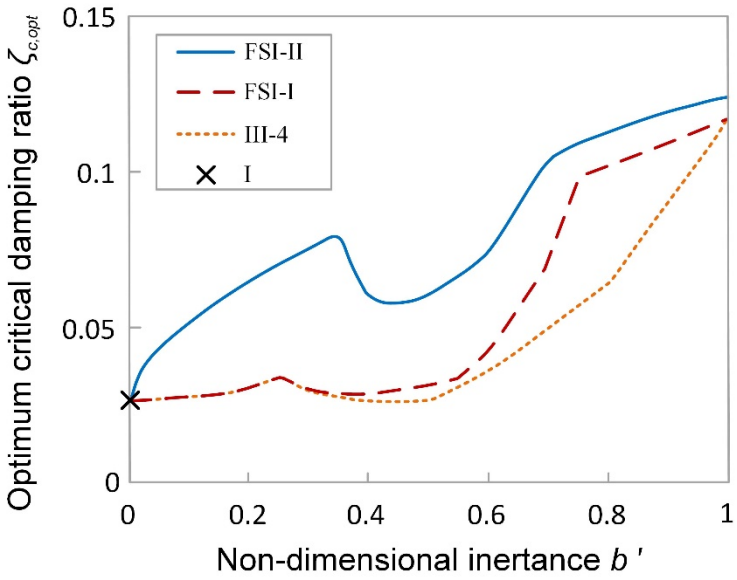

Figure 5.2: Optimum critical damping ratio versus non-dimensional inertance by Measure two for layouts of FSI-I, FSI-II, III-4 and I.

It can be seen from Figure 5.2 that both FSI layouts can provide greater optimum critical damping ratio than that of the most three-element beneficial layout with non-dimensional inertance $0 \leq b' \leq 1$. Compared with Layout FSI-I, Layout FSI-II is more beneficial as it provides better optimum critical damping ratio for all inertance studied. Especially, with small inertance value $b' < 0.36$, the benefits of FSI-II grow rapidly with increasing b'. However, for the range of $0.36 \leq b' \leq 0.45$, the optimum critical damping ratio of FSI-II decreases with the growth of b', due to the limitation that higher modes cannot meet the constraint.

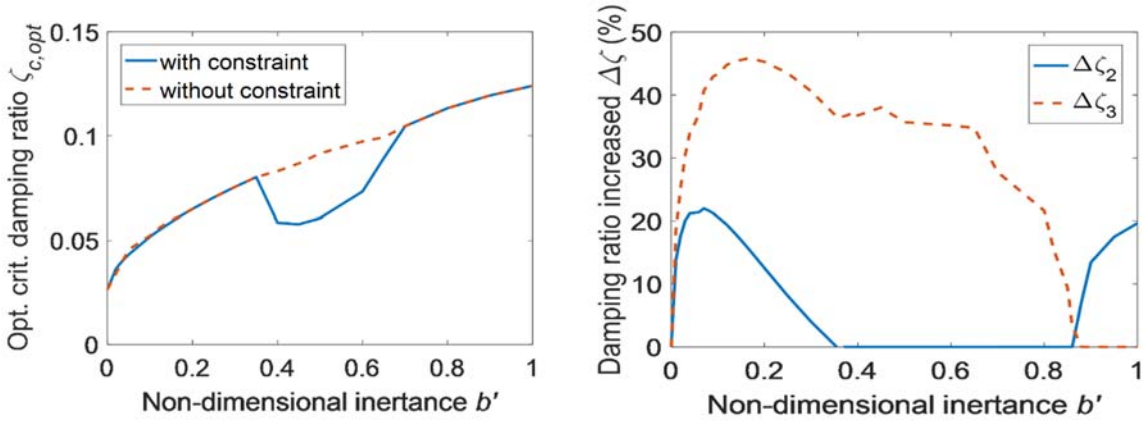

(a) (b)

Figure 5.3: Influence of the higher modes for FSI-II. (a) Optimum critical damping ratio versus non-dimensional inertance with and without the constraint, and (b) percentage increase in damping ratios of Modes 2 and 3 for FSI-II with the constraint over a damper only optimised for Mode 1.

The influence of higher-mode constraint on optimisation results of layout FSI-II are presented in Figure 5.3. The optimum results of FSI-II by Measure two, respectively with and without the higher mode constraint, are compared in Figure (5.3a), clearly showing the influence of the constraint. For non-dimensional inertance $0.36 \leq b' < 0.70$, the damping ratio is significantly influenced by the constraint, but for other inertance values, the difference between the optimised results respectively with and without the constraint is minimal.

In order to examine the influence of the higher mode constraint, the percentage increase in the damping ratio for Modes 2 and 3, compared between layout FSI-II with the higher mode constraint over layout I, a viscous damper optimised for Mode 1, are presented in Figure (5.3b) as example. When non-dimensional inertance $b' < 0.36$, the optimised results are not influenced by the higher mode constraint, neither for the Mode 2 nor Mode 3. While for the middle range of $0.36 < b' < 0.86$, the optimised result of layout FSI-II is limited by the Mode 2. While for $b' > 0.86$, the optimised result is limited

by the Mode 3 rather than the Mode 2. Modes 4 to 6 are not shown in the figure as they do not influence the results.

5.3.2 Optimum results for Measure three

The optimisation results for the two FSI layouts against Measure three are presented in Figure (5.4a), showing the relationship between optimised critical η_i and non-dimensional inertance b', with solid-curve for FSI-II and dash-curve for FSI-I respectively. The cross representing the performance of layout I, i.e., a viscous damper, is also presented as a standard for the comparison. Note that all modes in the frequency range $\omega_e \in (0, 6.5\omega_0)$ are included for consideration by the optimisation.

It can be seen from Figure (5.4a) that in most b' value considered, the FSI-II provides much greater optimised critical η_i than that of FSI-I. Obviously for FSI-II with $b' = 0$, the optimised critical $\eta_i = 0.026$, which is the same as that of Layout I. Compared with maximum optimum value of $\eta_i = 0.063$ for $b' = 1$, the local optimum value $\eta_i = 0.055$ with a small inertance of $b' = 0.09$ is only marginally less effective, and it can provide significant benefits compared with Layout I. While for relatively large inertance b', changing from 0.09 to 0.68, the optimised values of critical η_i of Layout FSI-II do not change significantly.

To illustrate the results further, Figure (5.4b) presents η_i of higher modes using the same parameters which provide FSI-II in Figure (5.4a). When non-dimensional inertance $b' \leq 0.09$, η_1 shows the lowest value, while for $0.09 \leq b' \leq 1$, the optimised result of FSI-II is provided by η_2. The values of η_i of higher modes are not limiting modes, so they are not shown in Figure (5.4b). However, no improvements are found from Layout III-4 for $b' = 0.36$ for the both measures, compared with Layout I.

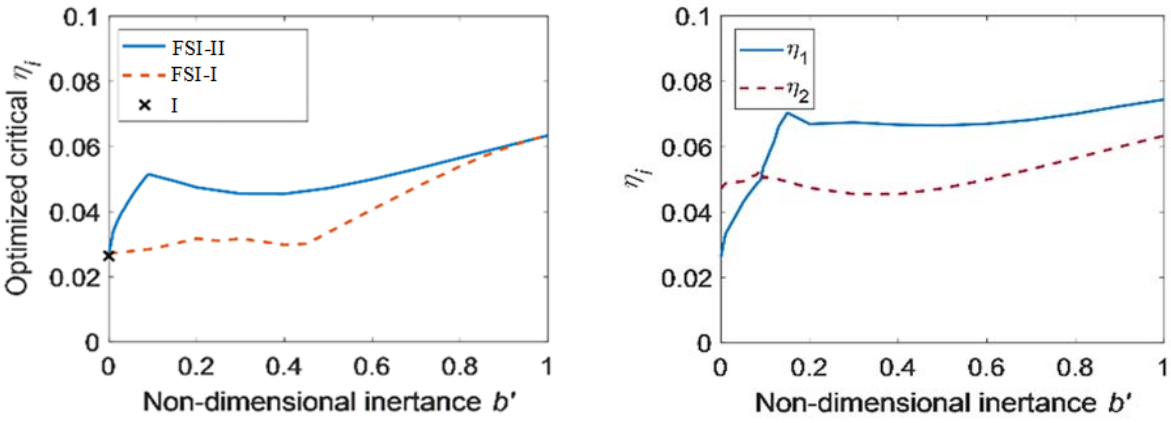

(a) (b)

Figure 5.4: Optimised η_i versus non-dimensional inertance using Measure three. (a) Optimum results for FSI-I and FSI-II, and (b) η_i for Modes 1 and 2 with the optimised solution of FSI-II.

5.3.3 Performance improvements from FSI layouts

Essentially, FSI-II covers a different set of candidate layouts from FSI-I. Layouts IV-1 and IV-2 are special cases, simplified from FSI-II, in which some element values were set to zero or infinity. The reason for Layouts IV-1 and IV-2 to be beneficial, especially with small inertance, can be explained as below. Compared with the most beneficial three-element layout III-4, Layouts IV-1 and IV-2 not only have a resonance network tuned to the first cable mode, the parallel damper, i.e., c_3 shown in Figure 5.6, also effectively damps out the vibrations of higher modes.

By using proposed performance measures, significant improvements obtained from FSI layouts, particularly from Layout FSI-II, have been found over optimised damper, i.e., Layout I, and also the most beneficial three-element layout, i.e., the identified Layout III-4 in Chapter 4.

Considering both physical implementation issue and also performance improvement extents, three typical inertance values of b' are taken as examples here, i.e., a very small b' of 0.05 which can be more for physical implementation, and 0.36 which corresponds

to local maximum optimum critical damping ratio using Measure two and 0.09 corresponding to local optimum using Measure three.

The optimisation results for Measure two are presented in Table 5.1, with the three different values of non-dimensional inertance b' as 0.05,0.09 and 0.36 respectively. For Measure three, the optimisation results with the three different values of non-dimensional inertance are presented in Table 5.2. For $b' = 0.36$, no improvements are found from the most beneficial three-element layout III-4.I

Table 5.1 Optimisation results ($\zeta_{c,opt}$) with different non-dimensional inertances for Measure two

Layouts	$b' = 0.05$	$b' = 0.09$	$b' = 0.36$
FSI-II	0.0452	0.0533	0.0840
FSI-I	0.0271	0.0278	0.0271
III-4	0.0271	0.0278	—

Table 5.2 Optimisation results (optimised η_i) with different non-dimensional inertances for Measure three

Layouts	$b' = 0.05$	$b' = 0.09$	$b' = 0.36$
FSI-II	0.0432	0.0508	0.0454
FSI-I	0.0271	0.0278	0.0301
III-4	0.0271	0.0278	—

Based on the optimisation results for Measures two and three (respectively for $\zeta_{c,opt}$ and η_i) with different non-dimensional inertances, respectively presented Tables 5.1 and 5.2, the relative improvements over a damper only can be obtained for observing the benefits from these layouts. The optimum results for a damper only equal to 0.0264 for both Measures two and three.

With all considered values of non-dimensional inertance, improvements over a viscous damper, for Layouts FSI-II, FSI-I and the three-element layout III-4 can be calculated based on Tables 5.1 and 5.2. For Layout FSI-I, the biggest improvements compared with a viscous damper for Measures two and three are 5.3% and 14%, respectively when b' are equals 0.09 and 0.36. And for the three-element Layout III-4, it is even less beneficial compared with FSI-I for both Measures two and three. On the other hand, it can be also calculated that Layout FSI-II provides the greatest relative improvements in all cases.

For non-dimensional inertance b' of 0.36 by using Measure two, the relative improvements of Layouts FSI-II to Layout I is up to 221.2%, indicating that optimum critical damping ratio can be over twice compared with a viscous damper only. For Measure three, relative improvements of FSI-II are also very significant for all considered values of non-dimensional inertance, respectively being 63.63%, 92.05% and 71.97% corresponding to b' of 0.05, 0.09 and 0.36. Hence, the fixed-size inerter layout FSI-II is identified as the most beneficial layout in the study.

5.4 Simplification procedure and identified four-element optimum configurations

In Section 5.3, significant advantages against both performance measures have been identified for the FSI-II layout, illustrated in Figure (2b), even with small inertance values. However, to realise these identified configurations, networks with seven elements are required. For example, using the Foster preamble (Van Valkenburg, 1962), one of the possible mechanical structures of FSI-II is shown in Figure 5.5. For physical implementation of a mechanical vibration absorber, it is highly desirable to minimise the number of elements, so in this section a simplification procedure is carried out. The optimum performance of the simplified configurations is then compared with that of the optimized results for FSI-II. The values of the damping coefficients and stiffnesses of the dampers and springs are still expressed in non-dimensional form as $b' = b/M$, but here the non-dimensional damping coefficient and spring stiffness are defined as $c' = (c/M)/(\omega_0)$ and $k' = (k/M)/{\omega_0}^2$, where c and k are the physical damping coefficients and stiffnesses, respectively. Note that only in Section 5.4, non-dimensional damping coefficients and spring stiffinesses are defined as $c' = (c/M)/(\omega_0)$ and $k' = (k/M)/{\omega_0}^2$, which are not same as those used in other chapters, as introduced in Sub-section 3.4.1.

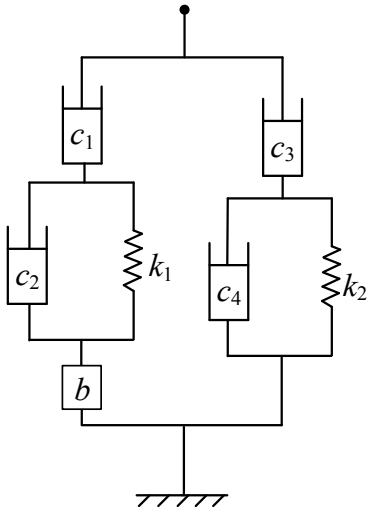

Figure 5.5: A seven-element network denoted as FSI-II.

5.4.1 Simplification procedure and simplified layouts

The simplification procedure is carried out in the following way. The optimisation in the previous section for FSI-II delivers multiple local maximum of the critical damping ratio (for Measure two) or critical η_i (for Measure three) with very similar results but for different values of the parameters in Equations (5.3) and (5.4). It was found that for some results where γ_1 in S_1 is smaller than 0.001, it can be approximated as zero, and for other results where α_1 in γ_1 is smaller than 0.001, it can be approximated as zero. If γ_1 and α_1 are respectively set to zero, the layout represents S_1 show in Figure (5.6a) can then be realised by the simplified layouts shown in Figures (5.6b) and (5.6c) correspondingly.

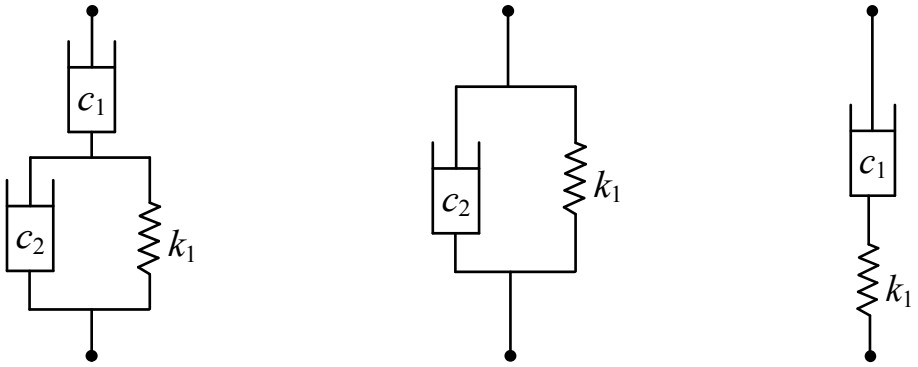

(a) (b) (c)

Figure 5.6: Simplification procedure of S_1. (a) The sub-network realising S_1 in FSI-II, and its simplification to (b) a spring-parallel-damper layout, and (c) to a spring-series-damper layout.

Similarly, it was found that the optimisation results for α_2 β_2 and γ_2 will make Equation (5.4) close to a constant value if we set Equation (5.4) to such a value, then S_2 shown in Figure (5.7a) can be realised by the layout with a damper only, shown in Figure (5.7b). Depending on the cases where S_1 is simplified to Figures (5.6b) or (5.6c), two four-element layouts IV-1 and IV-2 shown in Figure 5.8 are obtained.

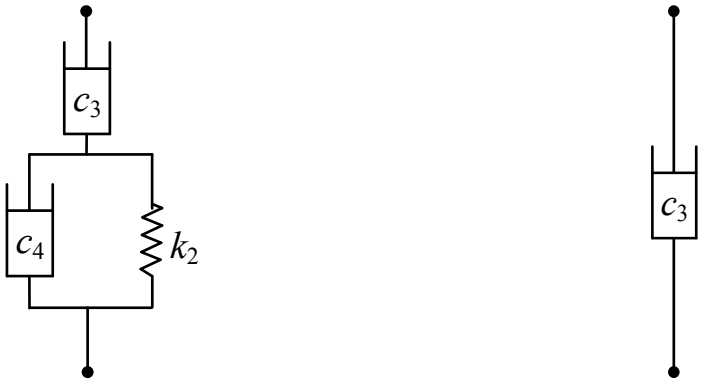

(a) (b)

Figure 5.7: Simplification procedure (a) S_2 in FSI-II and its simplification to (b) a layout with a damper only.

The corresponding cost function values of Measure two and Measure three with configuration with layouts are then compared with the optimum achieved by the seven-element FSI-II layout in Figure 5.5. Where the performance difference is within 1%, the element simplification is considered worthwhile.

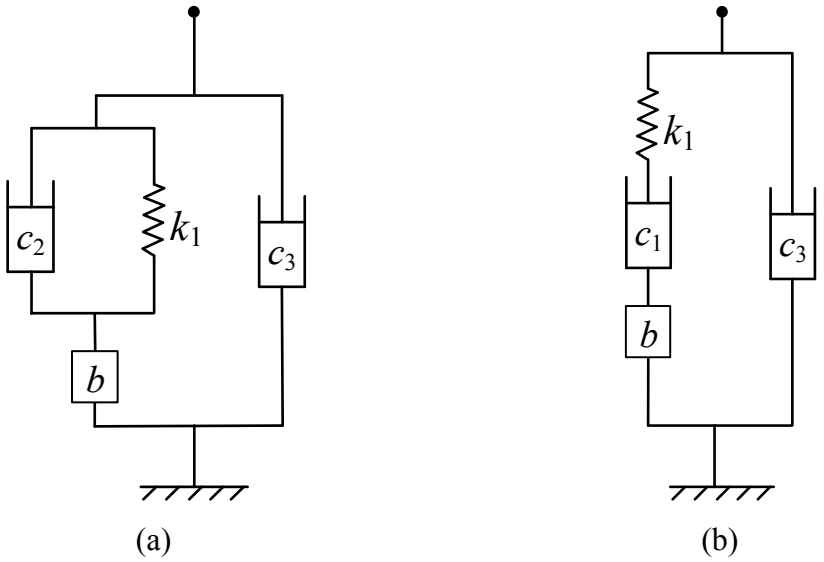

Figure 5.8: Mechanical structures of simplified four-element layouts. (a) Simplified layout IV-1, and (b) simplified layout IV-2.

5.4.2 Optimum results for Measure two

For Measure two, the optimum critical damping ratio $\zeta_{c,opt}$ for the configurations with layouts IV-1 and IV-2 are presented and compared in Figure 5.9 and 5.10, along with the corresponding element values. In order to examine the effectiveness of the proposed simplification approach, the results for the other layouts, i.e. seven-element layout FSI-II and also the layout of a damper only are also presented in Figure 5.9. The non-dimensional damping coefficients c'_1, c'_2, c'_3 and spring stiffness k'_1 versus non-dimensional inertance b′ are respectively shown in Figure 5.10.

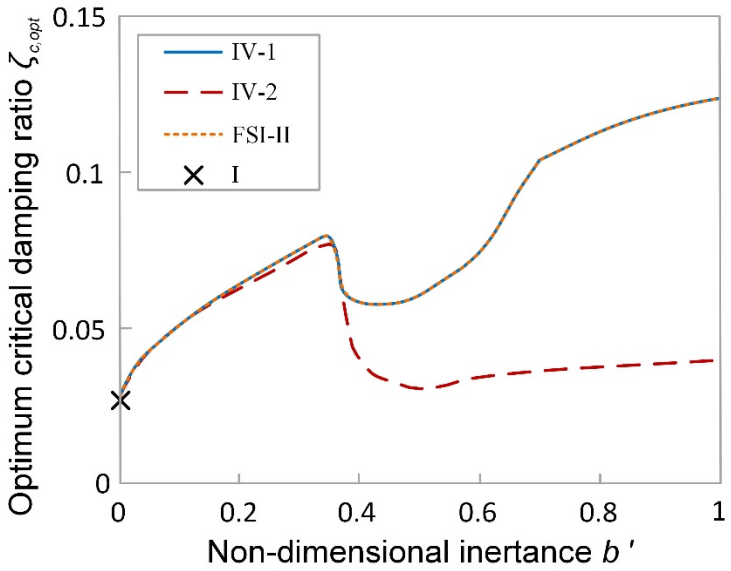

Figure 5.9: Optimum critical damping ratio of Layouts IV-1, IV-2, FSI-II and I using Measure two versus non-dimensional inertance.

It can be seen from Figure 5.9 that the optimum critical damping ratio $\zeta_{c,opt}$ provided by the simplified layout IV-1 is virtually the same as that for FSI-II with seven elements for the full range of b' considered, while IV-2 is similarly effective only for $b' \leq 0.36$. For both simplified layouts, the $\zeta_{c,opt}$ value not affected by the higher mode constraint with $b' \leq 0.36$ and a maximum improvement of 206% compared with a optimised viscous damper can be seen. It should be noted that layout IV-1 requires less or equal parameter values for both damping element and stiffness compared with layout IV-2.

Corresponding the optimum critical damping ratios of layouts, shown in Figure 5.9, the parameters value of the structure elements are presented in Figure 5.10. It can be seen from Figure (5.10a) that Layout IV-1 requires a lower damping coe□cient, however, for Layout IV-1, c'_2 is very small with $b' < 0.2$, it cannot be removed as there will be significant loss in optimum damping ratio. Figures (5.10b) and (5.10c) shows that for $b' \leq 0.36$ both layouts requires virtually the same values of c'_3 and k'_1.

It can be seen from Figure (5.10c) that compared with Layout IV-2, rather clear relationship can be found between $\zeta_{c,opt}$ element values (c'_2 , c'_3 and k'_1) for Layout IV-1.

It can be seen that for $b' \leq 0.36$, the developing trends of damping coefficients c'_2 and c'_3 are opposite, the former increases and the latter decreases with the growth of b'. In Figure (5.10c), an approximate linear relationship can be found between non-dimensional inertance b' and corresponding non-dimensional spring stiffness k'_1 within a wide range, i.e., $b' < 0.9$. While for Layout IV-2, only when $b' \leq 0.4$, the linear relationship is found after this value the impact of spring k'_1 decreases rapidly. This can be explained as follows. For IV-1 with $b' < 0.9$ and IV-2 with $b' < 0.4$, the frequency provided by the ratio of k'_1/b' is approximately equal to one, which has only marginal difference with the natural frequency of cable's undamped Mode 1, implying that the b' and k'_1 is basically tuned for the first mode of cable.

Results showed that with three-element layouts without the parallel damper (Luo et al., 2019), very beneficial damping ratios can be provided for the first mode of cable, however, damping ratio improvement for higher modes are marginal. While c'_3 is smaller than the value of damping coefficient for the damper only optimised for Mode 1 as shown in Figure (5.10b), it leads to most damping ratio enhancement for the higher modes.

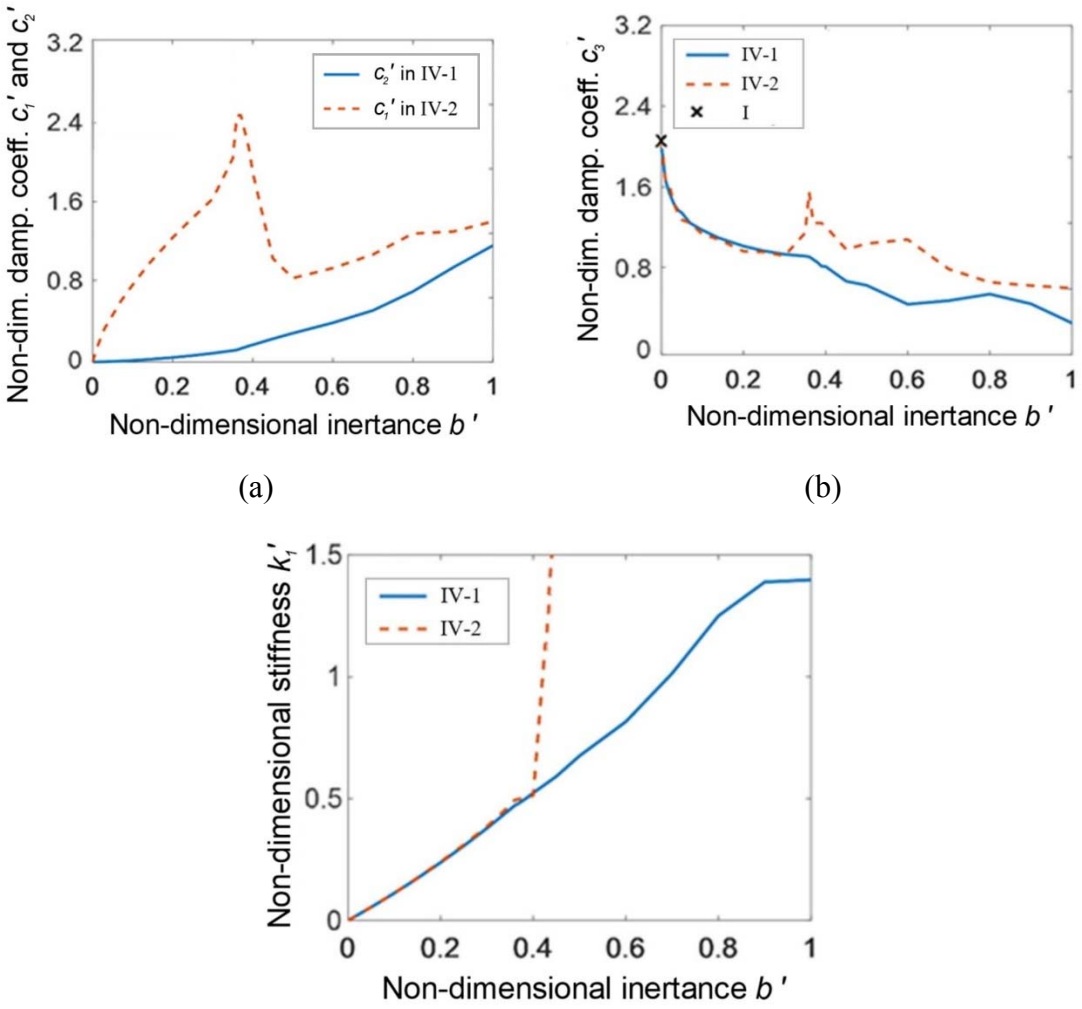

Figure 5.10: Corresponding non-dimensional parameter values for Layouts IV-1 and IV-2 using Measure two. (a) Damping coefficients c_1' and c_2', (b) damping coefficient c_3' and (c) spring stiffness k_1'.

5.4.3 Optimum results for Measure three

For Measure three, the optimal critical η_i for the configurations with IV-1 and IV-2 are presented and compared in Figure 5.11, along with the corresponding element values presented in Figure 5.13. As shown in Figure 5.11, the simplified four-element layout IV-1 provides almost the same performance as the seven-element FSI-II over the whole range of studied inertance, but the simplified layout IV-2 can only achieve the similar results with $b' \leq 0.25$.

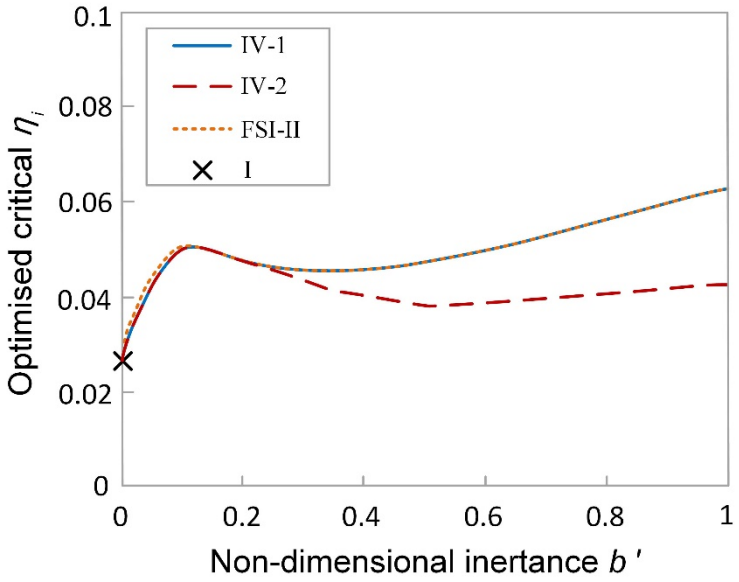

Figure 5.11: Optimised critical η_i versus non-dimensional inertance for Layouts FSII-II, IV-1 and IV-2 using Measure three.

Using Measure three, based on the optimised critical η_i shown in Figure 5.11, the corresponding non-dimensional parameter values for Layouts IV-1 and IV-2 are presented in Figure 5.12, including the non-dimensional damping coefficient c_1' of Layout IV-2, c_2' of Layout IV-1, damping coefficient c_3', and spring stiffness k_1', as illustrated by Figure 5.9 previously.

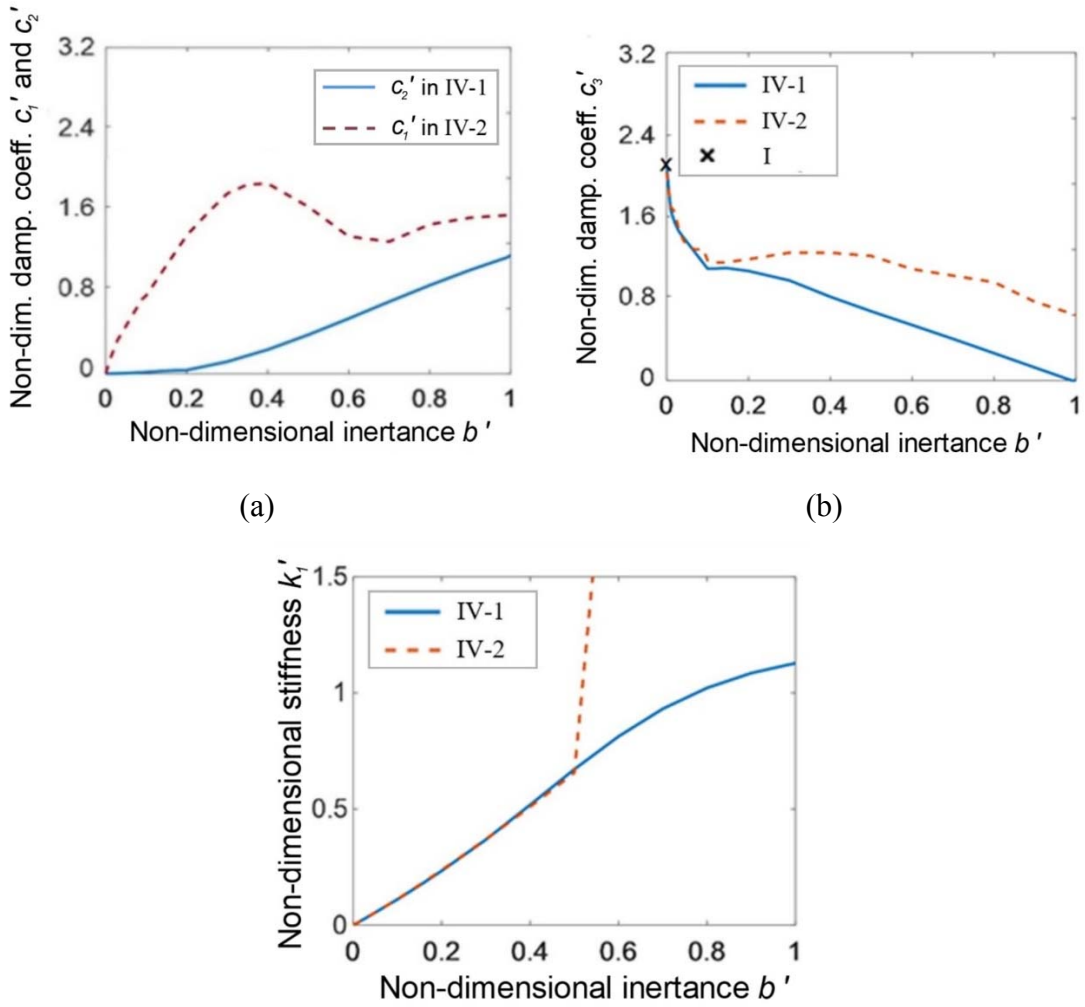

Figure 5.12: Corresponding non-dimensional parameter values for Layouts IV-1 and IV-2 using Measure three. (a) Damping coefficients c_1' and c_2', (b) damping coefficient c_3', and (c) spring stiffness k_1'.

It can be seen from Figures (5.12a) and (5.12b) that the simplified layout IV-1 requires same or less damping coefficients for both dampers compared with Layout IV-2. Also, the required parallel damping c'_3 is much less than that of the optimum damper. Figure (5.12c) shows that, in the range of $b' < 0.7$ for IV-1 and $b' < 0.5$ for IV-2, non-dimensional stiffness k_1' increase with the growth of b' are almost proportionally. This

means that the internal resonance of the absorber are close to the first mode of cable. For IV-2 with $b' \geq 0.5$, k' tends to be infinity, indicating that a three-element layout with two dampers and one inerter only, which leads to far less beneficial performance compared with the original FSI-II and the simplified IV-1.

Similar to the analysis for the results using Measure two, three typical values of non-dimensional inertance are taken as examples, i.e., a relatively small value of non-dimensional inertance $b' = 0.05$, the corresponding inertance providing local maximum $b' = 0.09$ and a relative large value $b' = 0.36$. The improvement of the performance criterion for Measure three, i.e., optimised critical η_i compared with the optimised damper for all modes within the damped natural frequency range of 0 to $6.5\omega_0$ are analysed and compared for different layouts, including the simplified four-element layouts IV-1 and IV-2, and the most beneficial three-element layout III-4 which is identified in (Luo et al., 2019).

The results showed that the three-element layouts can only provide marginal improvements compared with the damper only case. On the other hand, significant improvements of the critical η_i are obtained for both the configurations with the simplified layouts IV-1and IV-2. An extra η_i can be found with the same reason explained in Sub-section 5.4.2. For both simplified four-element layouts IV-1 and IV-2, it is found that for $b' = 0.05$, even though the extra mode is tuned for Mode 1, the original Mode 1 still provides the least η_i and remains as critical. For $b' = 0.09$ which provides the local maximum, the extra mode is tuned for Mode 1, and both Modes 1 and 2 are critical. The result analysis and the comparison for different layouts will be summariesed and presented in the following section in more details.

5.4.4 Improvements of simplified layouts with different inertances

Using the damper optimised for Mode 1 as a standard, corresponding damping ratios are compared among identified four-element layouts IV-1 and IV-2, along with the most beneficial three-element layouts identified in (Luo et al., 2019), respectively for Measures two and three.

First, for Measure two, taking two non-dimensionalised inertance values b', equal to 0.05 and 0.36 as examples, the relative damping improvements from IV-1 and IV-2 along with the three-element layout compared with viscous damper only are shown in Figure 5.13. Both simplified layouts can achieve significant improvements for Measure two. With non-dimensional inertance b' of 0.05 and 0.36, the relative improvements from IV-1 to viscous damper can be up to 72.05% and 221.2%, shown in Figures (5.13a) and (5.13b) correspondingly.

It should be noted that there could be more than six damped natural frequencies in the range from 0 to $6.5\omega_0$ due to the extra DOF(s) in the absorber layout, normally resulting in a pair of close modes. The two close modes have very similar damping ratios as well as natural frequencies. The resonances introduced by the inerter and spring are able to greatly increase the damping ratios of these modes relative to the original undamped mode. In this way, the resonances introduced by the inerter and spring elements are able to greatly enlarge the damping ratio of that mode.

It can be seen from Figure (5.13a) that for $b' = 0.05$, Layouts IV-1 and IV-2 are much more beneficial among all six modes than the three-element layout and the optimised viscous damper. For $b' = 0.36$ shown in Figure (5.13b), the relative improvement of the three-element layout over optimised damper is very marginal. It has been found that none of the three-element layouts studied previously can be more beneficial than a viscous damper only with these tested b', and the performance of identified Layouts IV-1 and IV-2 are limited by the Mode 2 of the cable.

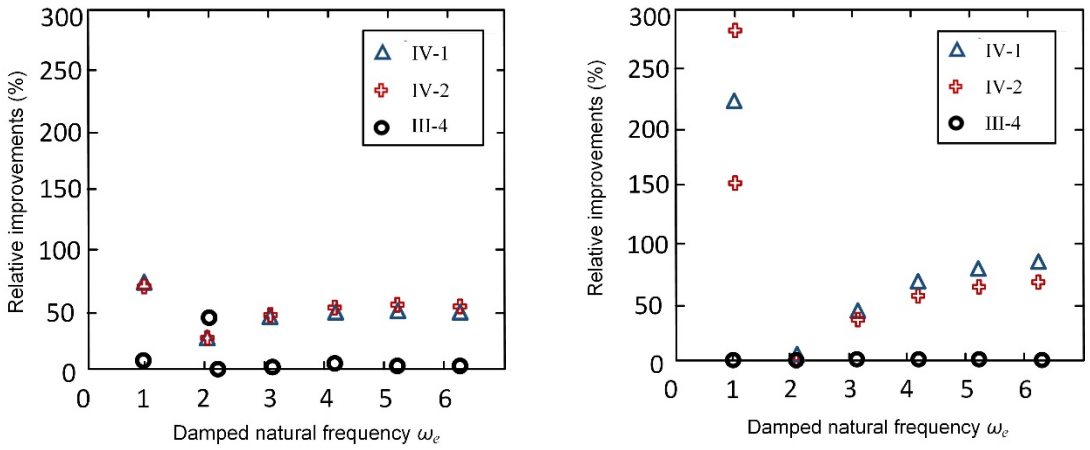

Figure 5.13: Relative improvement to optimised viscous damper by using Measure two. (a) For non-dimensional inertance b' of 0.05, and (b) for b' of 0.36.

Therefore, the results for Measure two show that, with considered two values of the non-dimensional inertance, the performance advantages of optimum three-element layout are marginal. In comparison, significant enhancement are observed for both IV-1 and IV-2. Comparing the two simplified beneficial layouts, IV-1 provides the greater relative improvements in most cases.

For Measure three, taking the non-dimensional inertance $b' = 0.09$ which provides the local maximum as example, the optimised performance criteria, i.e., critical η_i are compared with the optimised damper for all modes within the damped natural frequency range of 0 to $6.5\omega_0$, among the simplified layouts IV-1and IV-2, and the most beneficial three-element layout III-4. The relative improvements of corresponding η_i for all modes within damped natural frequency range of 0 to $6.5\omega_0$ for b' of 0.09 are compared in Figure 5.14.

It can be seen from Figure 5.14 that three-element layouts can only provide marginal improvements compared with the damper only case. On the other hand, an improvement of 102% for optimised critical η_i is achieved for simplified layout IV-1, while simplified layout IV-2 achieving a similar improvement. This reflects to 84% improvement compared with the most beneficial three-element layout III-4. It worth to point out that

because of the additional degrees of freedom introduced by Layouts IV-1and IV-2 tuned for Mode 1, there are two close modes around $\omega' = 1$. So, very similar values of η_i for both IV-1and IV-2 cases are shown in the figure.

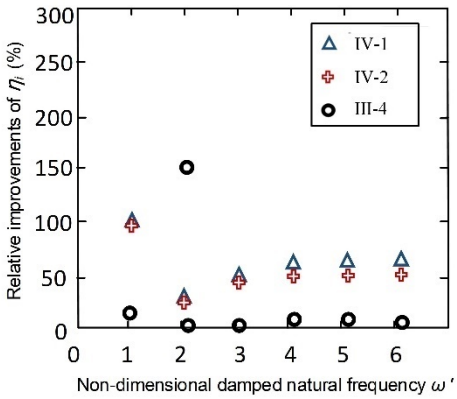

Figure 5.14: Relative improvements of corresponding η_i for all modes within damped natural frequency range of 0 to 6.5ω_0 for b' of 0.09.

Therefore, from the Figure 5.14, it can be seen that both Layouts IV-1 and IV-2 can provide much greater η_i compared with Layouts I and III-4 when $b' = 0.09$. Besides, taking a small non-dimensional inertance $b' = 0.05$ as example, the results show that the relative improvements of Layouts IV-1 over Layout I and III-4, i.e., the optimised damper and the most beneficial three-element layout, can be up to 72.1 and 66.8% respectively.

5.5 Summary

In this chapter, with a finite element model of the cable-absorber system and two proposed performance measures, i.e., Measures two and three, an investigation is carried out to identify absorber layouts that have substantially better performance than both viscous damper only and the most beneficial three-element layout identified in Chapter 4. The systematic identification is facilitated by using two fixed-sized-inerter (FSI) layouts generated via network synthesis and represented by corresponding admittance functions, respectively denoted as FSI-I and FSI-II. Their optimum results are searched with non-dimensional inertance in the range of 0 to 1. The results show that both FSI layouts can

provide enhanced performance, while Layout FSI-II, which is firstly introduced in this thesis, can provide significantly better overall damping performance for all values of inertance tested.

Two four-element layouts IV-1 and IV-2 are identified with similar performance results to the most beneficial seven-element layout FSI-II with a range of inertance values. The results indicate that for relatively low inertance values, both simplified layouts can provide very similar performance, while Layout IV-1 is as effective as FSI-II over wider range of inertance and meanwhile requires a lower damping coefficient for one of the dampers. It has been shown that benefit against both measures can be obtained with small inertance, which is critical for real-life implementation.

By using Measure two, the relative improvements to optimised viscous damper are significant from Layout IV-1. With non-dimensional inertance b' of 0.05 and 0.36 respectively, the relative improvements to viscous damper is up to 72.05% and 221.2% correspondingly. By using Measure three, for Layout IV-1 when b' =0.09 for example, an improvement of 102% for optimised critical η_i is achieved over the optimised damper and 84% improvement compared with the most beneficial three-element layout III-4 identified in Chapter 4. The results show that Layout IV-2 can achieve similar improvements.

Since large benefit against both measures can be obtained by simplified layouts even with small inertance, the simplified four-element layouts can be more realistic to implement in practice than the seven-element FSI layouts.

Due to its overall beneficial performance, it is concluded that the simplified four-element layout IV-1 is the most beneficial with a wide range of inertance. Therefore, it can be a good candidate layout to effectively suppress cable vibrations in practical applications.

Chapter 6

Effects of series compliance and absorber location

6.1 Introduction

In this chapter, based on the proposed mathematical approach introduced in Chapter 3, other effects on damping performances for suppressing cable vibration are investigated. For the identified beneficial layouts, comprehensive investigations are carried out to examine the effects of connection series compliance velues and absorber locations on damping performance, for both before and after tuning the absorber parameters. Due to the difficulties for examining the influences of various parameters which influence each other, all concerned parameters for a cable-absorber system are non-dimensionalised, including the series compliance represented by non-dimensionalised spring stiffness and the absorber location parameter which is non-dimensionalised, represented by its relative location to the total length of the cable.

In practice, the connections at either end of the absorber, with the support and with the cable, may not be fully rigid. Apart from compliance of the connections themselves and of any axial linkage element, for common bridge cables made up of multiple parallel strands in an outer sheath, there may be relative movement between the sheath, to which the absorber is usually attached, and the structural strands inside. The lack of rigidity may be expected to reduce the performance of the absorber. In order to quantify this effect, a compliant element is introduced in series with the absorber.

Firstly, considering the fact that the connections at either end of the absorber (with the support and with the cable) practically are not fully rigid in most cases, the effects of series compliance are investigated in this chapter. The influences of the series compliance along with structure parameters of various inerter-based absorber configurations on optimisation performance are examined. The effects on the beneficial absorber layouts, identified in Chapters 4 and 5, are comprehensively studied for both before and after retuning of their structure parameters.

Damper is usually installed near the cable support on the deck, which constrains the vibration mitigation effectiveness of the damper. The problem of the optimal damping constant of a viscous damper located close to one end of a taut cable was studied, showing that the optimum damping ratio of each mode are proportional to the damper's location (Pacheco et al., 1993). Moreover, the relevant study also showed that, that the modal damping provided by viscous dampers may drop dramatically, as the cable mode shape may be zero close to the support when the cable geometry-elasticity parameter is close to the frequency avoidance point (Xu and Yu, 1998).

Then, the effect of the absorber location is studied to examine the influence of non-dimensional inertance parameter and the location parameter on optimum critical damping ratio, taking two identified beneficial layouts, i.e., III-4 and IV-1 as example, which are identified in Chapters 4 and 5 respectively.

The proposed approach introduced in Chapter 3.3 is briefly recalled here, indicating the established finite element cable model, and the three performance measures. For generality, all values of element parameter are scaled introduced in Sub-section 3.4.1, including damping coefficient and stiffness of the absorber elements, defined as $b'=b/M$, $c'=(c/M)/(\omega_0/\pi)$ and $k'=(k/M)/(\omega_0/\pi)^2$ respectively. The circular natural frequencies ω_e of the damped system and the location of the damper relative to the total length of the cable a_f are also presented in non-dimensional forms as $\omega'=\omega_e/\omega_0$ and $a'_f=a_f/(n+1)$, respectively.

Based on the established generic model and proposed approach, the effects of series compliance, the structure parameters of the absorber and the installation location of the absorber are investigated as below.

6.2 Effects of series compliance

For simplicity, it is modelled as an ideal spring of non-dimensional stiffness k_{sc}'. The upper limit of possible stiffness values is considered infinite. The lower realistic limit is estimated using simplified assumptions as following. For vibrations of the main length of the cable (from the absorber to the other end) in a half sine wave mode shape, neglecting motion of the point where the absorber is attached and the short length of cable between that point and the near end, the force on the absorber is given approximately by $T\theta_{af}$ (as shown in Figure 3.1). The maximum value of θ_{af} approximately equals $\pi x_{max}/L$, where x_{max} is the maximum displacement at the anti-node of the mode. If this force causes a deformation between the end of the absorber and the cable, denoted as γ, the equivalent linear stiffness of the series spring, k_{sc}, is equal to $T\pi x_{max}/(L\gamma)$. Hence the non-dimensional stiffness k_{sc}' is simply $\pi x_{max}/\gamma$. Typically, it is aimed for x_{max} to be limited to the diameter of the cable, which is normally about 200 mm, whilst the deformation γ is estimated to be of the order of 10 mm. Hence the minimum value of k_{sc}' in practice is estimated to be around 60.

Therefore, in this section, to more than cover the range of expected values, non-dimensional stiffness k_{sc}' is taken to be in the range of 10 to infinity for investigating the effect of the series compliance which is idealised as a linear spring element.

The effects of series compliance are analysed by using the proposed performance measures, introduced in Sub-sections 3.3.1 and 3.3.2, i.e., Measures one and two, respectively without and with the higher-mode constraint. The higher mode constraint used here is the performance of a viscous damper with the same series compliance, rather than the universal curve (Pacheco et al., 1993).

The effect of series compliance is comprehensively investigated, firstly for those low-complexity beneficial layouts identified in Chapter 4. However, the beneficial layouts with two elements, i.e., Layouts II-3 and II-4, are not discussed here, as the optimisation results show that both layouts cannot achieve the same level of critical damping ratio when series compliance is included.

Therefore, four three-element beneficial layouts identified in Chapter 4 and two beneficial four-element layouts simplified from beneficial layout FSI-II are investigated

in this section. These totally six beneficial layouts, each including the series compliance represented by a non-dimensionalised spring k_{sc}', respectively are the three-element layouts, i.e. Layouts III-3_{sc}, III-4_{sc}, III-5_{sc} and III-6_{sc}, and four-element layouts IV-1_{sc} and IV-2_{sc}, presented in Figure 6.1.

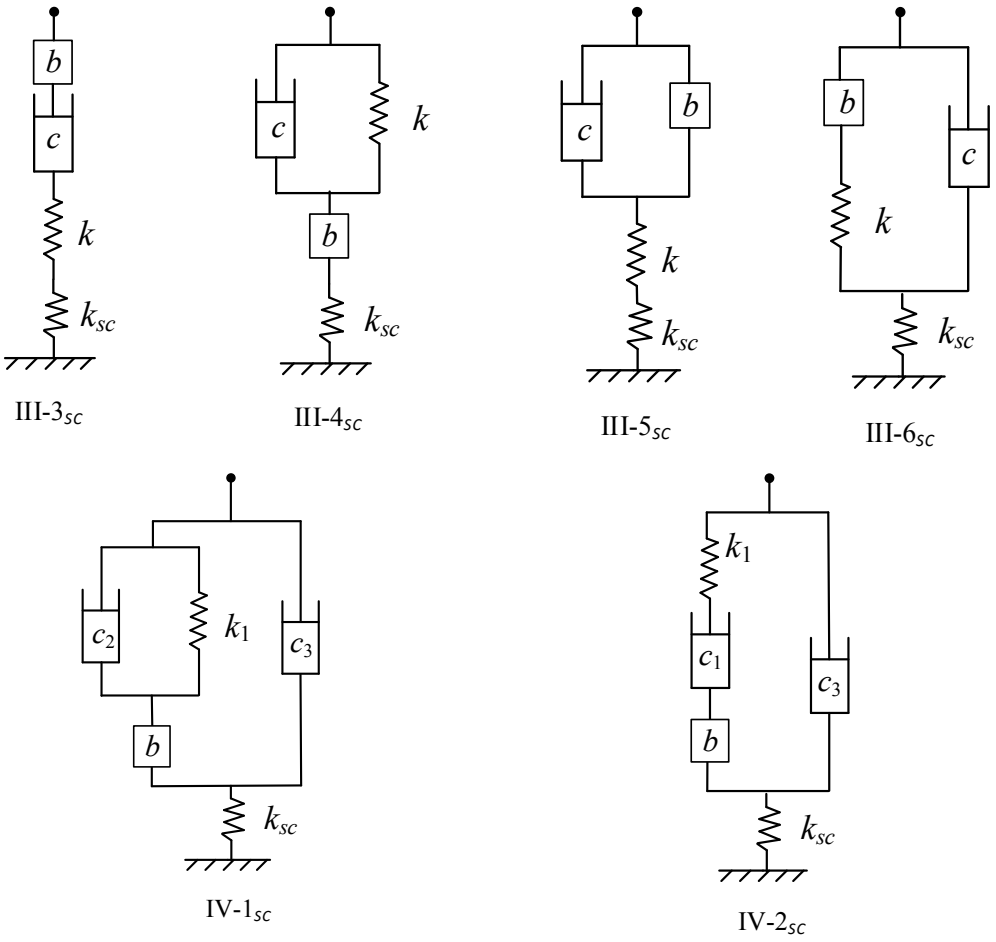

Figure 6.1: Beneficial three-element and four-element layouts with added series compliance.

By using proposed performance measure, i.e., Measure one described in Sub-section 3.3.1, the optimisation criterion for these layouts is to maximise the minimum damping ratio $\zeta_{c,opt}$ of all modes with frequencies in the range $\omega_e \in (0, 1.5\omega_0)$. The maximum critical non-dimensional inertance b_m', is introduced, which is defined as the non-dimensional inertance of the re-optimised absorber with series compliance. It at least the same

optimum critical damping ratio as the corresponding optimised absorber without series compliance can be achieved.

Since Layouts III-3_{sc} and III-5_{sc} have two springs in series, so it is clear that if $k_{sc}' \geq k_o'$, where k_o' is the original optimised non-dimensional stiffness without series compliance, they can be re-optimised to have identical properties to the original optimised layouts. The retuned k' can simply be calculated as $k' = 1/[(1/k_o') - (1/k_{sc}')]$. This is possible for of $b' < b_m'$, at which $k_{sc}' = k_o'$, and the maximum value of $\zeta_{c,opt}$ is achieved. For $b' > b_m'$ the performance of Layouts III-3_{sc} and III-5_{sc} rapidly decreases, but it is still larger than without retuning k'. For Layout III-6_{sc} it is still much more beneficial than the case where the parameters are not retuned cannot reach the original optimum even if the absorber is retuned. Thus the most beneficial three-element and four-element layouts Layout III-4_{sc} and Layout IV-1_{sc} are taken as example and analysed in this section.

Still using the previously optimised parameter values, when the series compliance is added, the critical damping ratios decrease significantly for all layouts. The effect of k_{sc}' on critical damping ratios for beneficial Layout III-4_{sc} and Layout IV-1_{sc} are presented in Figures 6.2 and 6.3 respectively.

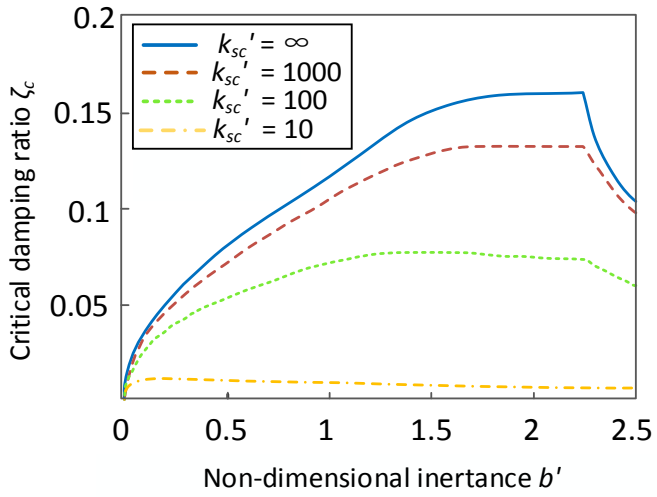

Figure 6.2: Critical damping ratio versus non-dimensional inertance with various values of non-dimensionalised series compliance k_{sc}' with parameters optimised for Layout III-4_{sc}.

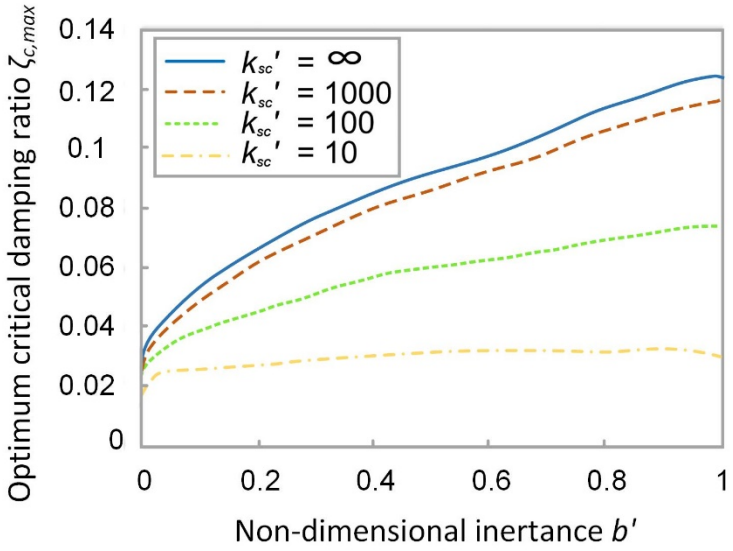

Figure 6.3: Critical damping ratio versus non-dimensional inertance with various non-dimensionalised series compliance k_{sc}' with parameters optimised for Layout IV-1_{sc}.

The effects of k_{sc}' on critical damping ratios for four-element beneficial layout, IV-1_{sc} which is the most beneficial four-element layout, simplified from Layout FSI-II, with added series compliance are presented in Figure 6.3. From the figure, it can be seen that, similarly results are found as Layout III-4_{sc}. But, the tested range of non-dimensional inertance is only from 0 to 1 since extreme large inertance value is not realistic and necessary duo to the reason explained in Chapter 5. Also, similar results have been found for Layouts III-3_{sc} and III-5_{sc} and IV-1_{sc}.

Within relatively large tested range for non-dimensional inertance b', it can be seen from Figure 6.2 that, without re-optimisation and without considering the higher mode constraint, for non-dimensionalised series compliance k_{sc}' equal to 1000, 100 and 10, the maximum optimum critical damping ratio $\zeta_{c,max}$ respectively are 83.0%, 47.2% and 2.7% of the original $\zeta_{c,max}$ only. Given the detrimental effect, the parameters of the absorbers should be re-optimised.

The re-optimised results for the most beneficial three and four element layouts, i.e., Layout III-4_{sc} and Layout IV-1_{sc} are shown in Figures 6.4 and 6.5 for the k_{sc}' equal to 10, 100 and 1000, as well as infinity. By comparison of the curves of critical damping ratio versus non-dimensional inertance with different values of k_{sc}', the effects series compliance can be found.

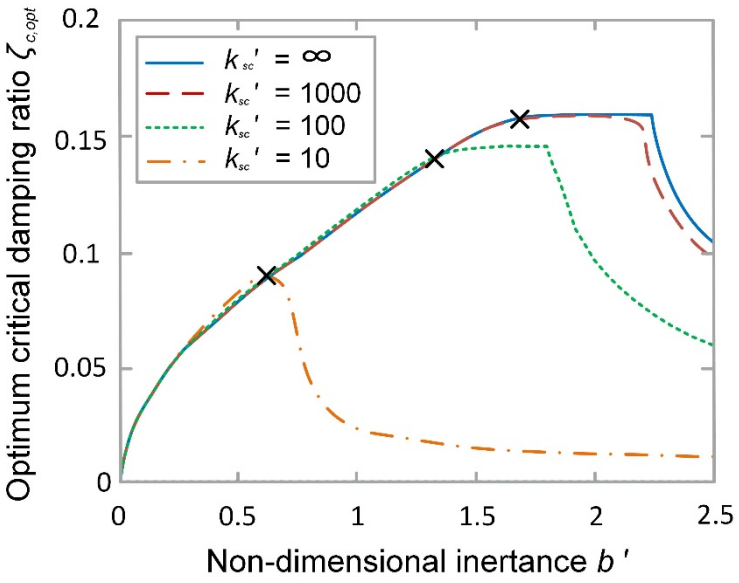

Figure 6.4: Re-optimised critical damping ratios with various non-dimensionalised series compliance k_{sc}' with parameters re-optimised for Layout III-4$_{sc}$.

As shown in Figure 6.4 for Layout III-4$_{sc}$, for different non-dimensionalised series compliance k_{sc}' within the tested range of non-dimensional inertance b' ranging from 0 to 2.5, for b' up to a certain value b_m', indicated by crosses, the optimum critical damping ratio of the re-optimised layout is at least as great as for the original layout. To achieve the optimum behaviour, both the non-dimensional damping coefficient c' and non-dimensional stiffness k' need to be adjusted. For $b' > b_m'$, the re-optimised $\zeta_{c,opt}$ for Layout Layout III-4$_{sc}$ cannot reach the original value, but it is still better than that without re-optimisation.

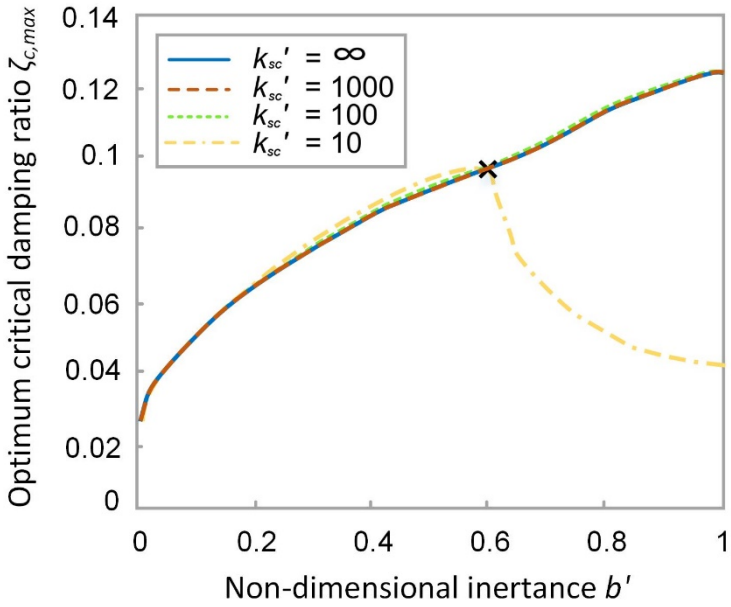

Figure 6.5: Re-optimised critical damping ratios with various non-dimensionalised series compliance k_{sc}' with parameters re-optimised for Layout IV-1_{sc}.

While for the most beneficial four-element layout IV-1_{sc}, very similar results are found, as shown in Figure 6.5, in which the tested range of non-dimensional inertance b' only ranging from 0 to 1. The b_m of approximately 0.6, represented by cross, which can be seen for the case with the softest series compliance tested when $k_{sc}' = 10$.

The re-optimised results presented in Figures 6.4 and 6.5 show that softer k_{sc}' can be beneficial if the system is retuned. For a range of b', which depends on k_{sc}', the re-optimised system can still provide a critical damping ratio the same good as, or in some cases even greater than the critical damping ratio provided by the original layout.

Figure 6.6 shows the relation of maximum critical inertance b_m' and its corresponding optimum critical damping ratio $\zeta_{c,opt}$ with series compliance k_{sc}' respectively for Layouts III-3_{sc}, III-4_{sc}, and III-5_{sc}. For all three layouts, when relatively stiff series compliance is considered, i.e. $k_{sc}' > 100$, only marginal effects can be seen on both $\zeta_{c,opt}$ and b_m'.

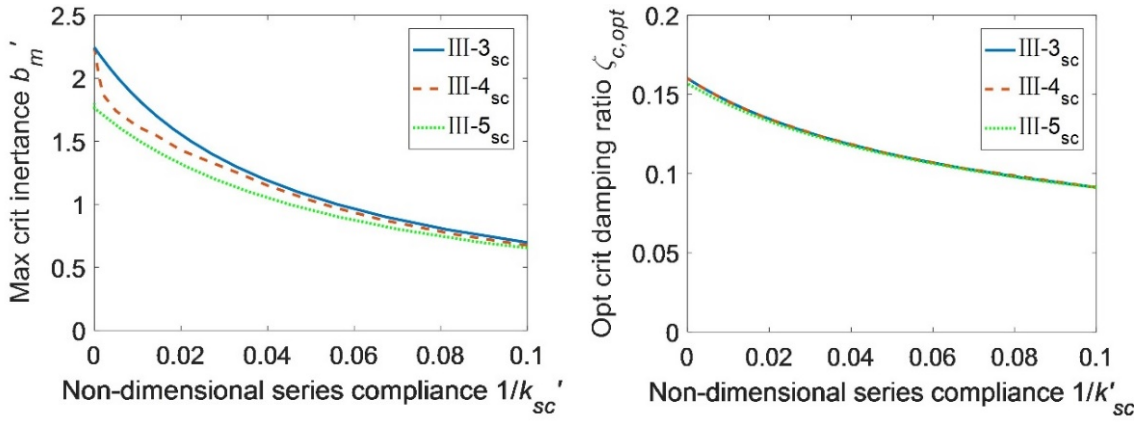

(a) (b)

Figure 6.6: Optimisation results for Layouts III-3_{sc}, III-4_{sc} and III-5_{sc}. (a) Maximum critical inertance b_m', and (b) corresponding optimum critical damping ratios versus non-dimensionalised series compliance.

Figure (6.6a) shows when series compliance is considered soft, i.e. the worst case considered when $k_{sc}' = 10$, the re-optimised $\zeta_{c,opt}$ can still reaches 60% of their original $\zeta_{c,max}$. Besides, when $k_{sc}' = 10$, the maximum critical non-dimensional inertance $b_m' \approx 0.6$ for all three layouts, which means within the range of inertance of most interest, i.e., $b' \leq 0.5$, same or even marginally better $\zeta_{c,opt}$ can be achieved compared with the case without the series compliances. Figure (6.6b) shows the corresponding optimum critical damping ratios versus non-dimensional series compliance, the higher mode constraint has influenced the local maximum $\zeta_{c,opt}$, for $k_{sc}' > 10$.

Considering the higher-mode constraint, the results using Measure two show that Layout III-6_{sc} cannot reach the original optimum even if the parameters of the absorber are retuned.

However, it is still much more beneficial than the case where the parameters are not retuned. For Layout III-4_{sc}, the re-optimised results are presented in Figure 6.7, showing that softer k_{sc}' can be beneficial if the system is retuned. For a range of b', which depends on k_{sc}', the re-optimised system can still provide a critical damping ratio as good as, or

in some cases even greater than, that the critical damping ratio provided by the original layout. Hence, it is concluded that the effect of series compliance may enhance damping performance if parameters of the absorber are properly tuned.

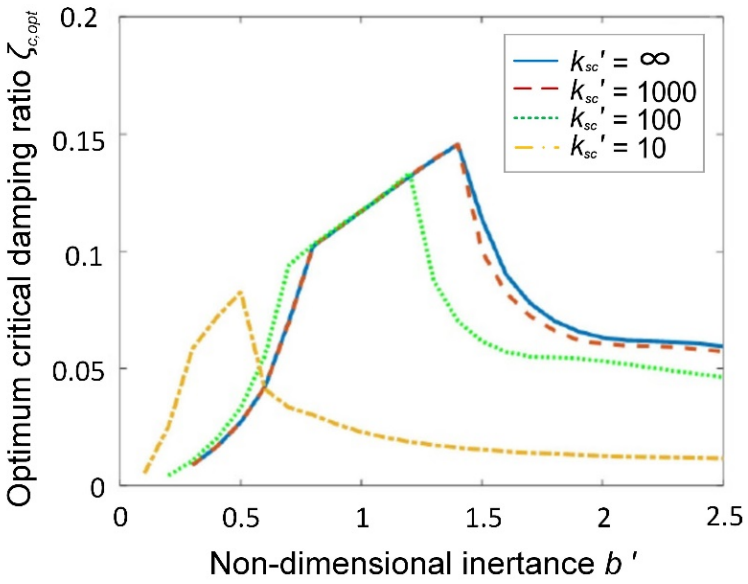

Figure 6.7: Optimum critical damping ratio for Layout III-4$_{sc}$ versus non-dimensional inertance for re-optimised results with the higher mode constraint and different non-dimensionalised series compliance.

6.3 Effects of absorber location

Due to the physical restriction, inerter-based absorbers have to be installed near the cable support on the deck, which constrains the vibration mitigation effectiveness of the absorber. The problem of the optimal damping constant of a viscous damper located close to one end of a taut cable was studied previously (Pacheco et al., 1993), suggesting that the maximum damping ratio that could be obtained by a concentrated viscous damper, would be about half the relative distance of the damper from the support, i.e., $\zeta_{c,max} = a'/2$ for a viscous damper within a realistic range. Meanwhile, when the damper is close to a support, an approximate value of the optimal external damping constant for the lower modes of vibration is also found. However, no relevant literature has been found on the location analysis for inerter-based absorber on cables.

In this section, the effects of the location for inerter-based absorber are investigated. The two most beneficial layouts, i.e., Layout III-4 and Layout IV-1 identified respectively in Chapters 4 and 5, are taken as an example. By using Measure one introduced in Sub-section 3.3.1, for non-dimensional location parameter in the range $a_f' \leq 0.5$, the overall maximum optimum critical damping ratio achievable are searched and then analysed for these beneficial layouts.

However, since the study is to examine damping performance of the inerter-based absorber for cable vibration, the effects of inertance are examined firstly. The relationship between the searched maximum optimum critical damping ratio $\zeta_{c,max}$ and the location parameter a' for the one-inerter layout with optimised inertance is presented in Figure 6.8.

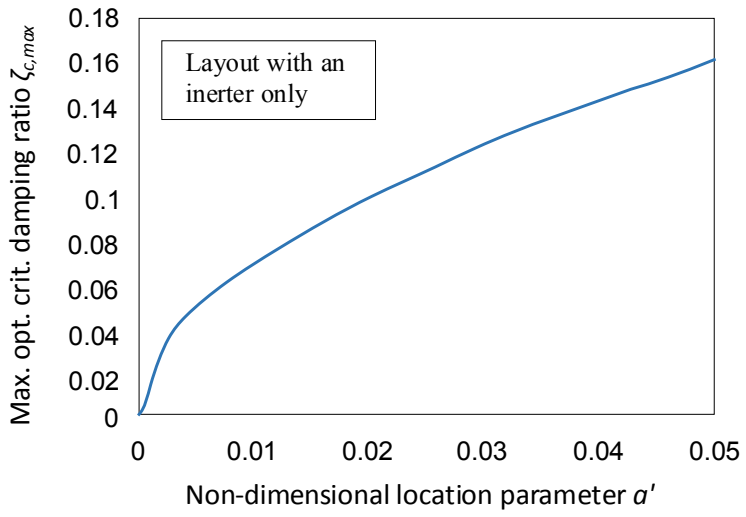

Figure 6.8: Maximum optimum critical damping ratio versus non-dimensional location parameter for one-inerter layout.

From Figure 6.8 it can be seen that, the maximum optimum critical damping ratio $\zeta_{c,max}$ increases with the growth of non-dimensional location parameter a'significantly. Obviously, better damping performances are resulted from larger non-dimensional location parameter.

Then, for the most beneficial three-element layout III-4 and the most beneficial four-element layout IV-1, the effects of the location parameter on damping performance are

examined. The relationships between their maximum optimum critical damping ratio $\zeta_{c,max}$ and non-dimensional inertance b' with different a' from 0.01 to 0.05 are presented in Figure 6.9.

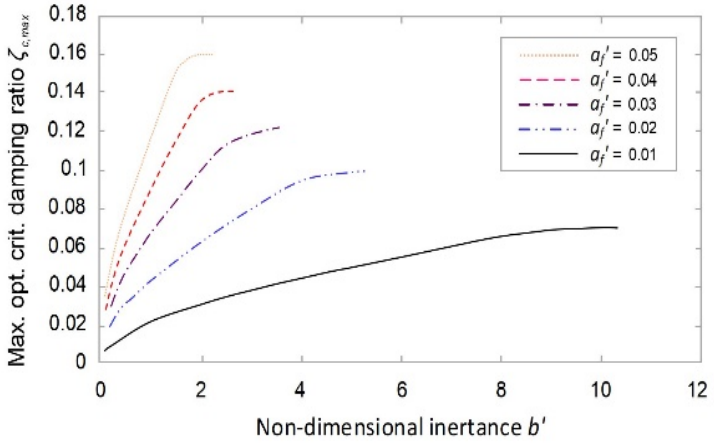

(a)

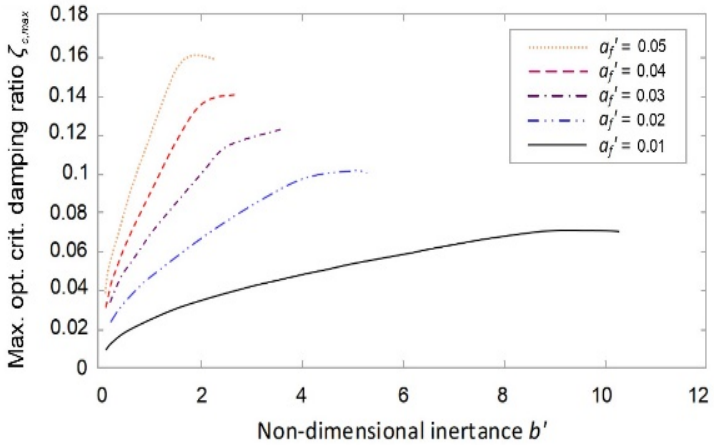

(b)

Figure 6.9: Maximum optimum critical damping ratio versus non-dimensional inertance with different location parameters for identified beneficial layouts. (a) III-4 and (b) IV-1.

By comparing the results from beneficial layouts III-4 and IV-1, respectively shown in Figures (6.9a) and (6.9b), slightly better performances can be found from four-element beneficial layout IV-1 though their trends are very similar. It can be seen from Figure 6.9

that, for both beneficial layouts, III-4 and IV-1, the non-dimensional location parameter has a significant effect on the searched optimum critical damping ratio $\zeta_{c,max}$. The maximum optimum critical damping ratio $\zeta_{c,max}$ increases with the growth of location parameter a' significantly. As expected, better damping performances are resulted from larger location parameter and greater inertance.

From both Figures (6.9a) and (6.9b), when a'=0.05, the best curve is obtained even with small non-dimensional inertance b'. The worst curve from the nearest location when a'=0.01, even with an extremely large non-dimensional inertance which close to 10.

Figure 6.9 shows that in order to achieve great $\zeta_{c,max}$, especially for a small a', an extreme larger inertance is needed. Obviously, it is not practical in terms the physical implementation, which implying that for inerter-based absorber for cable vibration suppression, the location parameter should be reasonably large for its effectiveness.

Many computations for the identified beneficial layouts show that inerter-based absorber can provide significantly larger optimum critical damping ratio $\zeta_{c,max}$ than that of a viscous damper in which $\zeta_{c,max} = a'/2$ within a realistic range. It should be pointed out that not only the seven-element FSI layouts or simplified four-element beneficial layouts IV-1 and IV-2, but other low-complexity layouts, including Layouts II-4, III-1, III-2, III-3 and III-4, all can achieve similar results. Also, it is found that, for any single-element structure listed in the present study, the product of a' and b' can be considered as constant.

Computations carried out for examining the relationships amongst b', a' and $\zeta_{c,max}$ for different cases indicate that, overall, optimum critical damping ratio is not proportional to increased location parameter with a range tested. The exhibited non-linear curves imply that there is a best compromise existing between a' and $\zeta_{c,max}$ for a configuration though the requirements for location parameter and optimum damping are conflicting in practice.

6.4 Summary

Based on the established model of cable-absorber system and the proposed mathematical approach introduced in Chapter 3, the effects of series compliance and absorber location are respectively investigated for different beneficial layouts.

First, the effect of series compliance at connections layouts are comprehensively investigated for the identified, beneficial layouts respectively with three and four elements, totally six layouts. Due to the existing coupling effects of the structural elements of absorber and the series compliance, the effects are investigated for both before and after retuning cases. The results show that without re-optimisation the series compliance is detrimental. However, up to a certain inertance which depends on the series compliance, the absorbers can provide virtually the same, or in some cases even better, performance as/than those without the series compliance if the values of structure element are properly retuned.

For two identified beneficial layouts, i.e., III-4, and VI-1, the effects of absorber location are investigated. The results show the significant influence of location of absorber on damping performance. It is found that the greater optimum critical damping ratio are resulted from larger non-dimensional location parameter and larger inertance non-linearly, implying the best compromise possibly existing between inertance, location and optimum damping ratio, since they are conflicting in practice. The obtained results can be useful in engineering application for absorber-cable system design, tuning and installation.

Chapter 7

Conclusion and outlook

This thesis is concerned with optimum absorber identification methodology for cable vibration suppression. A finite element taut cable model, with a generic vibration absorber represented by its admittance function, is firstly established. Three performance measures are introduced to quantify the damping performance for multiple modes. An efficient and systematic optimum configuration identification methodology is studied by using network synthesis and a simplification procedure.

First, with the proposed approach, potential advantages of low-complexity inerter-based absorber layouts, i.e., all layouts with three elements or fewer are systematically investigated, with corresponding element values in these layouts identified. By using proposed performance measures, the effects of these candidate absorbers for suppressing multiple modes are examined. However, there are many alternative inerter-based layouts containing more elements, which could potentially provide better performance. Due to the fact that the number of possible absorber layouts goes up exponentially with the increase of element number, and the difficulty for the identification of these layouts, an efficient and systematic optimum configuration identification methodology is then studied by making use of two types of fixed-sized-inerter (FSI) layouts. Considering more practical difficulties possibly existing in identifying complex layouts, and also for larger inertance to be physically implemented, a simplification procedure is adopted for the identified beneficial FSI layouts. Aiming to reduce the number of elements to the minimum while not compromising the performance gains, a beneficial, simplified configuration is identified which with fewer elements meanwhile with relatively small inertance.

For the identified beneficial layouts, other effects including series compliance, the structure parameters along with installation location of the absorber are also examined for beneficial absorber layouts.

In this chapter, the research conclusions and main contributions of the study are presented, and the remarks along with suggestions for future work are concluded, in Sections 7.1 and 7.2 respectively, as below.

7.1 Conclusions

In the mathematical modelling of a general representation for absorber layout for cable vibration suppression, a lumped-mass Finite Element (FE) model of a cable combined with an arbitrary linear passive absorber layout was built and described. Since the established integrated model of the cable with various absorber layouts represented by admittance functions, all possible passive linear absorbers can be investigated without the need of reformulating the system matrices in Equation (3.9). For general purpose, all structure parameters of absorber configurations were non-dimensionally scaled. The circular natural frequencies of the damped system were also presented in non-dimensional forms as respectively. Besides, the location parameter and series compliance (represented by a linear spring) were non-dimensionalised as well. For identifying beneficial layouts and a fair comparison, the locations of all candidate absorbers were all set same, at 5% length of the whole cable, for optimum absorber layouts identification investigation in Chapters 4 and 5.

A lumped mass FE model was built and the effect of the number of degrees of freedom is examined. The analysis for a number of absorber layouts showed that, typically, a lumped mass model with 99 degrees of freedom (DOFs) provided similar accuracy to a consistent mass model with 60 DOFs, but the consistent mass model took approximately twice the computational time. Hence, a lumped mass FE model rather than a consistent mass FE model was adopted for this study.

The two commonly used modelling for cable and absorber methods, i.e., Galerkin's method and FE method were mainly introduced, previous studies showed that the lumped mass FE model is more suitable for the present study, due to its better computational

efficiency, also being able to exhibit kink in results analysis. The preliminary computational results showed that the maximum relative difference of the calculated damping ratio between the lumped-mass FE models with 99 and 999 DOFs are very small, typically less than 0.1%. Considering only low-frequency modes with natural frequencies below 6.5 times of the circular natural frequency of the first mode for the undamped cable, therefore, a 99-DOF lumped mass FE model was used for the present study.

Performance measures were proposed to assess and qualify the damping performance of suppressing cable vibrations for all modes concerned depending on length of the cable and also forcing conditions. Three performance measures were proposed respectively considering the first mode only and higher modes (including the first six modes totally). Some extreme conditions were also considered to prevent galloping occur. Measure one is to maximise the minimum damping ratio of Mode 1 or around, i.e., including all modes with frequencies in the range $\omega_e \in (0,\ 1.5\omega_0)$. If with added the constraint that modes with natural frequencies in the range $\omega_e \in (1.5\omega_0,\ 6.5\omega_0)$ have no less damping than those for a cable with a viscous damper optimised for the first mode, then it is denoted as Measure two. Measure three is to maximise the minimum product of damping ratio and natural frequency (i.e., $\zeta_i \cdot \omega_i$) for avoiding dynamic insteability of the cable. By using these proposed measures, all interested modes were considered sufficient for the present study on vibration suppression of stay cables.

That is, for a systematic identification for different layouts, an optimisation approach was proposed, including the lumped mass FE model of the cable with an arbitrary linear passive absorber layout represented by its admittance function, and three proposed performances measures. For the generalised purpose and making comparisons fair, all parameters were non-dimensionalised. Some concerns in computation, e.g., MATLAB tools used for the computation, were also examined. The results showed that the proposed mathematical approach is computationally efficient for identifying beneficial layouts, which balanced well between calculation efficiency and accuracy for the comprehensive investigation.

In terms of different complexities for these inerter-based candidate absorbers, the results of optimisation and identification were respectively concluded, i) firstly for low-complexity layouts, i.e., with three elements or fewer; ii) secondly for two fixed-sized-

inerter (FSI) absorber layouts which are realised by a seven-element network; and iii) thirdly for the four-element beneficial layouts simplified from optimum FSI layout. The conclusions for these three classes, with different complexities, are respectively presented as below.

i) For low-complexity layouts

First, low-complexity inerter-based absorber layouts for cable vibration suppression were investigated and identified, with structure elements no more than three. To be specific, these low-complexity inerter-based absorber layouts refer to the layouts with no more than one inerter, damper and spring. All possible candidate low-complexity absorber layouts were presented with non-dimensionalised parameters. Based on the proposed approach, i.e., FE model of the cable with various absorber layouts represented by admittance functions, along with three performance measures which considering the first mode only and also the first six modes, absorbers with different layouts were optimised to identify beneficial low-complexity inerter-based absorber layouts for cable vibration suppression.

The performances of all possible low-complexity absorber layouts were analysed with non-dimensional inertance with the range of 0 to 2.5, with further focus on the more practical range of 0 to 0.5 respectively. The results showed that all layouts incorporating inerters can provide more beneficial optimum critical damping ratios than those for a viscous damper only.

Compared with two-element layouts for small inertance, three-element layouts can provide greater damping. If considering only the critical damping ratio, three layouts with three elements were found to be most beneficial, offering much greater damping ratios than other layouts when the inerter is small. Including the higher mode constraint, two three-element layouts were found to be most beneficial, even though their performance is restricted by the constraint.

ii) For FSI layouts with seven elements

Still based on the proposed mathematical approach, a systematic investigation was carried out to identify beneficial absorber layouts that have substantially better

performance than those low-complexity inerter-based absorber layouts. Considering the difficulty for choosing optimum absorber configurations increases, network synthesis was applied for identifying beneficial inerter-based absorber layouts with more structural elements. In this thesis, in order to further expand the range of network layouts covered, another FSI layout was firstly introduced in this study.

In the present study, two different fixed-sized-inerter absorber layouts respectively denoted as FSI-I and FSI-II, were introduced which covered a wide range of possible candidate seven-element absorber layouts. With the two FSI layouts which cover different seven-element layouts with one inerter and other six spring and damper elements, optimum absorber configurations are identified. The results demonstrated that the newly introduced fixed-sized inerter absorber layout, i.e., FSI-II, can significantly enhance the performance with small inertance values.

To be specific, the optimum results of the two FSI absorber layouts were searched with non-dimensional inertance in the range of 0 to 1 by using proposed performance measures. The results showed that both FSI layouts can provide much more beneficial results than for all low-complexity layouts, including the identified most beneficial three-element layout. It was found and should be mentioned that the firstly introduced fixed-sized inerter absorber layout in the present study, i.e., Layout FSI-II, showed the best overall damping performance for all values of inertance tested.

iii) For simplified beneficial layouts with four elements

Furthermore, since the identified FSI absorber configurations with seven elements still are complicated considering practical structure implementation, a simplification approach was proposed and adopted to reduce absorber structure elements, and meanwhile maintain their original optimum performance as much as possible. A simplification approach was implemented by neglecting parallel elements with an extreme small value and replacing a large-valued series element with rigid connections. The optimised results of the simplified layouts were compared with the original seven-element FSI layout results. If the performance reduction is small enough, typically less than 1%, then the simplified layouts were considered beneficial.

Based on proposed simplification approach, with a certain range of inertance, two four-element simplified beneficial layouts, respectively denoted Layout IV-1 and Layout IV-2, were identified with similar performance results to the most beneficial seven-element layout FSI-II, but with only four elements. The results indicated that for low inertance values, both simplified layouts can provide very similar performance, but compared with Layout IV-2, Layout IV-1 is as effective as FSI-II over a wider range of inertance and meanwhile requires a lower damping coefficient for one of the dampers.

Large benefits against both measures, i.e., Measures two and three, were obtained with even small inertance, which may be realistic to implement in practice. For relatively small inertance with non-dimensional inertance less than 0.09, the identified beneficial layouts still doubled the performance using both measures compared with the layout of a damper only.

Therefore, by adopting the proposed simplification approach, the identified seven-element fixed-sized-inerter absorber configuration was reduced to four elements. It can be concluded that the simplified layout, IV-1, is the most beneficial with a wide range of inertance. Thus, it can be a good candidate layout to effectively suppress cable vibrations in practical applications.

Finally, for the identified beneficial absorber layouts, respectively in Chapters 4 and 5, other effects including series compliance and the installation location of the absorber on optimum performance were examined and analysed in Chapter 6, summarised as below.

Considering the fact that the connections at either end of the absorber (with the support and with the cable) may not be fully rigid in practice, the effect of series compliance at connections for the identified, beneficial layouts respectively with three and four elements, totally six layouts were comprehensively investigated. Due to the existing coupling effects of absorber's structural elements and the series compliance, the effects were investigated for both before and after re-tuning cases. The results showed that without re-optimisation the series compliance was detrimental, however, up to a certain inertance, which depends on the series compliance, the absorbers can provide virtually the same, or in some cases even better performance as without the series compliance if the element values are properly retuned.

Then the effects of the installation location of absorber on damping performance were investigated. Two most beneficial layouts respectively identified in Chapters 4 and 5, i.e., Layouts III-4 and VI-1, were examined. It was found that the greater optimum critical damping ratio are resulted from larger non-dimensional location parameter and inertance, non-linearly anyhow, implying a best compromise possibly existing between inertance, location and optimum damping ratio through their practical requirements are conflicting in practice. The obtained results can be useful in engineering application for absorber-cable system design, tuning and installation.

The main contributions of this study lie in the proposed generic modelling and identification methodology to systematically investigate different absorber layouts. To be specific, they are summarised respectively as below,

- An integrated cable model, with a generic vibration absorber represented by its admittance function, is firstly established, in which all parameters are non-dimensionalised.
- Two optimum inerter-based absorbers configurations respectively with three and four elements were identified along with their structural parameters presented.
- The effects of series compliance at connections are firstly investigated considering a more realistic situation, and some interesting results are found. Besides, for two most beneficial inerter-based absorber layouts respectively with three and four elements as example, the effects of installation location on optimum performance are also examined.

The study results can be useful for inerter-based absorber for cable vibration problems in engineering application, e.g., in design, tuning and installation of the absorber. Besides, the proposed methodology in this study can be applied to cable vibration problems with other performance criteria, and also other mechanical structures.

The numerically-obtained performance improvement could be verified by applying the Real-Time Dynamic Substructure technique to physical inerter-based damping devices.

7.2 Remarks and outlook

Some remarks in the present study are addressed. Also, a few suggestions are made which could be useful for future work, respectively presented as below.

On the presented results throughout the whole thesis, the numerically-obtained performance improvement could be verified by applying the Real-Time Dynamic Substructure technique to physical inerter-based damping devices. Alternatively, as the analysis is presented in the non-dimensional form, a scaled, physical model of the device and cable could be used for testing.

Future work can be carried out on the aspects as below.

- Investigation of more complex inerter-based absorber layouts for further performance improvements.

  The inerter-based absorber layouts with more complexity, e.g. with structure elements over seven, may substantially provide further performance improvements than those inerter-based absorber layouts tested in this study. While in engineering application for cable vibration suppression, it is obviously in need for simplifying the structure of absorber device. Best compromise between optimisation performance and structural complexity is needed. Meanwhile, they can be further simplified for reducing structure elements in terms of physical implements.
- More considerations including nonlinearities.

  Since this thesis focused on an efficient and systematic optimum configuration identification methodology, to comprehensively investigate the damping performance of different layouts in a systematic way, the nonlinearities existing in the system in modelling, for example, the friction extra wear and parasitic damping in absorber devices can be studied in future work.
- More considerations for coupling effects with other structural members of the bridge.

  Although it is the vibration occurring on the cables which primarily induces vibration on the other structural members of the bridge, the cable vibrations are coupled with the vibration of the bridge deck and pylon towers, etc. More considerations for coupling effects with other structural members of the bridge can be included, and

sensibility analysis can be studied for the parameters of cable-absorber system along with other structure parameters for future work.

- Scaled model for testing.

  As in this study, all analysis is presented in non-dimensional form, a scaled physical model for the system with a device and cable could be used for testing. A further experimental study can be continued accordingly for investigating the optimum damping performance of different absorber configurations for suppressing cable vibration.

References

Acampora, A., Macdonald, J., Georgakisa, T., and Nikitas, N. (2014). 'Identification of aeroelastic forces and static drag coefficients of a twin cable bridge stay from full-scale ambient vibration measurements'. *Journal of Wind Engineering and Industrial Aerodynamics*, 124, 90–98.

Andersson, A., Karoumi, R. and O'Connor, A. (2013). 'External damping of stay cables using adaptive and semi-active vibration control'. *In ICSBOC, The 8th International Cable Supported Bridge Operators' Conference;* Sheraton Grand Hotel & Spa, Edinburgh, 3-5 June 2013.

Bakis, K. N., Massaro, M., Williams, M. S. and Graham, J. M. R. (2017). 'Passive control of bridge wind-induced instabilities by tuned mass dampers and movable flaps'. *Journal of Engineering Mechanics*, 143(9), pp. 04017078.

Bott, R. and Duffin, R. J. (1949). 'Impedance synthesis without use of transformers'. *Journal of Applied Physics*, 20(8), pp. 816.

Brune, O. (1931). 'Synthesis of a finite two-terminal network whose driving-point impedance is a prescribed function of frequency'. *Studies in Applied Mathematics*, 10(1-4), pp. 191–236.

Brzeski, P., Kapitaniak, T. and Perlikowski, P. (2015). 'Novel type of tuned mass damper with inerter which enables changes of inertance'. *Journal of Sound and Vibration*, 349, pp. 56-66.

Caetano, E. (2007). *Cable vibrations in cable-stayed bridges*. Zurich: IABSE.

Cai, C. S., Wu, W. J. and Shi X. M. (2006). 'Cable vibration reduction with a hung-on tmd system. part I: Theoretical study'. *Journal of Vibration and Control*, 12(7), pp. 801–814.

Cambridge University (2008). 'Professor Malcolm Smith's inerter raced in Formula One'. Available at: http://www.eng.cam.ac.uk/news/stories/2008/McLaren. (Accessed: 19 Aug 2008)

Cardenas, R. A., Viramontes, F. J. C., Gonzalez, A. D. and Ruiz, G. H. (2008). 'Analysis for the optimal location of cable damping systems on stayed bridges'. *Nonlinear dynamics,* 52(4), pp. 347-359.

Carne, T.G. (1981). 'Guy cable design and damping for vertical axis wind turbines.' SAND80-2669, Sandia National Laboratories, Albuquerque, NM.

Chen, M. Z. Q., Papageorgiou, C., Scheibe, F., Wang, F. C. and Smith, M. C. (2009). 'The missing mechanical circuit element'. *IEEE Circuits & Systems Magazine*, 09(1), pp. 10-26.

Chen, M. Z. Q. and Smith, M. C. (2009). 'Restricted Complexity Network Realizations for Passive Mechanical Control'. *IEEE Transactions on Automatic Control*, 54(10), pp. 2290-2301.

Chen, M. Z. Q. and Smith, M. C. (2007). 'Mechanical Networks Comprising One Damper and One Inerter'. *Proceedings of the European Control Conference*, Kos, Greece, July 2-5, 2007

Christenson, R.E., Spencer, B.F., Jr., Johnson, E.A., (2001) 'Experimental verification of semiactive damping of stay cables.' *Proceedings of the 2001 American Control Conference,* Arlington, Virginia, pp. 5058-5063, June 2001.

Cu, V. H. and Han, B. (2015). 'A stay cable with viscous damper and tuned mass damper'. *Australian Journal of Structural Engineering*, 16(4), pp. 316–323.

Den, Hartog, J. P. (1933). 'Transmission line vibration due to sleet'. *Transactions of the American Institute of Electrical Engineers*, 51(4), pp. 1074–1076.

De Domenico, D., Impollonia, N. and Ricciardi, G. (2018a). 'Soil-dependent optimum design of a new passive vibration control system combining seismic base isolation with tuned inerter damper'. *Soil Dynamics and Earthquake Engineering*, 105, pp. 37–53.

De Domenico, D. and Ricciardi, G. (2018b). 'An enhanced base isolation system equipped with optimal tuned mass damper inerter (tmdi)'. *Earthquake Engineering and Structural Dynamics*, 47, pp. 1169–1192.

Duflot, P. and Taylor, D. (2008). 'Fluid viscous dampers: an effective way to suppress pedestrian-induced motions in footbridges'. *In Third International Conference: Footbridge*

Faraj, R., Holnickiszulc, J., Knap, L. and Seńko, J. (2016). 'Adaptive inertial shock-absorber'. *Smart Materials and Structures*, 25(3), pp. 035031.

Firestone, F. A. (1933). 'A new analogy between mechanical and electrical systems'. *The Journal of the Acoustical Society of America*, 4(3), pp.249-267.

Fisco, N.R. and Adeli, H. (2011). 'Smart structures: part I—active and semi-active control'. *Scientia Iranica*, 18(3), pp. 275-284.

Flamand O., (1995) 'Rain-wind induced vibration of cables'. *Journal of Wind Engineering and Industrial Aerodynamics*, 57, pp. 353-362

Foster, R. M. and Ladenheim, E. L. (1963). 'A class of biquadratic impedances'. *IEEE Transactions on Circuit Theory*, 10(2), pp. 262–265.

Foster, R. M. (1924). 'A reactance theorem'. *Bell Syst. Techn. Jour.*, 3(2), pp.259-267.

Fujino, Y., Kimura, K. and Tanaka, H. (2012). 'Cable Vibrations and Control Methods', in *In Wind Resistant Design of Bridges*, Springer Japan, pp. 197-229.

Gartner, B. J. and Smith, M. C (2013). 'Damping and inertial hydraulic device'. US, 20130037362 A1 2013-02-14.

Giaralis, A. and Marian, L. (2016). 'Use of inerter devices for weight reduction of tuned mass-dampers for seismic protection of multi-story building: the tuned mass-damperinterter (TMDI)'. *Active and Passive Smart Structures and Integrated Systems*, (9799), p. 97991G.

Giaralis, A. and Taflanidis, A. A. (2018). 'Optimal tuned mass-damper-inerter (tmdi) design for seismically excited mdof structures with model uncertainties based on reliability criteria'. *Structural Control and Health Monitoring*, 25(2):e, pp. 2082.

Gimsing, N. J. and Georgakis, C. T. (2011). *Cable supported bridges: concept and design (3rd edition)*.Wiley & Sons, London, UK., 2011.

Gonzalez-Buelga, A., Irina F. Lazar, Jason Z. Jiang, Simon A. Neild, and Daniel J. Inman (2016). 'Assessing the effect of nonlinearities on the performance of a tuned inerter damper.' *Structural Control and Health Monitoring*, 24(3), pp. e1879.

Gonzalez-Buelga, A., Clare, Neild, L. R., S. A., Jiang, J. Z., and Inman, D. J. (2015). 'An electromagnetic inerter based vibration suppression device'. *Smart Materials and Structures*, 24.

Hanselka H. and Hoffmann U.(1999). 'Damping Characteristics of Fibre Reinforced Polymers' *Technische Mechanik*, Band 10. Heft 2: 91-101, Manuskrifteingang: 22. Juli 1998.

Hanazawa, Y., Suda, H. and Yamakita, M. (2011). 'Analysis and Experiment of Flat-Footed Passive Dynamic Walker with Ankle Inerter'. *Proceedings of the 2011 IEEE International Conference on Robotics and Biomimetics*, December 7-11, Phuket, Thailand.

Hessabi, R. M. and Mercan, O. (2016). 'Investigations of the application of gyro-mass dampers with various types of supplemental dampers for vibration control of building structures'. *Engineering Structures*, 126, pp. 174–186.

He, L., Liu, Y. and Han, S. (2016). 'Comparative study between two schemes of active-control-based mechatronic inerter'. *Proceedings of the 3rd International Conference on Mechatronics and Mechanical Engineering*, Shanghai, China, pp. 21-23.

Hikami, Y. and Shiraishi, N. (1988). 'Rain-wind induced vibrations of cables in cable-stayed bridges'. *Journal of Wind Engineering and Industrial Aerodynamics*, 29, pp. 409–418.

Hrovat, D. (1983). 'Semi-Active versus Passive or Active Tuned Mass Dampers for Structural Control'. *Journal of Engineering Mechanics*, 109(3), pp. 691–705.

Huang, H., Sun, L. and Jiang, X. (2012). 'Vibration mitigation of stay cable using optimally tuned MR damper'. *Smart Structures and Systems*, Vol.9(1), pp. 35-53.

Huang, S. C. and Lin, K. A. (2014). 'A new design of vibration absorber for periodic excitation'. *Shock and Vibration*, 2014, pp. 571421-571411.

Hu, Y., Chen, M. Z. Q. and Sun, Y. (2017a). 'Comfort-oriented vehicle suspension design with skyhook inerter configuration'. *Journal of Sound and Vibration*, 405, pp. 34-47.

Hu, Y., Chen, M. Z. Q., Xu, S. and Liu, Y. (2017b). 'Semiactive inerter and its application in adaptive tuned vibration absorbers'. *IEEE Transactions on control systems technology*, 25(1), pp. 294-300.

Ikago, K., Saito, K. and Inoue, N. (2012). 'Seismic control of single-degree-of-freedom structure using tuned viscous mass damper'. *Earthquake Engineering and Structural Dynamics*, 41, pp. 453-474.

Irvine, M. (1981) *Cable Structures*. 2nd ed. New York: Dove.

Irwin, P. A. (1997). 'Wind vibrations of cables on cable-stayed bridges'. *Building to Last ASCE*, pp. 383-387.

Iwanami, K. and Seto, K. (1984). 'Optimum design of dual tuned mass dampers and their effectiveness'. *Proceedings of the Japan Society of Mechanical Engineering(C)*, 50, pp. 44–52.

Jalili, N. (2002). 'A comparative study and analysis of semi-active vibration-control systems'. *Journal of vibration and acoustics*, *124*(4), pp. 593-605.

Jiang, J. Z. (2010). 'Passive electrical and mechanical network synthesis'. *PhD dissertation, University of Cambridge*, Cambridge, U.K..

Jiang, J. Z., Matamoros-Sanchez, A. Z., Goodall, R.M. and Smith, M. C. (2011a). 'Passive suspensions incorporating inerters for railway vehicles'. *Vehicle System Dynamics:International Journal of Vehicle Mechanics and Mobility*, 50(Sup1), pp. 263–276.

Jiang, J. Z. and Smith, M. C. (2011b). 'Regular positive-real functions and five-element network synthesis for electrical and mechanical networks'. *IEEE Transactions on Automatic Control*, 56(6), pp. 1275–1290.

Jiang, J. Z., Liu, X. and Harrison, A. (2015a). 'Passive suspension incorporating inerters for road damage improvement of heavy vehicles'. *Symposium on Dynamics of Vehicles on Road and Tracks*.

Jiang, J. Z., Matamoros-Sanchez, A. Z., Zolotas, A., Goodall, R. M. and Smith, M. C. (2015b). 'Passive suspensions for ride quality improvement of two-axle railway vehicles'. *Proceedings of Mechanical Engineering (Part F):Journal of Rail and Rapid Transit*, 229, pp. 315–329.

Jiang, J. Z., Alejandra Z. Matamoros-Sanchez, Roger M. Goodall, and Smith, M. C. (2011). 'Passive suspensions incorporating inerters for railway vehicles.' *Vehicle System Dynamics: International Journal of Vehicle Mechanics and Mobility*, 50(Sup1), pp. 263–276.

Jiang, J. Z., X. Liu, A. Harrison. (2015). 'Passive suspension incorporating inerters for road damage improvement of heavy vehicles', *Symposium on Dynamics of Vehicles on Road and Tracks*, Graz, Austria.

Karnopp, D., Crosby, M.J. and Harwood, R.A. (1974). 'Vibration control using semi-active force generators'. *Journal of engineering for industry*, *96*(2), pp. 619-626.

Koo, J. H., Ahmadian, M., Setareh, M. and Murray, T. (2004). 'In search of suitable control methods for semi-active tuned vibration absorbers'. *Modal Analysis*, 10(2), pp. 163-174.

Krenk, S. and Høgsberg, J. (2016). 'Tuned resonant mass or inerter-based absorbers: unified calibration with quasi-dynamic flexibility and inertia correction'. *Proc. R. Soc. A,* 472(2185), p.20150718.

Krenk, S. and Nielsen, S.R. (2002). 'Vibrations of a shallow cable with a viscous damper.' *Proceedings of the Royal Society of London A: Mathematical, Physical and Engineering Sciences*, 2018(458), pp. 339-357.

Krenk, S. (2000). 'Vibrations of a taut cable with an external damper', *Journal of Applied Mechanics*, 67(4), pp. 772-776.

Kumarasena, S., Jones, N. P., Irwin, P. and Taylor, P. (2007). 'Wind-induced vibration of stay cables'. *Federal Highway Administration*, Vol. Publication No. FHWA-RD-05-083.

Ladenheim, E. L. (1964). 'Three-reactive five-element biquadratic structures'. *IEEE Trans. on Circuit Theory*, 11, pp. 88–97.

Ladenheim, E. L. (1948). 'A synthesis of biquadratic impedances'. Master's thesis, Polytechnic Inst. of Brooklyn.

Langsoe H. E., and Larsen, O. D., (1987) 'Generating mechanisms for cable stay oscillations at the FARO bridges'. Proceeding, International Conference on Cable-stayed Bridges, Bangkok, November 18-20, 1987.

Lankin, J., Kilpatrick, J., Irwin, P. A., Alca, N., (2000) 'Wind-induced stay cable vibrations—measurement and mitigation'. Proceedings of the ASCE Structures Congress, Philadelphia, Pa., May 8–10, 2000.

Lazarek, M., Brzeski, P., Perlikowski, P. (2018). 'Design and identification of parameters of tuned mass damper with inerter which enables changes of inertance'. *Mechanism and Machine Theory,* 119, pp. 161–173.

Lazar, I. F., Neild, S. A. and Wagg, D. J. (2014). 'Using an inerter-based device for structural vibration suppression'. *Earthquake Engineering & Structural Dynamics*, 43(8), pp. 1129–1147.

Lazar, I. F., Neild, S. A. and Wagg, D. J. (2016). 'Vibration suppression of cables using tuned inerter dampers'. *Engineering Structures*, 122, pp. 62–71.

Li, C., Liang, M., Wang, Y. and Dong, Y. (2012). 'Vibration suppression using two-terminal flywheel. Part II: application to vehicle passive suspension'. *Journal of Vibration and Control*, 18(9), pp. 1353-1365.

Li, C. (2000). 'Performance of multiple tuned mass dampers for attenuating undesirable oscillations of structures under the ground acceleration'. *Earthquake Engineering and Structural Dynamics*, 29, pp. 1405–1421.

Li, P., Lam, J. and Cheung, K. C. (2014). 'Investigation on semi-active control of vehicle suspension using adaptive inerter'. *Proceedings of the 21th International Congress on Sound and Vibration*, Beijing, China, pp. 13-17.

Li, P., Lam, J. and Cheung, K. C. (2015). 'Control of vehicle suspension using an adaptive inerter'. *Proceedings of the Institution of Mechanical Engineers Part D: Journal of Automobile Engineering*, 229(14), pp. 1934-1943.

Li, Y., Howcroft, C., Jiang, J. Z. and Neild, S. A. (2017a). 'Using continuation analysis to identify shimmy-suppression devices for an aircraft main landing gear'. *Journal of Sound and Vibration*, 408, pp. 234–251.

Li, Y., Jiang, J. Z. and Neild, S. A. (2017b). 'Inerter-based configurations for main landing gear shimmy suppression'. *Journal of Aircraft*, 54, pp. 684–693.

Lilien, J. L. and Pinto da Costa, A. P. (1994). 'Vibration amplitudes caused by parametric excitation of cable stayed structures'. *Journal of Sound and Vibration*, 174(1), pp. 69–90.

Liu, Y., Chen, M. Z. Q. and Tian, Y. (2015). 'Nonlinearities in landing gear model incorporating inerter'. *IEEE International Conference on Information and Automation*, pages 696–701.

Liu, X. F., Jiang, J. Z., Titurus, B. and Harrison, A. (2018). 'Model identification methodology for fluid-based inerters'. *Mechanical Systems and Signal Processing*, 106, pp. 479–494.

Luo, J. N., Jiang, J. Z. and Macdonald, J. H. (2016). 'Damping performance of taut cables with passive absorbers incorporating inerters', *13th International Conference on Motion and Vibration Control (MOVIC 2016) joint with the 12th International Conference on Recent Advances in Structural Dynamics (RASD)*.

Luo, J. N., Macdonald, J. H. and Jiang, J. Z. (2017). 'Use of inerter-based vibration absorbers for suppressing multiple cable modes', *X International Conference on Structural Dynamic. EURODYN,* Rome, Italy.

Luo, J. N. , Jiang, J. Z. and Macdonald, J. (2019). 'Cable vibration suppression with inerter-based absorbers', *Journal of Engineering Mechanics,* 145(2):04018134.

Lu, L., Duan, Y. F., Spencer Jr, B. F., Lu, X. and Zhou, Y., (2017) 'Inertial mass damper for mitigating cable vibration', *Structure Control and Health Monitoring* 24(10):e1986.

Macdonald, J. H. and Larose, G. L. (2006). 'A unified approach to aerodynamic damping and drag/lift instabilities, and its application to dry inclined cable galloping', *Journal of Fluids and Structures*, 22(2), pp. 229-252.

Macdonald, J. H. G. (2016). 'Multi-modal vibration amplitudes of taut inclined cables due to direct and/or parametric excitation', *Journal of Sound and Vibration*, 363, pp. 473-494.

Maeda, H., Kubo, Y., Kato, K. and Fukushima, S. (1997). 'Aerodynamic characteristics of closely and rigidly connected cables for cable-stayed bridges', *Journal of Wind Engineering and Industrial Aerodynamics*, 69, pp. 263-278.

Main, J. A. and Jones, N. P. (2002). 'Free vibrations of taut cable with attached damper. I: Linear viscous damper', *Journal of Engineering Mechanics*, 128(10), pp. 1062-1071.

Makris, N. (2017). 'Basic response functions of simple inertoelastic and inertoviscous models'. *Journal of Engineering Mechanics*, 143(11), pp. 04017123.

Makris, N. and Kampas, G. (2016). 'Seismic protection of structures with supplemental rotational inertia', *Journal of Engineering Mechanics*, 142(11), pp. 04016089.

Marian, L. and Giaralis, A. (2014). 'Optimal design of a novel tuned mass-damper-inerter (TMDI) passive vibration control configuration for stochastically support-excited structural systems'. *Probabilistic Engineering Mechanics*, 38, pp. 156-164.

MATLAB (2010). *Version 7.10.0 (R2010a)*. Natick, Massachusetts: *The MathWorks Inc*.

Matsumoto, M., Shiraishi, N., Kitazawa, M., Knisely, C., Shirato, H., Kim, Y. and Tsujii, M. (1990). 'Aerodynamic behaviour of inclined circular cylinders-cable aerodynamics', *Journal of Wind Engineering and Industrial Aerodynamics*, 33(1-2), pp. 63-72.

Nakaminami, S., Kida, H., Ikago, K. and Inoue, N. (2017). 'Dynamic testing of a full-scale hydraulic inerter-damper for the seismic protection of civil structures', *7th International Conference on Advances in Experimental Structural Engineering*.

Ni, Y., Spencer, B., Ko, J. (2001) 'Feasibility of active control of cable-stayed bridges: an insight into Ting Kau Bridge', *Smart Structures and Materials. Proceedings of SPIE*, 4330, pp. 387–398.

Ou J. P. (2003). *Structural vibration control: active, semi-active and intelligent control.* Beijing: *Science Press.* (in Chinese)

Ouni, E. l., Kahla, M. H., N. B. and Preumont, A. (2012). 'Numerical and experimental dynamic analysis and control of a cable-stayed bridge under parametric excitation'. *Engineering Structure*, 45, pp. 244-256.

Pacheco, B.M., Fujino, Y. and Sulekh, A. (1993). 'Estimation curve for modal damping in stay cables with viscous damper', *Journal of Structural Engineering*, 119(6), pp. 1961-1979.

Pantell, R. H. (1954). 'A new method of driving point impedance syntheses. *Proc. IRE*, 42, pp. 861.

Papageorgiou, C. and Smith, M. C. (2005). 'Laboratory experimental testing of inerters', *44th IEEE Conference on Decision and Control, and the European Control Conference.* Seville, Spain.

Peeters, B., Couvreur, G., Razinkov, O., Kündig, C., Van der Auweraer, H. and De Roeck, G. (2009). 'Continuous monitoring of the Øresund Bridge: system and data analysis'. *Structures and Infrastructure Engineering*, *5*(5), pp. 395-405

Pinkaew, T. and Fujino, Y. (2001). 'Effectiveness of semi-active tuned mass dampers under harmonic excitation'. *Engineering Structures*, 23(7), pp. 850-856.

Pires, L., Smith, M. C., Houghton, N. E., and McMahon, R. A. (2013). 'Design trade-offs for energy regeneration and control in vehicle suspensions'. *International Journal of Control,* 86(11), pp. 2022-2034.

Poincare, H. (1907). 'Study of telephonic reception'. Eclairage Electrique, 50, pp. 221–372.

Post-Tensioning Institute. (2012). *Recommendations for stay cable design, testing, and installation.* Farmington Hills, MI, Post-Tensioning Institute.

Reza, F. M. (1955). 'A supplement to Brune synthesis'. *Transactions of the American Institute of Electrical Engineers, Part I: Communication and Electronics,* 74(1), pp. 85–90.

Richard, E. C. and Spencer, B. F. (2006). 'Experimental verification of smart cable damping', *Journal of Engineering Mechanics,* 132(2), pp. 268-278.

Richards, P. I. (1947). 'A special class of functions with positive real parts in a half-plane'. *Duke J. of Math*, 14, pp. 777–786.

Riordan, J. and Shannon, C. E. (1942). 'The number of two-terminal series-parallel networks', *Studies in Applied Mathematics*, 21(1-4), pp. 83-93.

Sarkar, P. P., Mehta, K.C., Zhao, Z.S., Gardner, T. (1999). 'Aerodynamic approach to control vibrations in stay cables'. Report to Texas Department of Transportation, TX.

Smith, M. C., Houghton, N. E., Long, P. J. and Glover, A.R. Mclaren Racing Limited and Cambridge Enterprise Ltd. (2014). *'Force-controlling hydraulic device'*. U.S. Patent 8,881,876.

Smith, M. C. and Wang, F. C. (2004). 'Performance benefits in passive vehicle suspensions employing inerters', *Vehicle System Dynamics*, 42(4), pp. 235-257.

Smith, M. C. Cambridge University Technical Services Ltd. (2008). *'Force-controlling mechanical device'*. U.S. Patent 7,316,303.

Smith, M. C. (2002). 'Synthesis of mechanical networks: the inerter'. *IEEE Transaction on Automatic Control*, 47(10), pp. 1648–1662.

Seshu, S. (1959). 'Minimal realizations of the biquadratic minimum function'. *IRE Transactions on Circuit Theory*, 4, pp. 345–350.

SETRA. (2002). *Cable Stays: Recommendations of French Inter ministerial Commission on Prestressing*. Bagneux Cedex.

Shen, Y., Chen, L., Yang, X., Shi, D. and Yang, J. (2016). 'Improved design of dynamic vibration absorber by using the inerter and its application in vehicle suspension', *Journal of Sound and Vibration*, 361, pp. 148-158.

Shi, X. and Zhu, S. (2018) 'Dynamic characteristics of stay cables with inerter dampers', *Journal of Sound and Vibration,* 423, pp. 287-305.

Song, B., Wang, Z., Ko, J. M. and Ni, Y.Q. (2013). 'Design and modelling of a fluid inerter', *International Journal of Control*, 86(11), pp. 2035-2051.

Song B., Wang, Z., Ko, J. M. and Ni, Y.Q. (2003). 'Parametrically excited oscillation of stay cable and its control in cable-stayed bridges', *Journal of Zhejiang University Science*, 4(1), pp. 13-20.

Storer, J. E. (1957). *Passive network synthesis*. New York: McGraw-Hill Book Company.

Storer, J. E. (1954). 'Relationship between the Bott-Duffin and Pantell impedance synthesis'. *Proc. IRE*, 42(9), pp. 1451.

Sun, X. Q., Chen, L., Wang, S. H., Zhang, X. L. and Yang, X. F. (2016). 'Performance investigation of vehicle suspension system with nonlinear ball-screw inerter', *International Journal of Automotive Technology*, 17(3), pp. 399-408.

Swift, S. J., Smith, M. C., Glover, A. R., Papageorgiou, C., Gartner, B. and Houghton, N. E. (2013). 'Design and modelling of a fluid inerter'. *International Journal of Control*, 86(11), pp. 2035-2051.

Tabatabai, H. and Mehrabi, A.B. (1999). 'Tuned dampers and cable fillers for suppression of bridge stay cable vibrations', IDEA program final report, Construction Technology Laboratories, Inc., Skokie, IL.

Tagata, G. (1977) 'Harmonically forced finite amplitude vibration of a string', *Journal of Sound and Vibration*, 51(4), pp. 483-492.

Takewaki, I., Murakami, S., Yoshitomi, S. and Tsuji, M. (2012). 'Fundamental mechanism of earthquake response reduction in building structures with inertial dampers', *Structural Control and Health Monitoring*, 19.

Tang K. and Yan X. (2018) 'A review on the damping properties of fiber reinforced polymer composites'*, J. of Industrial Textile*, DOI:10.1177/1528083718795914.

TERATEC Inc. (2018) 'Cable Dampers for Civil Markets'. Available at: http:// http://www.teratec.ca/markets/structural-civil/cable-dampers/. (Accessed: 25 Aug 2008)

Tseng, H.E. and Hrovat, D. (2015). 'State of the art survey: active and semi-active suspension control'. *Vehicle system dynamics*, *53*(7), pp. 1034-1062.

Thomson, W. and Dahleh, M. (1997). *Theory of Vibration with Applications*. 15th Edn. London: Pearson.

Tokoro, S., Komatsu, H., Nakasu, M., Mizuguchi, K. and Kasuga, A. (2000). 'A study on wake-galloping employing full aeroelastic twin cable model', *Journal of Wind Engineering and Industrial Aerodynamics*, 88, pp. 247-261.

Tran, T. T., Hori, C. and Hasegawa, H. (2014). 'Integrated inerter design and application to optimal vehicle suspension system', *International Journal of Computer-Aided technologies*, 1(2/3), pp. 1-16.

Tseng, H. E. and Hrovat, D. (2015). 'State of the art survey: active and semi-active suspension control', *Vehicle System Dynamics*, 53(7), pp. 1034-1062.

Van Valkenburg, M. E. (1962). *Introduction to modern network synthesis*. 2nd edn. New York *:John Wiley & Sons*.

Wang, F. C., Hsieh, M. R. and Chen, H. J., (2012). 'Stability and performance analysis of a full-train system with inerters', *Vehicle System Dynamics*, 50(4), pp. 545-571.

Wang, F. C., Hong, M. F. and Lin, T. C. (2011a). 'Designing and testing a hydraulic inerter', *ARCHIVE Proceedings of the Institution of Mechanical Engineers (Part C): Journal of Mechanical Engineering Science*, 1(C1), pp. 1-7.

Wang, F. C. and Chan, H. A. (2011b). 'Vehicle suspension with a mechatronic network strut', *Vehicle System Dynamics*, 49(5), pp. 811-830.

Wang F. C., Min-Ruei Hsieh, and Hsueh-Ju C. (2011c). 'Stability and performance analysis of a full-train system with inerters'. *Vehicle System Dynamics*, 50(4), pp. 545–571.

Wang, F. C. and Liao, M. K. (2010a). 'The lateral stability of train suspension systems employing inerters', *Vehicle System Dynamics*, 48(7), pp. 619-643.

Wang, F. C., Hong, M. F. and Chen, C. W. (2010b). 'Building suspensions with inerters', *Proceedings of the Institution of Mechanical Engineers, Part C, Journal of Mechanical Engineering Science*, 224, pp. 1650-1616.

Wang, F. C., Liao, M. K., Liao, Su, B. H., W. J., and Chan, H. A. (2009a). 'The performance improvements of train suspension systems with mechanical networks employing inerters'. *Vehicle System Dynamics*, 47(7), pp. 805–830.

Wang, F. C. and Lin, T. C. National Taiwan University. (2009b). *'Hydraulic inerter mechanism'*. U.S. Patent Application 12/048,652.

Wang, F. C. and Su, W. J. (2008). 'Impact of inerter nonlinearities on vehicle suspension control', *International Journal of Vehicle Mechanics and Mobility*, 46, pp. 575-595.

Wang, F. C. and Chan, H. A. (2008). 'Mechatronic suspension design and its applications to vehicle suspension control', *Proceedings of the 47th IEEE Conference on Decision and Control*, Cancun, Mexico, 9-11.

Wang, F. C., Chen, C. W., Liao, M. K. and Hong, M. F. (2007). 'Performance analyses of building suspension control with inerters', *Proceedings of the 46th IEEE Conference on Decision and Control,* New Orleans, USA, 3786-3791.

Wang K, Michael Z.and Chen Q. (2012). Realization of biquadratic impedances with at most four elements 24th Chinese Control and Decision Conference, 2012

Wang, M. and Sun, F. (2018). 'Displacement reduction effect and simplified evaluation method for sdof systems using a clutching inerter damper', *Earthquake Engineering and Structural Dynamics,* 47(7), pp.1651-1672.

Wang, X., Blaabjerg, F. and Liserre, M. (2014). 'An active damper to suppress multiple resonances with unknown frequencies'. *Applied Power Electronics Conference and Exposition (APEC), 2014 Twenty-Ninth Annual IEEE (pp. 2184-2191). IEEE.*

Warnitchai, P., Fujino, Y. and Susumpow, T. (1995). 'A nonlinear dynamic model for cables and its application to a cable-structure system', *Journal of Sound and Vibration*, 187(4), pp. 695-712.

Washington State Department of Transportation (2018). *'Tacoma Narrows Bridge: "Galloping Gertie" Collapses November 7, 1940'*. Available at: http://www.wsdot.wa.gov/tnbhistory/connections/connections3.htm#2. (Accessed: 20, May, 2018)

Wen, Y., Chen, Z. and Hua, X. (2016). 'Design and evaluation of tuned inerter-based dampers for the seismic control of mdof structures', *Journal of Structural Engineering*, 143(4), pp.04016207.

Xu, K. and Igusa, T. (1994). 'Vibration control using multiple tuned mass damper', *Journal of Sound and Vibration*, 175, pp. 491-503.

Xu, L., Yu, Z. (1998) 'Vibration of Inclined sag cables with oil dampers in cable-stayed bridges', *Journal of Bridge Engineering,* 3(4), pp. 194–203

Yang, J. N. (2016). 'Force transmissibility and vibration power flow behaviour of inerter-based vibration isolators', *13th International Conference on Motion and Vibration Control (MOVIC 2016) joint with the 12th International Conference on Recent Advances in Structural Dynamics (RASD)*.

Yang, J. N., and Giannopoulos, F. (1979) 'Active control and stability of cable-stayed bridge', Journal of Engineering Mechanics Division, ASCE, 105(EM4), pp. 677-694.

Yang, S., Xu, T., Li, C., Liang, M. and Baddour, N. (2016). 'Design, Modeling and Testing of a Two-Terminal Mass Device With a Variable Inertia Flywheel', *Journal of Mechanical Design*, 138(9), pp. 095001-095010.

Yoshimura, T., Savage, M. G., Tanaka, H. and Urano, D. (1995). 'Wind-induced oscillations of groups of bridge stay-cables', *Journal of Wind Engineering and Industrial Aerodynamics*, 54, pp. 251-262.

Zdravkovich, M. M. (1987). 'The effects of interference between circular cylinders in cross flow', *Journal of Fluids and Structures*, 1(2), pp. 239-261.

Zhang, S. Y., Jiang, J. Z. and Neild, S. (2017). 'Optimal configurations for a linear vibration suppression device in a multi-storey building', *Structural Control and Health Monitoring*, 24(3), pp. e1887.

Zilletti, M. (2016). 'Feedback control unit with an inerter proof-mass electrodynamic actuator', *Journal of Sound and Vibration*, 369, pp. 16-28.

Zuo, D. and Jones, N. (2010). 'Interpretation of field observations of wind-and rain-wind-induced stay cable vibrations', *Journal of Wind Engineering and Industrial Aerodynamics*, 98, 73–87.

Appendices

i) Table for all candidate layouts

I

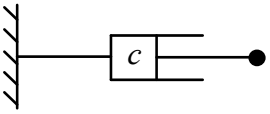

II-1

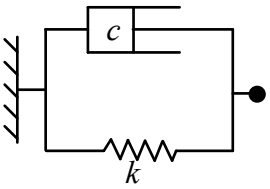

II-2

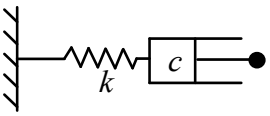

II-3

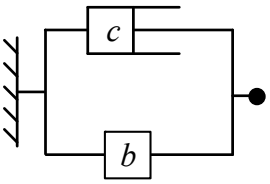

II-4

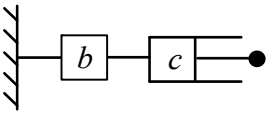

III-1

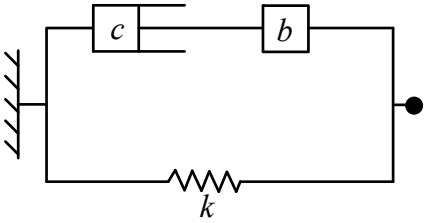

III-2

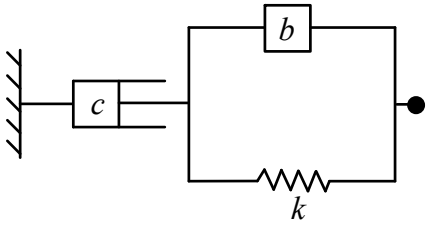

III-3

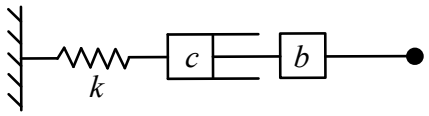

III-4

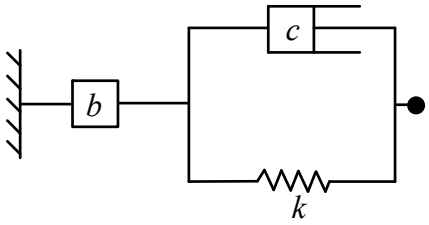

III-5

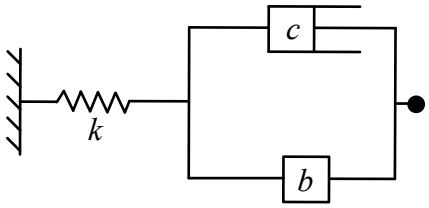

III-6

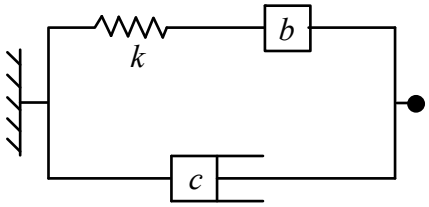

III-7

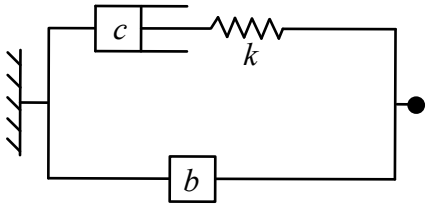

III-8

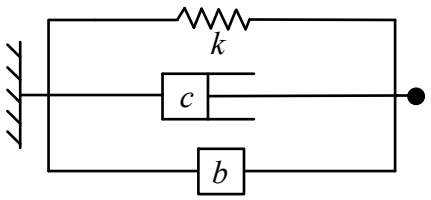

FSI-I

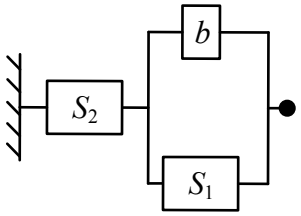

FSI-II

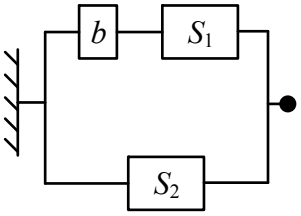

IV-1

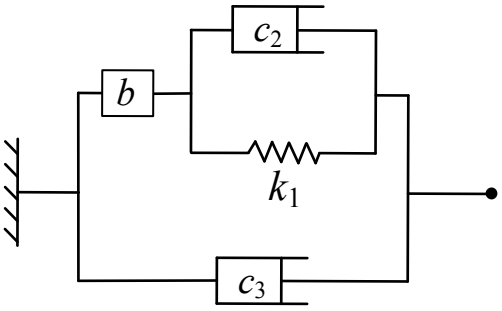

IV-2

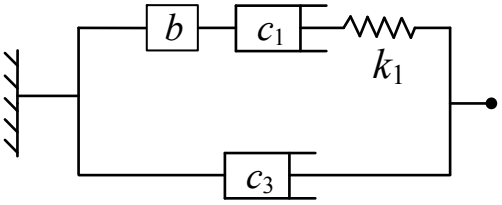

III-3$_{sc}$

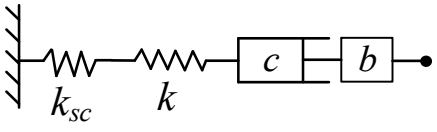

III-4$_{sc}$

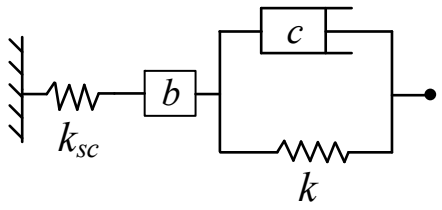

III-5$_{sc}$

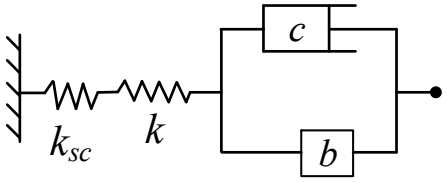

III-6$_{sc}$

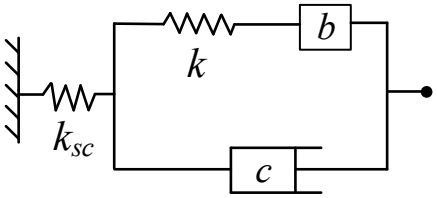

IV-1$_{sc}$

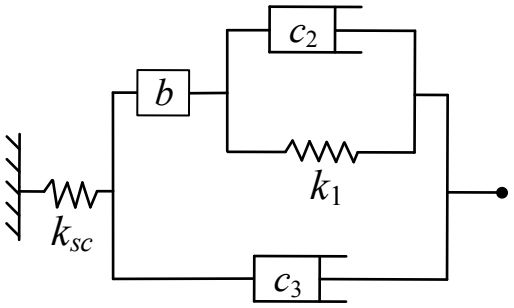

IV-2$_{sc}$

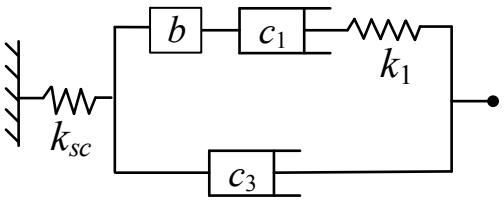

ii) Sample loop of optimisation of a viscous damper

```
function R6=func0(x)
% Calculation of eigenvalue for structure with extra DOF
syms s
% Starting conditions
%xc   location of the absorber
%n    DOF of the cable
xc=1;
n=19;
%%%%%%%%%%%%%%%%%%%%%%%%%%%%%%%%%%%%%%%%%%%%%%%%
%Transfer function of absorber's structure
%TF=c;
%%%%%%%%%%%%%%%%%%%%%%%%%%%%%%%%%%%%%%%%%%%%%%%%

% Calculation for M F K
f1=zeros(n);
f1(xc,xc)=1;
F=f1;

m1=eye(n)/(n);
M=m1;

k1=eye(n);
k2=ones(n-1,1);
k3=diag(k2,1);
k4=diag(k2,-1);
k5=2*k1-k3-k4;
k6=k5*(n+1);
K=k6;
%%%%%%%%%%%%%%%%%%%%%%%%%%%%%%%%%%%%%%%%%%%%%%%%
%Calculation of eigonvalue with TF method
O=zeros(n);
I=eye(n);
A01=[O,I;-inv(M)*K,-inv(M)*F*TF];
A02=eye(2*n)*s;
A03=A01-A02;
A04=det(A03);

D01=solve(A04,'s');
D02=double(D01);
D03=D02;
[~,D04]=sort(imag(D03));
D05=D03(D04);
D06=imag(D05)>=0;
D07=D05(D06);
R0=D07;
%%%%%%%%%%%%%%%%%%%%%%%%%%%%%%%%%%%%%%%%%%%%%%%%
R1=R0;
R2=imag(R1)<1.5*pi;
R3=R1(R2);
[~,R4]=sort(-real(R3)./imag(R3));
R5=R3(R4(1 function R6=func0(x)
% Calculation of eigonvalue for structure with extra DOF
syms s
% Starting conditions
%xc   location of the absorber
%n    DOF of the cable
xc=1;
n=19;
%%%%%%%%%%%%%%%%%%%%%%%%%%%%%%%%%%%%%%%%%%%%%%%%
```

```
%Transfer function of absorber's structure all parallel
%TF=c;
%TF=b*s+c;
%TF=b*s+c+k/s;

%all series
%TF=1/(1/c+1/(b*s));
%TF=1/(1/(b*s)+1/c+1/(k/s));

%six simple structures
%TF=1/(1/(c+k/s)+1/(b*s));
%TF=1/(1/(b*s+k/s)+1/(c));
TF=1/(1/(b*s+c)+1/(10/s));

%TF=1/(1/c+1/(k/s))+b*s;
%TF=1/(1/(b*s)+1/(k/s))+c;
%TF=1/(1/(b*s)+1/c)+k/s;
%%%%%%%%%%%%%%%%%%%%%%%%%%%%%%%%%%%%%%%%%%%%%%%%%%%%%%%%%%%%%%%%%%%%%%%%%%%%%%%%

% Calculation for M F K
f1=zeros(n);
f1(xc,xc)=1;
F=f1;

m1=eye(n)/(n);
M=m1;

k1=eye(n);
k2=ones(n-1,1);
k3=diag(k2,1);
k4=diag(k2,-1);
k5=2*k1-k3-k4;
k6=k5*(n+1);
K=k6;
%%%%%%%%%%%%%%%%%%%%%%%%%%%%%%%%%%%%%%%%%%%%%%%%%%%%%%%%%%%%%%%%%%%%%%%%%%%%%%%%
%Calculation of eigonvalue with TF method
O=zeros(n);
I=eye(n);
A01=[O,I;-inv(M)*K,-inv(M)*F*TF];
A02=eye(2*n)*s;
A03=A01-A02;
A04=det(A03);

D01=solve(A04,'s');
D02=double(D01);
D03=D02;
[~,D04]=sort(imag(D03));
D05=D03(D04);
D06=imag(D05)>=0;
D07=D05(D06);
R0=D07;
%%%%%%%%%%%%%%%%%%%%%%%%%%%%%%%%%%%%%%%%%%%%%%%%%%%%%%%%%%%%%%%%%%%%%%%%%%%%%%%%
R1=R0;
R2=imag(R1)<1.5*pi;
R3=R1(R2);
[~,R4]=sort(-real(R3)./imag(R3));
R5=R3(R4(1,1));
R6=real(R5)./abs(R5);
,1));
R6=real(R5)./abs(R5);
```